LIVING AND IMMORTAL POLYMERIZATION OF CYCLIC ESTERS WITH A DINUCLEAR INDIUM CATALYST

by

Cuiling Xu

B.Sc., Peking University, 2009

A THESIS SUBMITTED IN PARTIAL FULFILLMENT OF
THE REQUIREMENTS FOR THE DEGREE OF

MASTER OF SCIENCE

in

THE FACULTY OF GRADUATE STUDIES

(Chemistry)

THE UNIVERSITY OF BRITISH COLUMBIA

(Vancouver)

April 2012

Abstract

The dinuclear indium catalyst [(NNO)InCl]$_2$(μ-OEt)(μ-Cl) (**30**), previously reported to be highly active and living in the ring-opening polymerization (ROP) of lactide (LA), was synthesized *via* a previously published procedure and is studied to be active for the ROP of β-butyrolactone (BBL), ε-caprolactone (CL) and allyl-β-butyrolactone (fBL). A series of diblock copolymers PLLA-*b*-PDLLA were synthesized for the first time and their thermal properties were studied. A series of triblock copolymers PLLA-*b*-PDLLA-*b*-PLLA/PDLA were synthesized for the first time. Studies on the polymerization of BBL by **30** reveal that it is highly solvent dependent and the rate is first order in BBL and catalyst concentration. The activation parameters were obtained from an Eyring plot. The polymerization is controlled, providing PHB with molecular weights in agreement to theoretical values up to 300 kDa in narrow distribution. Triblock copolymers PLLA-*b*-PHB-*b*-PDLA were synthesized *via* the sequential addition technique. Polymerization of CL by **30** showed an unusual slower rate than LA. Copolymers of allyl-β-butyrolactone with LA and BBL were made, supporting the feasibility of incorporating functionality into pendent groups of polyesters with this catalyst.

The catalyst **30** is capable of immortal polymerization of LA and BBL with high loading of monomers and alcohols ([BBL]:[**30**]:[ROH] = 10000:1:100), providing polymers with molecular weights in well agreement with calculations inverse to the total amount of **30** and alcohols. The tacticity of polymers was not affected by the addition of ethanol. Poly(ethylene glycol) monomethyl ethers with molecular weights of 350 Da and 5000 Da were used as chain transfer agent to synthesize PEG and polyester block copolymers *via* iROP for the first time. Nanoparticles of PEG_{114}-*b*-$PLLA_{200}$ and PEG_{114}-*b*-$PLLA_{105}$ were made through nanoprecipitation and thin film rehydration/dialysis methods.

Preface

The studies on the polylactide diblock copolymers were carried out in collaboration with Prof. Savvas G. Hatzikiriakos and Norhayani Othman at UBC Chemical and Biological Engineering. In this collaborative project, the thermal, rheological and mechanical measurements were done by Norhayani Othman. The rest, including synthesis of the polymers, preparing the blending samples and characterization by NMR and GPC were done by Cuiling Xu. The results have been submitted to a journal, with the name of the paper as "Thermorheological and mechanical behavior of polylactide and its enantiomeric diblock copolymers and blends". Part of the thermal results is used in Chapter 2 in this thesis.

The studies on the copolymers containing poly(ethylene glycol) block were carried out in collaboration with Prof. Helen Burt and Dr. Kevin Letchford at UBC Pharmaceutical sciences. The studies on the solution behaviors of these copolymers and encapsulation of drugs were done by Dr. Kevin Letchford. Part of the results is used in Chapter 3.

The synthesis of allyl-β-butyrolactone was done by Dr. Thusith Pothupitiya. Preliminary polymerization of this monomer was done by Cuiling Xu and part of the results is listed in Chapter 2.

Table of Contents

List of Tables

List of Figures

List of Schemes

List of Abbreviations

BBL	β-butyrolactone
Bn	benzyl, -$CH_2(C_6H_5)$
*t*Bu	*tert*-butyl, -$C(CH_3)_3$
CL	ε-caprolactone
Conv.	conversion
DMF	dimethylformamide
DMSO	dimethyl sulfoxide
equiv	equivalent(s)
Et	ethyl
g	grams
GPC	gel permeation chromatography
h	hour(s)
h	Planck's constant
HNNO	2-[[[(dimethylamino)cyclohexyl]amino]methyl]-4,6-bis(tert-butyl) phenol
iROP	immortal ring-opening polymerization
k	rate constant for polymerization reactions
k_b	Boltzmann's constant
k_{obs}	observed rate constant for polymerization reactions
LA	lactide
M	monomer
M_n	number average molecular weight
M_w	weight average molecular weight
Me	methyl
MePEG	poly(ethylene glycol) monomethyl ether
MW	molecular weight
M/I	monomer to initiator ratio

NMR	nuclear magnetic resonance
NNO	deprotonated HNNO
NOESY	nuclear Overhauser effect spectroscopy
OTf	triflate, $CF_3SO_3^-$
PCL	poly(ε-caprolactone)
PDI	polydispersity index
PEO	poly(ethylene oxide)
PEG	poly(ethylene glycol)
PET	poly(ethylene terephthalate)
Ph	phenyl
PLA	polylactide, poly(lactic acid)
PLLA	poly(L-lactide)
PDLA	poly(D-lactide)
PDLLA	poly(racemic lactide)
PHA	poly(hydroxyalkanoate)
PHB	poly(β-hydroxybutyrate)
PHBHH	poly(β-hydroxybutyrate-*co*-β-hydroxyhexanoate)
PHBV	poly(β-hydroxybutyrate-*co*-β-hydroxyvalerate)
rac	racemic
ROP	ring-opening polymerization
s	second(s)
t	time
T	temperature
T_g	glass transition temperature
T_m	melting temperature
THF	tetrahydrofuran
TMB	1,3,5-trimethoxybenzene
Tol	toluene

Acknowledgements

I would like to appreciate many people who have helped me with my project and this thesis. I would like to say thank you first to my supervisor Prof. Parisa Mehrkhodavandi for her patience and support. Her enthusiasm and diligence in the academic field encouraged me a lot. I would like to say thank you to the previous and present members of the Mehrkhodavandi Group for their help and accompanies. Specially, thank you to Kimberly Osten and Dinesh Aluthge for revising my thesis with great patience and carefulness. Thank you to Insun Yu for useful suggestions. Thank you to Dr. Alberto Acosta-Ramírez for teaching me lab techniques. Thank you to Dr. Thusith Pothupitiya for synthesizing monomers.

I would like to thank Prof. Laurel L. Schafer and Prof. Jayachandran N Kizhakkedathu for being my committee and bringing precious advices to my thesis. Thank you to Prof. Savvas G. Hatzikiriakos in Chemical and Biological Engineering for his guidance and support in the collaborative project. Thank you to Norhayani Othman for measuring thermal, rheological and mechanical properties of polymer samples. Thank you to Prof. Helen Burt and Dr. Kevin Letchford in Pharmaceutical Sciences for studying the behavior of PEG block copolymers in drug delivery. Thank you to Kevin for running GPC of some special samples for me. Thank you to the Gates group in Chemistry Department for the use of their GPC instrument.

Thank you to all the staff in UBC Chemistry Department. Thank you to Maria Ezhova and Jason Traer for their help with NMR spectroscopy. Thank you to the staff in glass shop, mechanic shop and chem store.

Thank you to my family for their unconditional love and support. Thank you to my friends.

CHAPTER 1. General Information

1.1 Introduction to biodegradable polymers

Fossil fuel feedstocks have played an important role in the rapid modernization of our world. They provide energy and raw materials for the chemical industry to produce necessary products, especially polymers. Synthetic fibers, plastics, and rubbers surpass natural counterparts greatly in variable properties; therefore, they are utilized in various fields ranging from transportation to packaging.[1] However, with the current oil crisis, the need for alternative sustainable synthetic routes towards these products is becoming urgent.[2] In addition, synthetic materials like polyethylene are difficult for the natural environment to degrade, which results in plastic pollution, making biodegradability another goal for next generation materials.[3]

Regardless of whether a synthetic material is based on renewable or petrochemical resources, biodegradability pertains to the ability of a material to be degraded in the natural environment by microorganisms to carbon dioxide and water.[4] There are three major categories of biodegradable polymers: (1) natural polysaccharides and other biopolymers; (2) polyesters synthesized by microorganisms, such as poly(hydroxyalkanoate)s (PHAs); (3) synthetic polymers.[4] Large scale of natural polysaccharides, such as starch, can be produced with low cost. However, they usually need to be blended with other synthetic polymers to achieve the most desirable properties, and attractive blendings are limited.[5]

PHA is a family of diverse polyesters produced by microorganisms as an energy reserve material (Figure 1.1). Poly(β-hydroxybutyrate) (PHB) was the first PHA that was isolated and discovered from bacteria. Later, it was found that depending on the species of bacteria and carbon sources around them, various hydroxyalkanoate monomers can be utilized to synthesize PHA. Therefore the physical properties and biodegradability of PHAs can be different, based on their monomer composition and ratios.[6] Versatile materials, from hard crystalline plastic to elastic rubber, can be made from different PHAs. Recently, genetic

engineering of microorganisms has led to use of microorganisms for the targeted synthesis of PHA.[7] Microbial polyesters can be easily degraded in soil, sludge or sea water. Among PHAs, poly(β-hydroxybutyrate-*co*-β-hydroxyvalerate) (PHBV), poly(β-hydroxybutyrate-*co*--β-hydroxyhexanoate) (PHBHH) and PHB are now available in large quantities for applications in research.[8] For example, because of their biocompatibility, PHAs have been used as tissue engineering materials.[9]

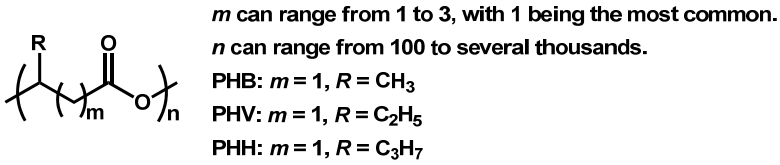

Figure 1.1 General molecular structure of PHA

Compared to natural polymers, synthetic polymers are more versatile for different applications. There are three categories of synthetic biodegradable polymers, all of which contain ester linkages in the main chain. The first category is polyesters. The second category includes poly(ester amide)s, poly(ester ether)s, poly(ester carbonate)s, poly(ester urethane)s and poly(ester urea)s, which represents polymers possessing both esters and other heteroatom-containing linkages in the main chains. The last category contains only heteroatom-containing linkages other than ester linkages in the main chain, with examples including polypeptides, some biodegradable polyamides, polyether and poly(urethane)s.[4]

Usually, synthetic polymers such as polyamides, polyurethanes, and polyethers are not readily biodegradable unless modified by the introduction of different substituents.[10] Incorporation of ester groups into these heteroatom-containing polymers changes their biodegradability.[11] These polymers often undergo enzyme degradation at the ester linkage first. Other modifications, such as copolymerization and physical processing can also increase their biodegradability.[4, 12]

Polyesters, a category of polymers which contain ester functional groups in their main chains, are representatives of synthetic biodegradable polymers. Natural polyesters and a few

synthetic polyesters are biodegradable. Polyesters are classified into aliphatic and aromatic ones, both of which contains commercialized products, such as poly(ε-caprolactone) (PCL), polylactide (PLA), poly(lactide-*b*-glycolide) and poly(ethylene terephthalate) (PET). Synthetic routes towards polyesters include polycondensation of an alcohol and acid and ring-opening polymerization of cyclic esters. Lactide and β-butyrolactone are monomers which have gained much interest and can be polymerized to produce PLA and PHB.

1.2 Polylactide

Polylactide or poly(lactic acid) (PLA) is a biodegradable polyester that can be made from renewable resources, such as corn starch or cane sugar, which form lactic acid under fermentation conditions. PLA is unique amongst biodegradable polymers, not only because of its similar properties to polymers like polyethylene and poly(ethylene terephthalate) (PET), but also because of its good processability into films, fibers and other useful materials.[13] It's widely used in biomedical engineering and food packaging and applications.[14]

In light of increasing environmental concerns, PLA is being commercially produced in larger scales in the past few years with a decreasing cost. NatureWorks LLC is a pioneer in commercially available biopolymers derived from 100% renewable resources. The company applies its unique technology to the processing of natural plant sugars to create polylactide, merchandised under Ingeo™ fibers brand names.[15] It is also the largest producer of bio-based lactide. Other companies involved in manufacturing PLA include PURAC, Futerro, KAIST and several Chinese manufacturers.

1.3 Lactide and tacticity of polylactide

Lactide (LA), a dimer of lactic acid, is usually produced by a series of poly-merization/depolymerization reactions from lactic acid. Lactide is widely used as the monomer to produce PLA *via* ring-opening polymerization (ROP). As Figure 1.2 shows,

there are two chiral centers in every LA unit. Therefore, there are four types of monomers based on different configurations of the two chiral carbons: D-LA (*R*,*R*-lactide), L-LA (*S*,*S*-lactide), *meso*-LA (*R*,*S*-lactide) and *rac*-LA (50% D-LA and 50% L-LA). Natural LA is in L, or (*S*,*S*) configuration. PURAC produces D-lactide and L-lactide under the brand name PURALACT^{TM}, with high stereochemical purity.[16] The enantiopure monomers allow synthesis of PLA copolymers with different features.

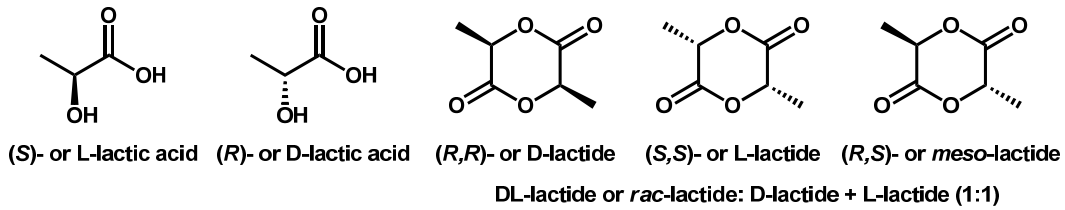

Figure 1.2 Lactic acid and isomers of lactide

The chirality of LA translates to the resulting PLA. If the configurations of the two neighboring chiral carbons in two connected monomeric units in PLA are the same, this connection is called a meso linkage. Otherwise, it is called a racemic linkage. P_m and P_r describe the probabilities of finding meso or racemic linkages, respectively, in the polymer chain. Depending on the chirality of the monomer used and the connections between neighboring units in the polymer chain, there are several possible microstructures of PLA (Scheme 1.1). In isotactic polymers composed of entirely L- or D- lactide, *i.e.* poly(L-LA) (PLLA) or poly(D-LA) (PDLA), P_m = 1. Polymerizing *meso*-LA with syndioselective catalysts yields syndiotactic PLA. In polymerization of *rac*-LA, several different polymer microstructures are possible. Without any selectivity, atactic PLA is formed. If D- and L-LA are enchained in an alternating fashion, then heterotactic PLA with P_r = 1 is formed. Stereoblock PLA can be achieved by using a selective catalyst for the kinetic resolution of *rac*-LA or by sequential polymerization of D-LA/L-LA with a living catalyst.

Scheme 1.1 Different microstructures of PLA formed from isomers of lactide

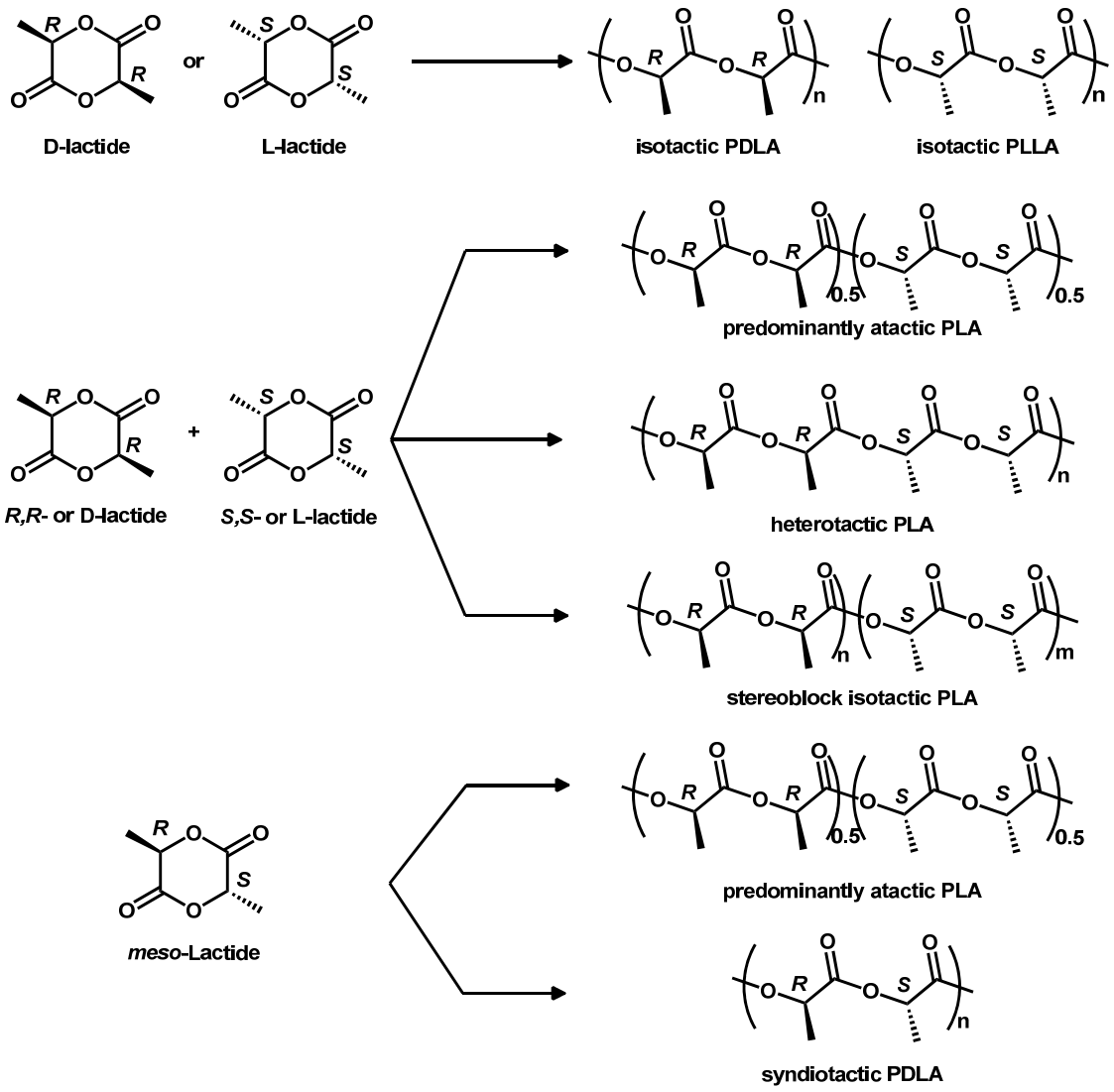

The microstructure of PLA can be probed by NMR spectroscopy. $^{1}H\{^{1}H\}$ and $^{13}C\{^{1}H\}$ NMR spectroscopy have been used to designate the sequences in PLA polymer. In $^{1}H\{^{1}H\}$ spectrum, a tetrad* sensitivity of the methine proton can be observed and used to determine P_m and P_r values. For PLA derived from *rac*-LA, five tetrad sequences can be seen: *mmm*, *mrm*, *mmr*, *rmr* and *rmm*.

Tacticity has a strong influence on the properties of PLA such as crystallinity, melting point

* Tetrad means four repeating units in the polymer chain. Similarly, diad and triad means two and three repeating units, respectively.

and biodegradability. PLLA is a crystalline polymer with an equilibrium melting point (T_m) of 207 °C (experimental data is 180 °C) and a glass transition temperature (T_g) of 60 °C, while atactic PLA is an amorphous polymer with no T_m and only a T_g of 50–60 °C.[17] Reduced stereoregulatiry of PLA can lead to reduction in the melting point, rate of crystallization and extent of crystallization.

The brittleness of crystalline PLLA usually reduces its processability, resulting in the limitation of their applications.[18] Blending PLLA with a second polymer has been used to modify its processability and mechanical properties.[19] Amorphous poly(*rac*-LA) (PDLLA) was one of the effective polymers to be blended with PLLA to alleviate the brittleness. In PLLA/PDLLA blends, crystallization of PLLA occurred when the percentage of PLLA was higher than 0.20.[20] A single T_g was observed for the blends, indicating the miscibility of these two polymers.

Higher melting point PLA can be made by mixing PLLA and PDLA to form a stereocomplex. Ikada *et al.* reported in 1987 that a melting point of 230 °C was observed by mixing PLLA and PDLA with a 50:50 ratio.[21] PLLA chains adopted left-handed helical structure in crystalline form and therefore PDLA a right-handed helical structure. Thus, by mixing PLLA and PDLA, a stereocomplex with a new crystalline structure was formed through van der Waals forces such as dipole-dipole interactions between the two different helical chains. Stereocomplexes of PLA can be made not only by simply blending PLLA and PDLA together, but also by synthesizing PLLA/PDLA stereoblock copolymers (Scheme 1.1).[22] PURAC is developing commercial products with higher heat stability based on stereocomplexes of PLA.[16]

1.4 Ring-opening polymerization of lactide

Two different methodologies are employed in the synthesis of PLA: polycondensation of lactic acid and ring-opening polymerization (ROP) of lactide. Polycondensation of lactic acid

requires the removal of water from the reaction mixture and often heating and vacuum are necessary for this purpose. With this method, however, only low molecular weight polymer with high polydispersity index (PDI, *i.e.* M_w/M_n) can be achieved. ROP is very convenient and efficient for the production of polyesters. It uses mild reaction conditions and has better control over the molecular weight and the microstructure of the resulting polymers.

Polycondensation involves the condensation of diols and diacids or bifunctional monomers through step growth polymerization. The major advantage of polycondensation is that it allows access to a broader range of polymer structures. For example, Meyer *et al.* used polycondensation to produce novel copolymers of lactic acid and glycolic acid with repeating sequences.[23] Segmers with different sequences were presynthesized and then polycondensed. Scheme 1.2 shows how segmers of (lactic acid)-(glycolic acid) (LG) sequence were made and polymerized. Other similar repeating sequence copolymers were also made, such as ones with LLG and GLG sequence. The accomplishment of sequence design in synthetic polymers has potential spectacular advantages in making frontier materials.

Scheme 1.2 Synthesis of repeating sequence copolymers by segmer assembly

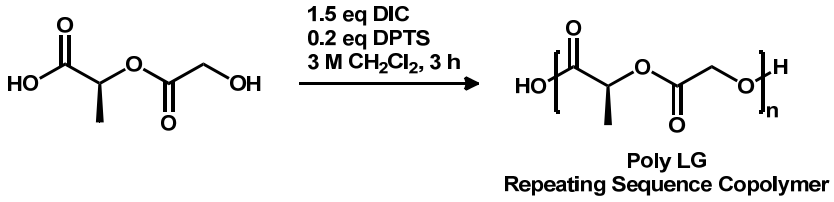

ROP, especially coordination-insertion ROP, is a very convenient and efficient method to produce polyesters. It uses mild reaction conditions and has better control over the molecular weights and microstructures. The driving force of ROP is the relief of ring strain of cyclic esters. Ring strain differs with different monomers. Ring strain of LA is considerably high as a result of its boat conformation due to two carbonyl bonds in the ring.[24]

Scheme 1.3 Mechanism of coordination-insertion ROP of LA using metal oxide catalysts

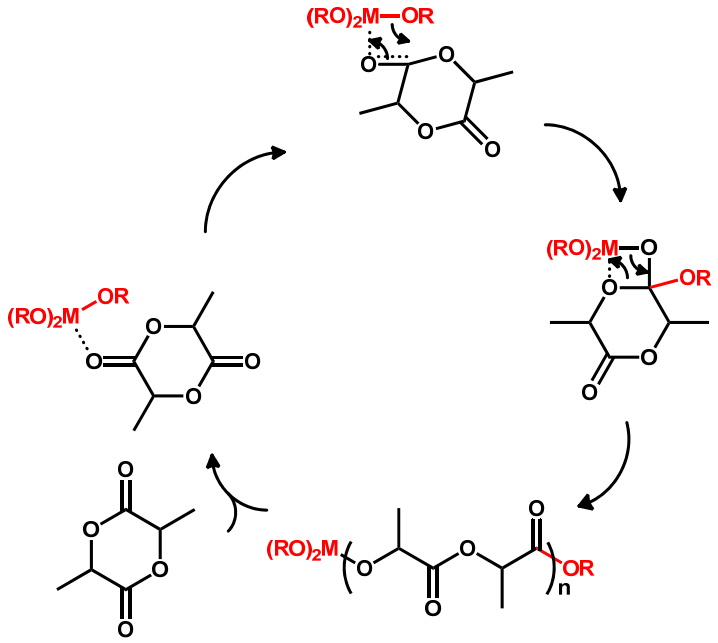

The mechanism of coordination-insertion ROP of LA involves coordination of LA to the metal center, followed by insertion of LA into metal-oxide bond *via* acyl–oxygen cleavage of LA (Scheme 1.3).[24b]

There are two types of mechanisms governing stereocontrol in polymerization reactions.[25] One is called enantiomorphic site control, where a chiral ligand on the catalyst forms an asymmetric environment which results in the inclination of the catalyst to incorporate a monomer with a specific configuration. The second is chain-end control, where the enchainment of the next monomer unit is influenced only by the stereochemistry of the last unit in the growing polymer chain.

Sometimes these two mechanisms are difficult to distinguish. However, if there are stereochemical errors occurring during the polymerization, examining these errors, by NMR spectroscopy for example, can provide insight into which mechanism may be present. In an enantiomorphic site control mechanism, enchainment of the disfavored monomer isomer may be corrected when the next monomer is enchained. This is the opposite in a chain-end control

mechanism, whereby enchainment of the disfavored monomer isomer would result in propagation of the error at the next insertion of monomer, generating polymers with stereoblocks. The distributions of the tetrad sequences in PLA are different under these two mechanisms. Statistical analysis of the tetrad distributions in the homonuclear decoupled ^{1}H NMR spectrum can be used to differentiate these two processes.

Early initiators for coordination-insertion ROP of LA were mainly simple homoleptic metal complexes, tin(II) bis(2-ethylhexanoate), zinc(II) lactate and aluminium(III) isopropoxide ($Al(OiPr)_3$).[24b] These initiating systems were used industrially to produce commercialized PLA. However, side reactions such as intramolecular and intermolecular transesterification are significant. They have not much control over the molecular weight and no control over the stereochemistry of polymers.

Well-defined single-site catalysts with ancillary ligands were designed to overcome those limits and enhance catalytic activity.[26] Selective catalysts which possess both high stereoselectivity and good control over molecular weights are shown in Figure 1.3 and Figure 1.4.

There was only one example of efficient syndioselective catalysts published.[27] The chiral aluminum isopropoxide complex **1a** (Figure 1.3) supported by a salen ligand was able to polymerize *meso*-LA, resulting in a highly syndiotactic PLA (P_r up to 96%). The racemate of this catalyst was later found to polymerize *meso*-LA to heterotactic PLA.[28] A polymer exchange mechanism was proposed to account for the tacticity of this polymer, where runs of enantiomerically pure lactide were interrupted by periodic changes in stereochemistry caused by interchange between enantiomeric catalyst species.

For synthesis of isotactic PLA, Spassky *et al.* were the first to discover that Schiff's base (salen type) aluminum complexes are highly selective catalysts.[29] In 1996, they reported an aluminum methoxide complex **1b** (Figure 1.3) supported by a binaphthyl Schiff-base ligand was able polymerize *rac*-LA to give isotactic PLA through a chain-end control mechanism.

At low conversions, D-LA was preferentially incorporated, taking up to over 80% of the monomeric units in the polymer; at high conversions, a stereocomplex between D- and L-enriched stereocopolymers was formed.

Inspired by their work, other aluminum complexes supported by Schiff's base and other N,O-donor ligands were reported. In 2002, Feijen *et al.* reported a complex based on (*R*,*R*)-cyclohexanediamine Schiff base.[30] This catalyst **2** (Figure 1.3) was easy to synthesize and preferentially polymerized L-LA with a rate difference as k_{SS}/k_{RR} = 14 *via* a chain-end control mechanism. Stereocomplexes of PLA were synthesized by polymerization of *rac*-LA with the racemate of the catalyst, showing a T_m of 183.5 °C higher than pure PLLA. Aluminum complex **3** (Figure 1.3) supported by an achiral salen ligand synthesized by Nomura *et al.* showed high isoselectivity (P_m = 0.91, T_m = 192 °C) *via* a chain-end control mechanism.[31] In 2004, Gibson *et al.* found quite remarkable stereocontrol in the polymerization of *rac*-LA by aluminum initiators **4** (Figure 1.3) supported by tetradentate aminophenoxide ligands.[32] The polymerizations were well-controlled and living, affording PLA materials ranging from highly isotactic to highly heterotactic, depending upon the ligand substitution pattern. Isotactic PLAs were produced in the case of complexes bearing unsubstituted phenoxide groups whereas heterotactic PLAs were obtained when the phenoxide units of the salan ligand contained substituents in the 3 and 5 positions (e.g. for complexes **4c** and **4d**). The tacticity was also significantly influenced by the substituents R^1 on the amido nitrogen. By modifying the substituent from methyl group (**4a** with P_m = 0.68) to benzyl group (**4b** with P_m = 0.79) higher isotacticity was achieved.

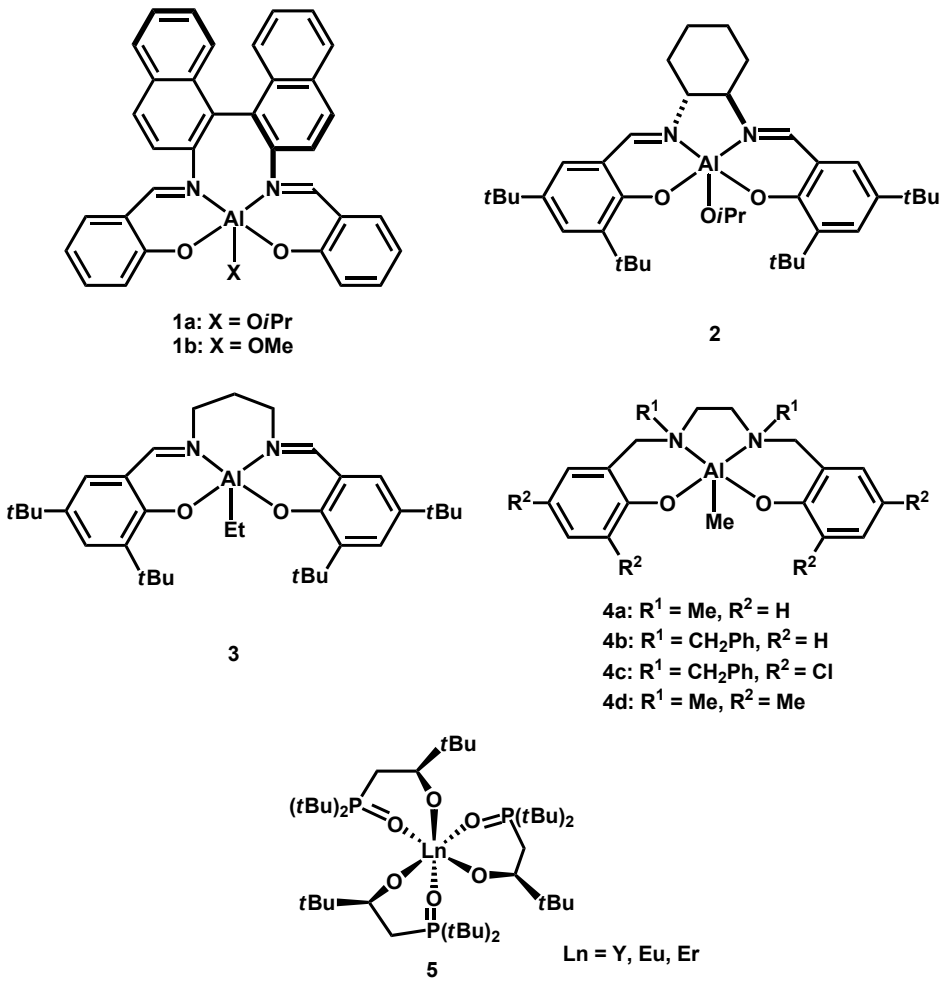

Figure 1.3 Stereoselective systems for ROP of lactide

For other metal-based systems, in 2008, Arnold *et al.* reported a racemic phosphine oxide/alkoxide ligand HL which, upon lanthanide complexation, generated a racemic mixture of homochiral, C_3-symmetric complexes, *RRR*- and *SSS*-[LnL_3] **5** (Figure 1.3).[33] The complexes were active ([LA] = 0.156 mol/L, at −18 °C, in 10 mins, 98% conversion was reached) to polymerize *rac*-LA into highly isotactic PLA (P_m = 0.81) and also stereocomplexes of PLA.

Catalysts for synthesis of heterotactic PLA are more common. Coates *et al.* reported a series of zinc(II) and magnesium(II) alkoxides based upon a β-diiminate ligand framework (Figure 1.4).[34] Complex **6c** was the most active and stereoselective zinc complex for the polymerization of lactide. **6c** polymerized *rac*-LA into heterotactic PLA (P_r = 0.94 at 0 °C), and *meso*-LA into syndiotactic PLA (P_r = 0.76 at 0 °C). Changing the ligand substituents R

from isopropyl to either ethyl groups (**6a** with P_r = 0.79) or n-propyl groups (**6b** with P_r = 0.76) resulted in a decrease in heterotacticity.

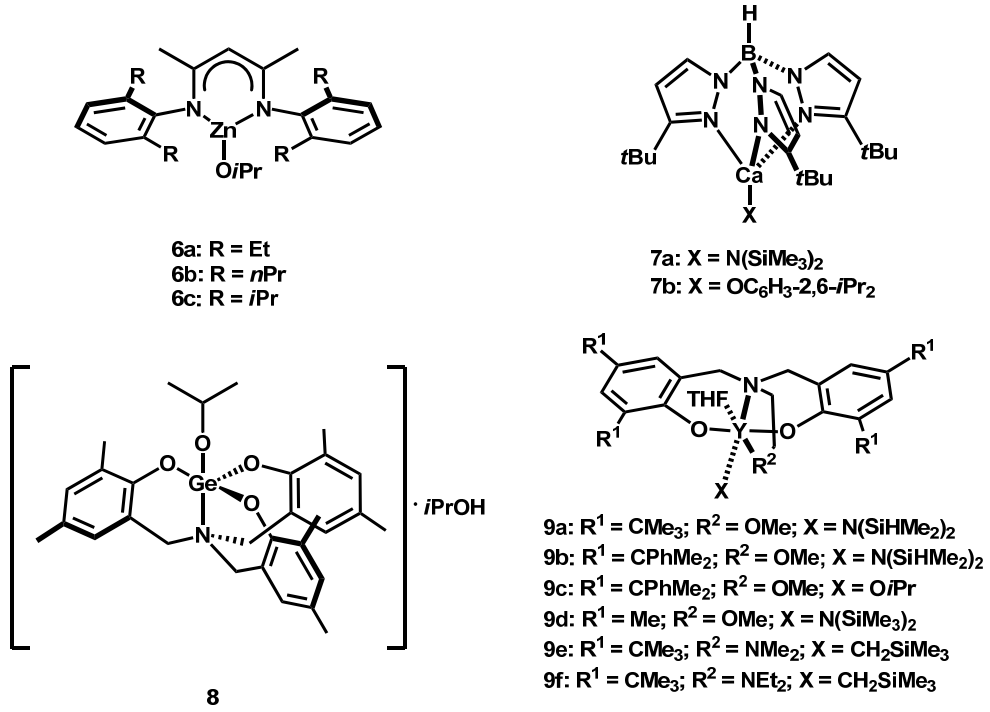

Figure 1.4 Heteroselective systems for ROP of *rac*-lactide

Chisholm *et al.* reported the first examples of monomeric heteroleptic calcium complexes **7a–b** supported by amido and alkoxy groups (Figure 1.4) for the ROP of LA.[35] Tridentate trispyrazolyl borates (Tp) were shown to be a better ligand for calcium than the aforementioned β-diiminate ligand by Coates *et al*[34]. The bulky substituents on the Tp$^{t\text{Bu}}$ ligand was important for the realization of single-site living polymerization and the stereoselectivity (P_r = 0.93). No stereocontrol was observed for the less sterically demanding Tp$^{i\text{Pr}}$ ligand supported complex. The reactivity followed the trend: Ca > Mg > Zn for a series of compounds Tp$^{t\text{Bu}}$ MOR.

Davidson *et al.* reported the first sing-site germanium alkoxide initiators **8** (Figure 1.4) supported by C_3-symmetric amine(triphenolate) for the ROP of LA. It was able to afford highly heterotactic PLA under solvent-free conditions.[36] Hillmyer and Tolman *et al.* used readily available reagents, indium trichloride, benzyl alcohol, and triethylamine, to generate a

catalyst *in situ* for the room temperature polymerization of *rac*-LA affording highly heterotactic PLA (P_r = 0.97 at 0 °C) with controlled molecular weight and narrow molecular weight distribution.[37]

In recent years, complexes based on lanthanide metals have been studied for ROP of LA.[38] Carpentier *et al.* reported a series of complexes of yttrium, lanthanum and neodymium supported by alkoxyaminobis(phenolate) ligands.[39] The resulting Group 3 metal complexes were able to perform ROP of *rac*-LA in living way. Complex **9b** (Figure 1.4) polymerized *rac*-LA into heterotactic PLA (P_r = 0.90 at 20 °C) and *meso*-LA to syndiotactic PLA (P_r = 0.75 at 20 °C). Reaction of **9b** and 2-propanol formed **9c** *in situ*, with which highly heterotactic PLAs with narrow PDI were obtained with high activities and productivities at room temperature. The steric bulk of the substituents on the aromatic rings, and particularly the ortho-phenolate substituents, were critical for high heteroselectivity for ROP of *rac*-LA *via* a chain-end control mechanism.

1.5 Poly(β-hydroxybutyrate)

Apart from polylactide, poly(hydroxyalkanoate) (PHA) is another category of polyesters which has been widely used. Among PHAs derived from different monomers, poly(β-hydroxybutyrate) (PHB) is the most common type (Figure 1.1). Naturally derived PHB is a biodegradable and biocompatible thermoplastic with similar application range to isotactic polypropylene.[6] The monomeric unit in naturally-occurring PHB is in the *R* configuration. Natural PHB is highly crystalline with high molecular weight and a melting point of 180 °C. Compared to polypropylene (PP), poly(ethylene terephthalate) (PET) and Nylon-6,6, PHB has similar Young's modulus and tensile strength but much smaller extension needed to break, meaning it's stiffer and more brittle (Table 1.1).[6]

Table 1.1 Physical and thermal properties of PHB and other similar materials[6]

Properties	PHB	PP	PET	Nylon-6,6
Melting temperature (°C)	177	170	267	265
Glass-transition temperature (°C)	4	−10	69	50
Crystallinity (%)	60–80	50–70	30–50	40–60
Density (g/cm^3)	1.250	0.905	1.385	1.14
Water uptake (wt%)	0.2	0.0	0.4	4.5
Young's modulus (GPa)	3.5	1.7	2.9	2.8
Tensile strength (MPa)	43	34	70	83
Extension at break (%)	5	400	100	60

Table 1.2 Physical and thermal properties of PHB and other PHAs[9]

Polymers	PHB	poly(HB-*co*--10% HV)[a]	poly(HB-*co*--20% HV)[a]	poly(HB-*co*--10% HH)[b]	poly(HB-*co*--17% HH)[b]
T_m (°C)	177	150	135	127	120
T_g (°C)	4	—	—	−1	−2
Tensile strength (MPa)	43	25	20	21	20
Extension needed to break (%)	5	20	100	400	850

[a]HB = β-hydroxybutyrate; HV = β-hydroxyvalerate. [b]HH= β-hydroxyhexanoate. Structures of PHB, PHV and PHH were shown in Figure 1.1

Materials based on PHB, such as copolymers and composites, can have various properties suitable for different applications. Copolymers between β-hydroxybutyrate and other β-hydroxyalkanoate monomers have higher elongation at break (Table 1.2), meaning that they are less brittle than PHB.[9] Chen *et al.* made films and scaffolds from blends of PHB and poly(β-hydroxybutyrate-*co*-β-hydroxyhexanoate) (PHBHH).[40] The elongation to break increased from 15% to 106%, when PHBHH content in the blend was increased from 40% to 60%. PHA and PHA based materials have been used in biomedical application. Yagi *et al.* reported an efficient transdermal drug delivery system made from a poly(amidoamine)

dendrimer containing PHA, which allowed the required drug to permeate through a skin model.[41]

Yoon *et al.* synthesized diblock copolymers by chemically coupling poly(HB-*co*-HV) or poly(HB-*co*-γ-hydroxybutyrate) with poly(ethylene glycol) monomethyl ether (MePEG) through transesterification.[42] The amphiphilic copolymers assembled in aqueous solution to form nanoparticles with a hydrophilic shell of MePEG and a hydrophobic core of PHA. Studies on the release of a hydrophobic drug and the *in vitro* cytotoxicity of these nanoparticles showed that this system could be safe for the controlled release of various hydrophobic drugs.

Blending PHB with other polymers can even enhance its biocompatibility. Cheng *et al.* prepared a series of blends based on PHB and polyethylene glycol (PEG) with different ratios ranging from 80:20 (wt%) to 20:80 (wt%). Results on platelet clotting time showed that PEG played an important role in resisting platelet adhesion.[43]

Hydrolysis of PHA, particularly by enzymes, was affected not only by the stereoregularity, but also by the crystallinity, molecular weight and composition of the polymer itself. Generally, less crystalline polymer and lower molecular weight polymer were degraded more slowly.[44] Environmental degradation studies have shown that the biodegradability of (*R*)-PHB was greater than PLLA.[45] With depolymerases, highly crystalline (*R*)-PHB can be hydrolyzed very quickly. However, (*R*)-PHB cannot. PHB with P_m ranging from 0.68 to 0.92 had increased erosion compared to (*R*)-PHB, resulting in a higher fraction of oligomers. Atactic PHB degraded more slowly than (*R*)-PHB.[46] Syndiotactic PHB was hardly hydrolyzed, which is a result of the fact that the binding domain of PHB depolymerase has an affinity toward the isotactic (*R*)-PHB crystalline phase.[47]

Chemically synthesized PHB can have different microstructures. It is a goal for researchers to synthesize isotactically rich, but not completely isotactic PHB (ideal P_m will be around 0.7–0.9) to make it less brittle.

PHAs are more expensive than PLA. So far, commercial PHB, PHBV, poly(β-hydroxybutyrate-*co*-γ-hydroxybutyrate) and medium-chain-length PHAs have been produced in large scales by microbial fermentation of natural biomaterials, such as sugar, starch and wood. Various wild type strains of bacteria were found to be able to produce PHB and other PHAs in large density containing a high percentage of products.[8]

ICI was one of those companies who produced PHA in the 1980s in a large scale.[8] Due to the high cost, production stopped in the 1990s. Monsanto produced PHBV under the name of Biopol. Later, the rights to Biopol were sold to Metabolix. Metabolix created a joint venture with Archer Daniels Midland Company, named Telles, which produces PHAs under the brand name Mirel^{TM} *via* large-scale microbial fermentation technology.[48] These products have been applied in many fields, such as agricultural, food, marine and packaging areas. In recent years, several companies in China have joined in the production of PHA, such as Tianjin Green Bio-science, whose scale has reached 10,000 tons per year.[8]

1.6 Carbonylation of epoxides to β-lactones

There are different routes to synthesize PHB, either from β-hydroxybutyric acid or β-butyrolactone (BBL). (*R*)-β-hydroxybutyric acid can be made through chemical synthesis, enzymatic hydrolysis and metabolic engineering of bacteria strains, among which the chemical synthesis route is not economically favored. Tokiwa *et al.* separated a PHB depolymerase from a thermophilic Streptomyces sp. MG. This enzyme was able to hydrolyze PHAs such as PHB, PHBV, and also synthetic aliphatic polyesters such as polypropiolactone.[49] Chen *et al.* produced (*R*)-β-hydroxybutyric acid directly from glucose by simultaneously expressing genes of 4 enzymes in *E. coli* strain DH5α.[7] The concentration of chiral β-hydroxybutyric acid was highly increased. The monomer obtained can be modified with other functional groups and further applied in organic synthesis or even as biofuels.[50]

Among chemical synthesis, carbonylation of epoxides remains a powerful way to produce enantiopure β-butyrolactone (BBL) and functionalized BBL (Scheme 1.4). One of the most significant contributions to this field came in 2002, when the Coates group discovered catalysts with unprecedented activity and selectivity for the carbonylation of a variety of epoxides.[51]

Scheme 1.4 Carbonylation of epoxides

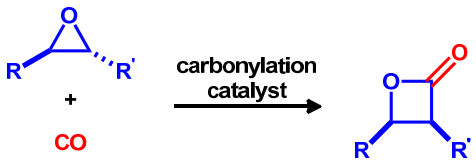

In 2002, the complex [(salph)Al(THF)$_2$][Co(CO)$_4$] **10** (Figure 1.5) was found to be active for the carbonylation of epoxides.[51] *R*-BBL was generated from propylene oxide with more than 98% retention of configuration. 1-butene oxide reached more than 99% conversion in 2.5 hours, with 1 mol% **10**, at 50 °C, under a pressure of 880 psi CO. When carbonylating isobutylene oxide, two possible regioisomers were produced, indicating two different pathways. The postulated primary pathway involved nucleophilic attack of the epoxide at the less hindered site by the Co anion. The other route involved ring-opening of epoxide by the Al cation. This catalyst was later applied to the carbonylation of *cis*/*trans*-2-butylene oxide, producing *trans*- and *cis*- products.[52]

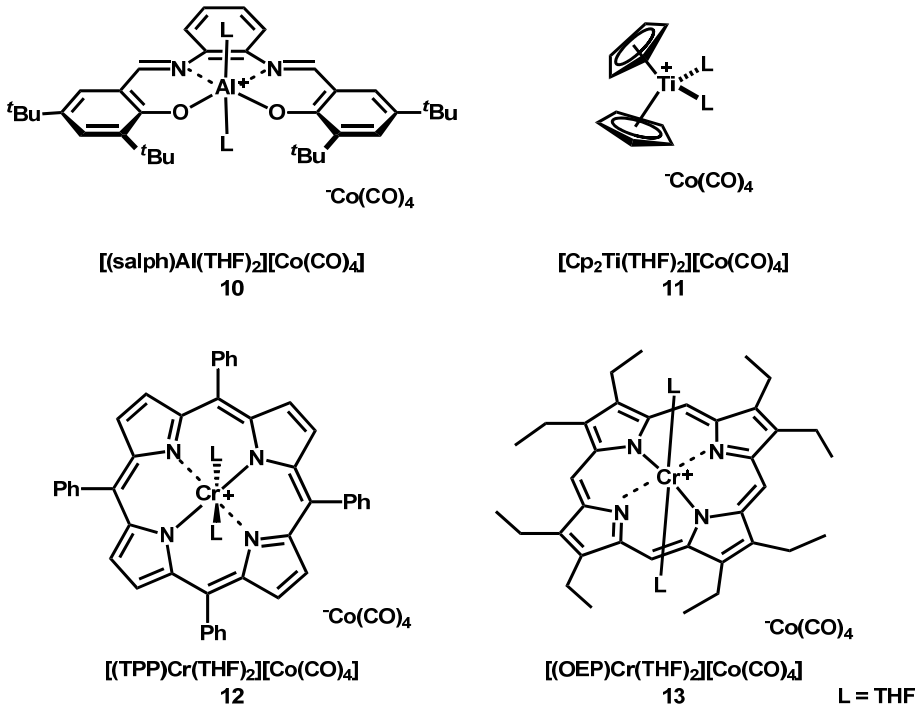

Figure 1.5 Structures of selective catalysts for carbonylation of epoxides

Another catalyst of the type [Lewis acid]$^{+}$[$CoCO_4$]$^{-}$, [$Cp_2Ti(THF)_2$][$CoCO_4$] **11** (Figure 1.5) expanded the epoxide scope. Functionalized epoxides such as 1,2-epoxy-5-hexene and epichlorohydrin reacted with high conversion and retention of configuration (5 mol% **11**, 60 °C, 900 psi CO). Subsequently, another Lewis acid, Cr(III) porphyrin, combined with $CoCO_4^{-}$ (**12,** Figure 1.5), was found to be more active than the aforementioned catalysts.[53] In addition, it was able to produce mono- and bi-cyclic β-lactones. The catalyst worked very well for several epoxyalkanes with carbon lengths between 4 and 12 (0.125–1.5 mol% **12**, 60 °C, 900 psi CO). Slightly tailoring the porphyrin ligand led to the discovery of an even more active complex **13** (Figure 1.5).[54] Under the same condition as above, only 0.001–0.2 mol% catalyst was required to reach full conversion. Epoxides containing ester and amide chains were also tolerated well in this system.

This reaction was optimized to be able to tolerate CO pressures as low as 1 atm, under the catalysis of [(salph)Cr(THF)$_2$][$CoCO_4$] (in **10** of Figure 1.5, Al was replaced by Cr).[55] With this catalyst, weakly coordinating polar solvents like dimethyl ether worked best for the reaction and room temperature was used. Compared to previous results at higher temperature,

the formation of ketone byproducts was decreased.

In 2006, the mechanism of epoxide carbonylation by the catalyst **10** was explored in detail (Scheme 1.5).[56] The rate-determining step was the formation of the lactone product from the (β-metalloxy)acylcobalt species (**A** in Scheme 1.5).

Scheme 1.5 Mechanism of the catalytic carbonylation of epoxides by $[(salph)Al(THF)_2][Co(CO)_4]$

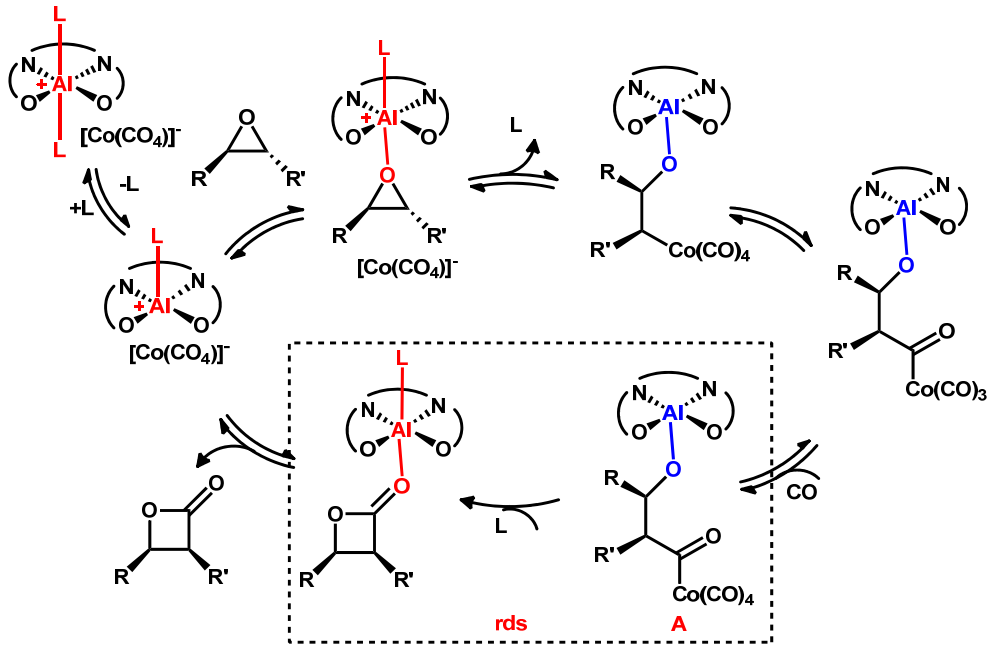

1.7 Ring-opening polymerization of β-butyrolactone

There are three major routes to synthesize PHB: (1) fermentation by microorganisms; (2) alternating copolymerization of propylene oxide and carbon monoxide; (3) ring-opening polymerization (ROP) of β-butyrolactone.

Fermentation produces highly isotactic PHB with high molecular weights (over 100 kDa, with PDI 1.7–2.9).[6] However, better technology to separate PHB from bacteria has to be developed.[57] Another drawback is that highly isotactic PHB is brittle and does not have many

applications.[6] Copolymerization of propylene oxide and carbon monoxide* is not efficient in generating high molecular weight polymer.[58] In contrast, ROP has more control over the microstructure, molecular weight and PDI of the polymer, especially through the coordination-insertion mechanism of ROP.[24b] Other mechanisms of ROP include lipase-catalyzed, cationic, anionic and organocatalytic mechanisms.[59]

Lipase-catalyzed polymerization emerged almost 20 years ago and in 1993, it was found to be feasible for ROP of lactones.[60] The mechanism for the lipase-catalyzed polymerization of lactones is thought to proceed *via* an acyl-enzyme intermediate (enzyme-activated monomer, EM).[61] The rate-determining step is the monomer activation by the enzyme to open the ring of the lactone to produce an acyl-enzyme intermediate (as shown as EM in Scheme 1.6). EM then reacts with nucleophiles such as water to yield ω-hydroxycarboxylic acid in the initiation step. In the propagation stage, the ω-hydroxycarboxylic acid acts as the growing polymer species by repeatedly attacking EM. Thus, the ω-hydroxycarboxylic acid incorporates one more unit of monomer after each attack.

Scheme 1.6 Mechanism for the lipase-catalyzed polymerization of lactones[61]

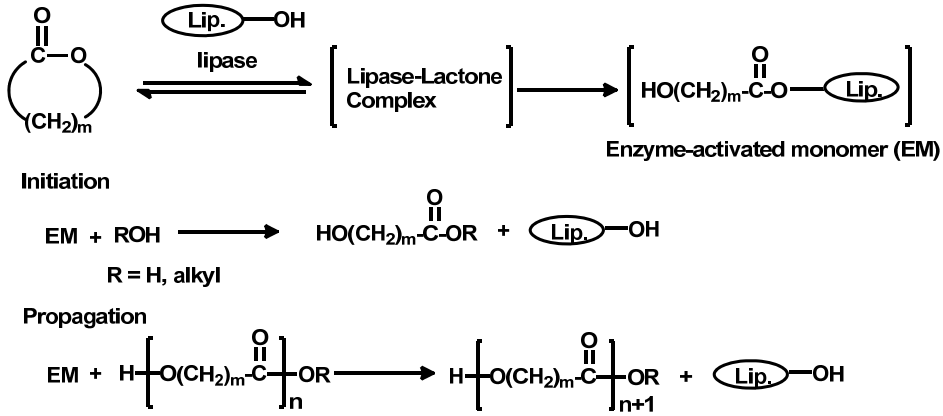

* The catalyst and condition used for copolymerization of propylene and CO are different from those in the carbonylation of epoxides. In the copolymerization, a simple base such as pyridine was used to assist in the electrophilic attack of the cobalt-bonded acyl carbon atom on the epoxide to grow the polymer chain.

Compared to other methods, lipase-catalyzed was characteristic in its monomer scope and functional group tolerance.[61b, 62] Large member ring lactones can be efficiently polymerized by lipases. Monomer scopes extend to macrolides, carbonates and phosphates. Lipase-catalyzed ROP can produce copolymers, such as poly(ester-*co*-carbonate)s, copolycarbonates and PEG-*b*-polyesters. The functionality tolerance allows initiating alcohols to contain alkenes, which can be further crosslinked. Macrolides carrying various biofunctional groups can also be polymerized.

The BBL depolymerase mentioned before can also polymerize lactones. It is active for smaller lactones, such as 4-membered β-propiolactone and 6-membered δ-valerolactone (VL). On the other hand, larger lactones like CL, 11-undecanolide were polymerized better by lipases.[62]

Lipase-catalyzed ROP can provide regio- and stereoselectivity as well, however, with very low molecular weights (less than thousands). Recent achievement includes the discovery of new enzymes and using green solvents such as water, ionic liquids and super critical carbon dioxide.[61b]

Examples for cationic ROP for lactones are not very common for several reasons. Cationic catalysts are usually very sensitive to moisture. Examples of cationic ROP for BBL are even more rare. In 1991, triethyloxonium hexafluorophosphate (**14**, Figure 1.6) was found to be able to initiate cationic ROP of CL even in the presence of alcohol.[63] BBL could be polymerized as well, with a lower activity compared to CL. Other cationic catalysts like zirconocene (**15**, Figure 1.6)[64], scandium trifluromethanesulfonate ($Sc(OTf)_3$) (**16**, Figure 1.6)[65], an N-heterocyclic carbene complex of silver (**17**, Figure 1.6)[66], hetero-scorpionate aluminum complexes (**18**, Figure 1.6)[67] have been used to polymerize CL and LA. Recently a zwitterionic ("inner salt") complex of yttrium (**19**, Figure 1.6) was found to be active for the amine-initiated immortal ROP of *rac*-LA, yielding heterotactic PLA (P_r = 0.93) with a fast rate.[68]

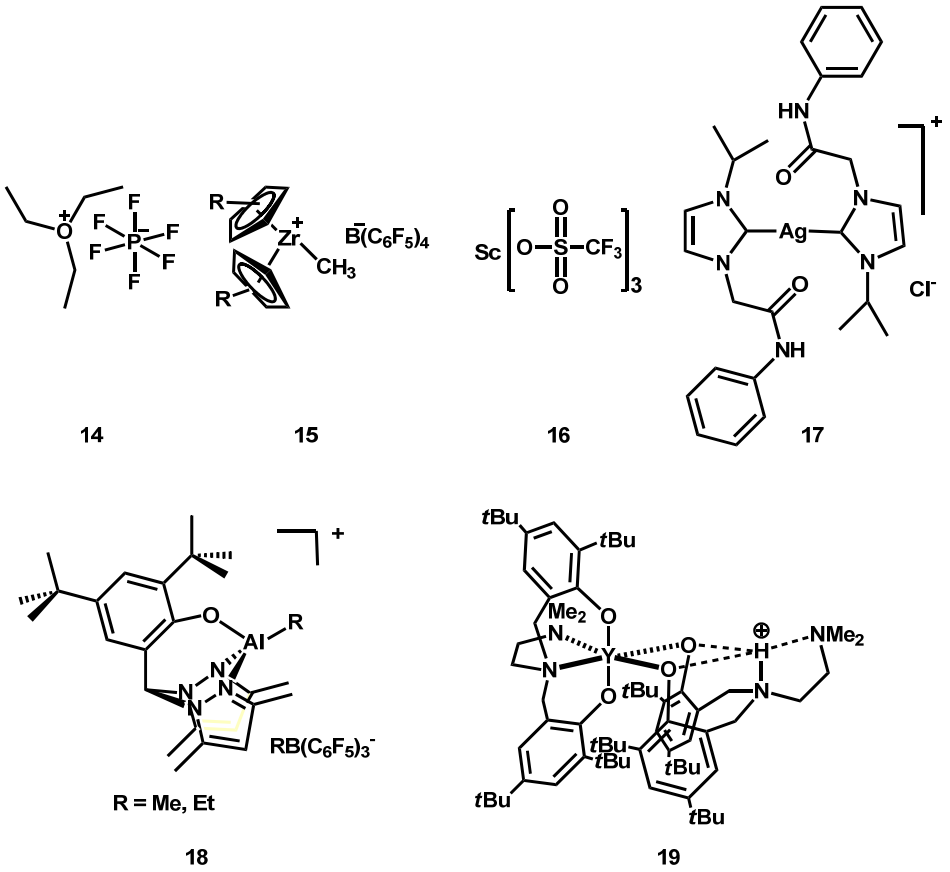

Figure 1.6 Selective catalysts for cationic ROP of cyclic esters

The cationic ROP proceeded through an activated monomer mechanism (**A**, Scheme 1.7), taking $Sc(OTf)_3$ catalyzed polymerization of CL.[65] First $Sc(OTf)_3$ activates the monomer by coordinating to CL, yielding the cationic complex **A**. The complex is attacked by nucleophiles like ROH to produce **B**. There are rapid equilibria between **B**, **C** and **D**. **D** can continuously attack complex **A** to grow the polymer chain.

Scheme 1.7 Proposed mechanism of the cationic ROP of CL by $Sc(OTf)_3$[65]

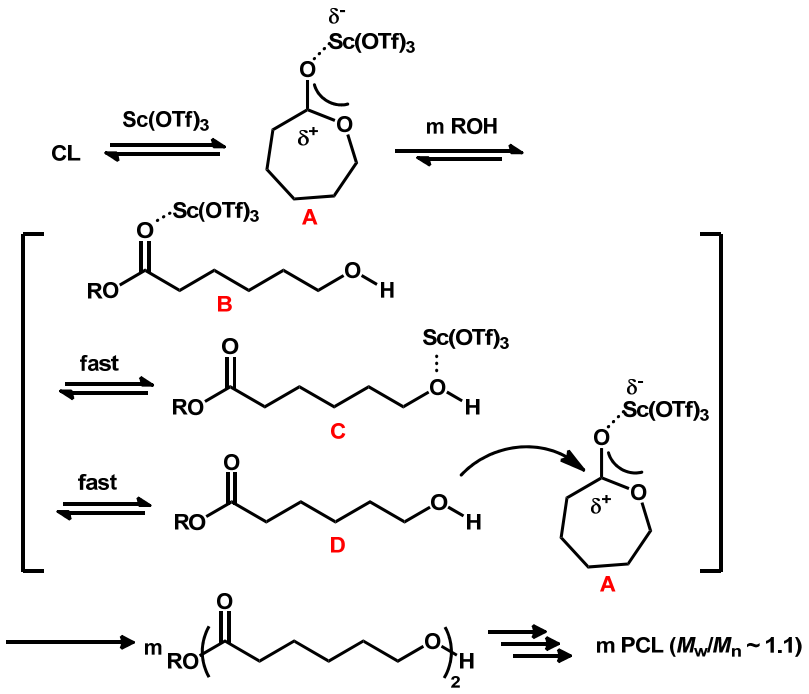

Unlike cationic ROP, anionic ROP of BBL has been widely studied, although only polymers with low molecular weights were obtained with low yields. Most of the anionic ROP catalysts were alkali metal compounds, such as hydrides[69], alkoxides or carboxylates complexed with crown ethers[70] and naphthalenides[71]. Other metal compounds have been used, such as aluminoxane[72]. Even metal-free systems, like ammonium carboxylate[70c], ammonium hydroxide[70c] and other novel examples[73] were developed.

Alkali metal hydrides polymerized BBL with low yields and low molecular weights. It was able to copolymerize BBL and CL with a higher yield, for CL was a preferred monomer.[69b] Reaction required a large amount of NaH, with the monomer to initiator ratio (M/I) less than 20, yielding copolymers of several thousand Dalton. The PDI was around 1.5.

In alkali metal alkoxide/crown ether or alkali metal carboxylate/crown ether systems, the crown ether activated the anion, enabling the polymerization of BBL. Carbon-oxygen cleavage and inversion of configuration occurred.[70b] Carboxylate salts were less sensitive to impurities than other anionic species; they were able to produce PHB with higher molecular

weights (170 kDa). Studies on the counterion and solvent effects on the anionic ROP of BBL by acetate salts showed that in the catalysts with a large counterion, more polar solvents such as dimethyl sulfoxide (DMSO) reduced the reaction rate.[74] However, when a small counterion was applied, the opposite tendency was observed. In a recent article, it was found that in polar aprotic solvents such as DMSO which could activate the anion by separating the ion pair, sodium carboxylate salts were able to polymerize BBL without a crown ether, although the reaction took a week to reach completion.[75]

Apart from ammonium catalysts, another novel metal-free catalytic system was created by adding either primary alcohols or carboxylic acids to 1 equivalent of a stable carbene (Figure 1.7).[73] The carbene was protonated by the alcohol or the acid and then worked as associated counterion. Well-defined high molecular weight PHB was synthesized with M_n up to 32 kDa and PDI ranging from 1.1 to 1.3. More interestingly MePEG attached with a carboxylic acid end group was able to act as a macroinitiator to produce block copolymers.

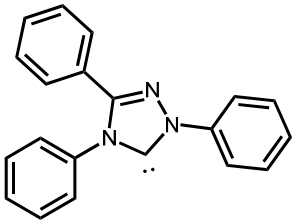

Figure 1.7 Structure of a stable carbene used to produce a metal-free initiator for anionic ROP

The mechanism of anionic ROP of BBL is shown using carboxylate and alcoholate catalysts as examples (Scheme 1.8).[73] With carboxylates, the β-carbon is attacked by the carboxylate anion to grow the chain exclusively through alkyl–oxygen cleavage. With alcoholates, however, acyl–oxygen cleavage also occurs to some extent. For example, in the alcohol and carbene system mentioned above, there was 36% acyl–O cleavage.[73]

Scheme 1.8 Mechanism of anionic ROP of BBL by carboxylate and alcoholate catalysts

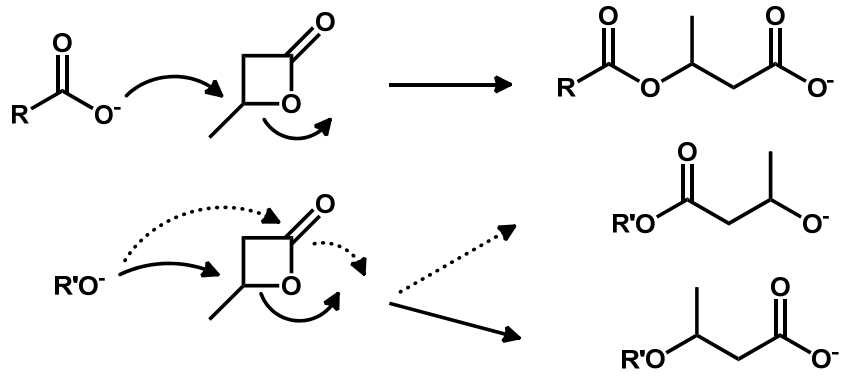

Anionic ROP usually utilizes non-toxic metals or even no metals. Therefore, the catalyst residue, which is hard to remove from the polymers, is not harmful to humans. This makes it an attractive way to produce PHB, especially for biomedical applications. However, apart from the main drawback of typically producing only low molecular weight polymers, anionic ROP also has problems such as chain transfer to the monomer and extensive back-biting.[59]

ROP through the coordination-insertion mechanism, compared to other ROP methods, works the best for BBL in regards to regulating the molecular weight, composition and microstructure. Therefore, many studies have been carried out to synthesize various metal-based initiators and study their activities towards coordination-insertion ROP of BBL. PHB chemically synthesized with various microstructures would be of more interest, considering naturally synthesized PHB is isotactic and brittle.

In the early 1990s, simple homoleptic metal complexes, such as tin(II) bis(2-ethylhexanoate), zinc(II) lactate and aluminium(III) isopropoxide ($AlO\textit{i}Pr_3$) were used for the ROP of cyclic esters.[76] They were easily obtained and robust in the polymerization reaction. $Sn(Oct)_2$ is used to polymerize PLA industrially. Compared to LA and CL, these catalysts are still not very active for the polymerization of BBL.[77]

It has been showed in the above sections that coordination-insertion ROP of LA involves the coordination of the monomer to the metal center and then the insertion of the monomer into

the metal-alkoxide initiating species. Studies on various catalysts in the coordination-insertion ROP of BBL also support this mechanism (Scheme 1.9).[78] BBL proceeds through acyl-oxygen bond cleavage to insert into the metal-alkoxide bond, forming a new metal-alkoxide species. This leads to retention of the configuration of the monomer, in contrast to anionic ROP (Scheme 1.10). The driving force of ROP is the ring strain release from cyclic esters.

Despite of the high ring strain of four-membered lactones (thermodynamic parameters for polymerization of β-propiolactone: ΔH_{polym} = −82.3 kJ·mol^{-1}, ΔS_{polym} = −74 J·mol^{-1}·K^{-1}; no data of BBL was available in the literature), BBL appears less reactive than other lactones like LA (ΔH_{polym} = −22.9 kJ·mol^{-1}, ΔS_{polym} = −25 J·mol·K^{-1}).[24a, 79] A range of side-reactions, such as transesterification and chain transfer, are more prone to occur in the ROP of BBL than of other six- or seven-membered lactones. Therefore, quite a large amount of studies on ROP of BBL showed slow rates and deficient control over molecular weights.

Scheme 1.9 Mechanism of coordination-insertion ROP of BBL polymerization

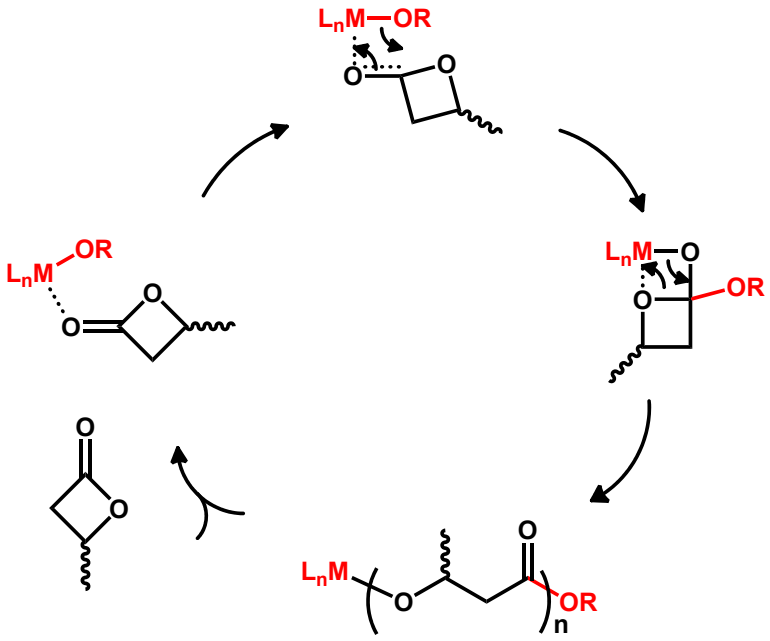

Scheme 1.10 Possible routes for the ROP of BBL using metal alkoxide catalysts: (a) coordination-insertion mechanism and (b) anionic mechanism

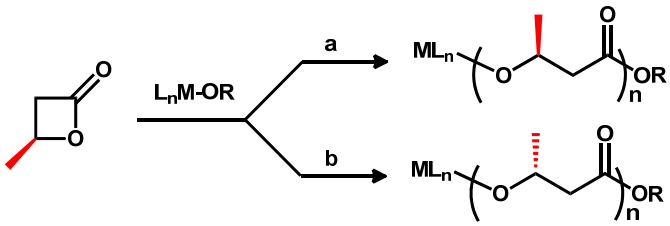

With the homoleptic catalysts mentioned above, polymerization was not very active, obtaining polymers with wide PDI, due to slower initiation compared to propagation and transesterification.[77] This led to the development of catalysts supported by various ancillary ligands. These well-defined heteroleptic metal complexes had higher activity and selectivity in the polymerization.

The tacticity in PHB can be determined from NMR, since the chemical shift of ^{13}C NMR resonances is sensitive to the PHB chain conformation due to shielding effects of the three-bond gauche interaction of the γ-carbons. Inverse gated $^{13}C\{^{1}H\}$ NMR is used to observe the tacticity of PHB. In the carbonyl region of PHB, the upfield (~169.0 ppm) and downfield (~169.1 ppm) signals in the carbonyl region correspond to the meso (*m*) diad sequences, *i.e. R–R* and *S–S*, and the racemic (*r*) diad sequences, *i.e. R–S* and *S–R*, respectively. The methylene region (40.7–40.9 ppm) shows triad sensitivity.[54, 78b] Therefore, P_m and P_r can be determined by calculating the ratio of the integration of *m* diad sequences in the carbonyl region of the ^{13}C NMR spectrum to the total integration of the carbonyl region.

Not many catalysts possessing both high activity and isoselectivity towards ROP of BBL were reported. In 2008, Rieger *et al.* reported highly active chromium(III) salophen complexes **20** (Figure 1.8), which were able to polymerize *rac*-BBL to PHB with high molecular weight (780 kDa) and isotacticities of 60–70%.[80] The reaction was carried out in neat monomer, which might be the reason for the unexpected high molecular weight (780 kDa, with only 1000 equivalents of BBL) and high PDI (7–9). Aryl substituents on the

salophen framework exerted an influence on the catalyst performance, indicating better catalyst design can be achieved by substituent modification.

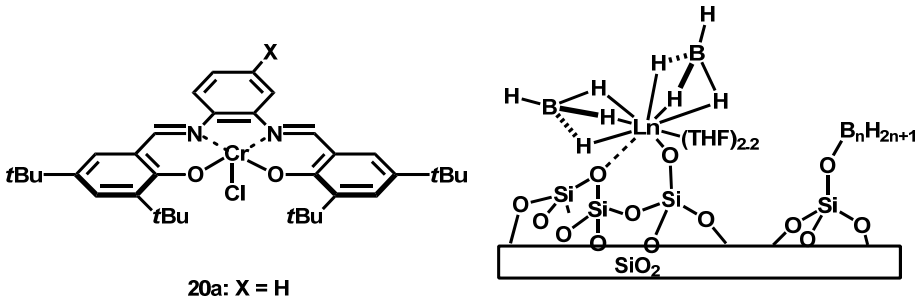

Figure 1.8 Selective stereoselective systems for the isotactic ROP of *rac*-BBL

Another special isoselective example was reported by Thomas *et al.* in 2010 that grafting of $[Ln(BH_4)_3(THF)_3]$ (Ln = La, Nd) onto silica afforded materials containing well-characterized bis(borohydride) surface species (**21**, Figure 1.8).[81] The neodymium-decorated silica was able to convert *rac*-BBL into highly isotactic PHB (P_m = 0.85). The grafted system was easy to make and time-saving. This heterogeneous catalyst was special, for under similar conditions, the molecular precursor only gave rise to an atactic polymer. However, it was not very active, with 200 equivalents of BBL reaching only 75% conversion after 24 h, though the PDI was low (PDI = 1.18).

There are more systems with syndiotactic selectivity during coordination-insertion ROP of *rac*-BBL. In 1993, Gross *et al.* documented the ability of tributyltin methoxide, $SnBu_3OCH_3$, to catalyze the ROP of *rac*-BBL, with P_r from 0.6 to 0.7.[82] Later, $(n\text{-}Bu_3Sn)_2O$, $(Ph_3Sn)_2O$, and $Sn(n\text{-}Bu)_2(OCH_3)_2$ were also reported.[83] However, the molecular weights obtained were extremely low (2.5 to 5.3 kDa, 84 kDa respectively). In the same year, Hori *et al.* found that polymerization of *rac*-BBL by distannoxane complexes **22** (Figure 1.9) gave predominantly syndiotactic PHB.[84] Other tin compounds like dialkyltin oxides, Bu_2SnO and Et_2SnO, were also reported to be active for syndioselective ROP of BBL was well (P_r up to 72%).[85]

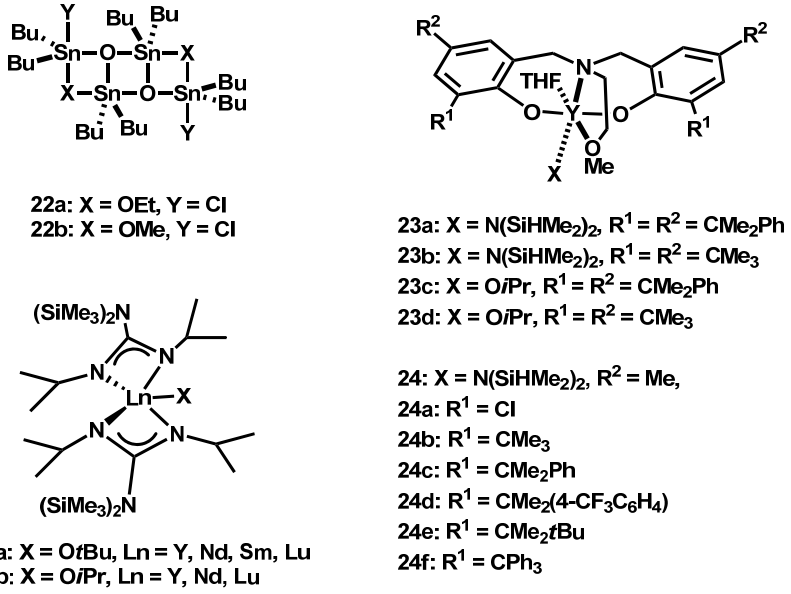

Figure 1.9 Selective stereoselective system for the syndiotactic ROP of *rac*-BBL

A system with both considerably high activity and syndioselectivity towards ROP of BBL was based on well-defined single-site bis(phenolate) complexes of Group 3 metal (**23**, Figure 1.9), able to generate highly syndiotactic PHB (P_r up to 0.94).[78b] It has been mentioned earlier that these catalysts (**9**, Figure 1.4) were highly active initiators in the synthesis of heterotactic and syndiotactic PLA from *rac*-LA and *meso*-LA, respectively.[39] Catalyst **23c** and **23d** were very active for the ROP of BBL, especially in toluene and benzene. With [BBL] = 2.44 M, 200 equivalents BBL could be converted 97% in 1 minute at room temperature. When equivalents of BBL used were below 1000, the resultant polymers had narrow molecular weight distributions and experimental M_n values close to the theoretical values. The highly order in the microstructure of the synthesized PHB led to a melting temperature up to 183 °C, even higher than that of pure isotactic PHB (*ca.* 180 °C).[86] Later, lanthanide alkoxide complexes supported by bis(guanidinate) (**25**, Figure 1.9) was also found to have syndioselectivity.[87]

The steric and electronic effects of complexes **23** on the ROP of LA and BBL were studied.[88] A series of these yttrium complexes with different substituents on the ortho position of the aryl ring were synthesized (denoted as **24**, Figure 1.9) and polymerization with them were carried out. For the polymerization of *rac*-LA, bulkier ortho substituents on the phenolate

rings resulted in higher heterotacticities, regardless of their electronic effect: **24a** (P_r = 0.56) << **24b** (P_r = 0.80) << **24c** (P_r = 0.90) < **24d** (P_r = 0.93–0.94) ≤ **24e** (P_r = 0.94–0.95) ≤ **24f** (P_r = 0.95–0.96). On the other hand, for the polymerization of *rac*-BBL, only ligands bearing a phenyl group in the ortho substituents led to higher syndiotacticities, indicating the existence of electronic interactions: **24a** (P_r = 0.42–0.45) << **24e** (P_r = 0.62–0.70) < **24b** (P_r = 0.80) ≤ **24d** (P_r = 0.82–0.84) < **24c** (P_r = 0.89) < **24f** (P_r = 0.94). DFT computations based on model intermediates agreed with these hypotheses. There was a C–H···π interaction between a methylene C–H of the ring-opened BBL unit and the π system of one of the ortho-aryl substituents of the ligand, which stabilized some intermediates; by contrast, such interaction was not observed for the methyl group of lactate.

Recently, similar syndiospecific yttrium complex was applied to synthesize alternating copolymers *via* ROP of enantiopure functionalized β-lactone monomers, made by the aforementioned carbonylation of epoxides.[89] The syndiospecific catalyst was used to polymerize β-lactone monomers with different configurations and functional side-chains (Scheme 1.11). In this way, alternating copolymers of BBL analogues were made.

Scheme 1.11 Alternating copolymer of BBL analogues synthesized by a syndiospecific catalyst

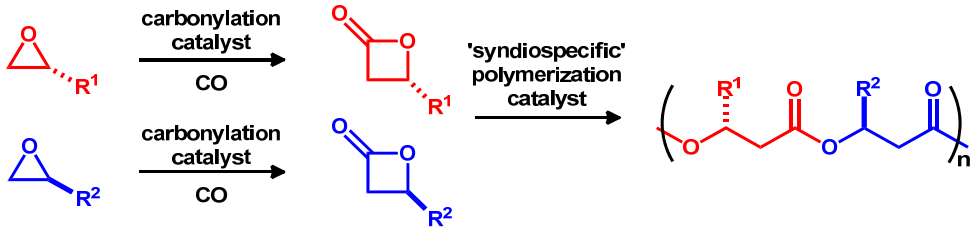

The single-site β-diiminate (BDI) zinc catalysts **6** (Figure 1.4), previously reported by Coates *et al.* to be highly active and stereoselective for the ROP of lactide (P_r = 0.94)[34], was found to be able to polymerize BBL rapidly under mild conditions, however, without stereoselectivity.[78a] With 200 equivalents of BBL, M_n was proportional to conversion throughout the reaction. PDI was narrow, supporting a living polymerization. High molecular

weight PHB (M_n > 100 kDa) could be achieved as well, although only atactic PHB was obtained.

1.8 Immortal ring-opening polymerization of cyclic esters

Many systems for ring-opening polymerization of cyclic esters mentioned above can conduct the polymerization in a living way. In living polymerization, the initiation rate is much faster than the propagation, allowing all the chains to grow at the same time with a same rate. No termination and irreversible transfer exist.[90] The amount of polymer chains equals the amount of active sites on the initiators. *i.e.* the amount of initiators for single-site catalysts. The catalytic productivity in living polymerization is low, since to grow each polymer chain needs one molecule of catalyst. In consequence, the contamination of the polymers from catalyst residues is considerably large. Nevertheless, immortal ring-opening polymerization can overcome these limitations.[91]

Immortal polymerization, as defined by the discoverer Inoue, "is the polymerization that gives polymers with a narrow molecular distribution, even in the presence of a chain transfer reaction, because of its reversibility, which leads to the revival of the polymers once dead, that is, the immortal nature of the polymers".[92]

Scheme 1.12 Chain transfer in iROP

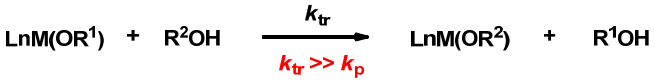

In immortal ROP, a catalyst/chain transfer agent binary system allows reversible chain transfer reaction during polymerization. The growing chain is transferred between the alkoxide species at a speed much faster than the propagation rate (Scheme 1.12), thus making the polymerization immortal. With one molecule of metal complex, multiple polymer chains can grow. Therefore, lower catalyst loading is needed through iROP. By utilizing

functionalized chain transfer agent (CTA) immortal ROP also provides easy access to end-functionalized polymers.

Immortal ROP was first discovered by Inoue *et al.* in 1985, when they found that in the polymerization of epoxides by aluminum porphyrin, (tetrapheny1porphinato)aluminum chloride (TPPAlCl) (**26**, Figure 1.10), adding alcohol did not terminate the polymerization.[93] Instead, polymers with a narrow molecular weight distribution were produced. Their M_n corresponded well with the ratio of monomer to the amount of alcohol plus initiator. These facts indicated a fast exchange between TPPAlOR and alcohol, thus indicating the immortal nature of the polymerization. The TPPAlCl system was even tolerant to other protic compounds, such hydrochloric acid, carboxylic acid and water.[94] Later, other metals such as zinc coordinated by porphyrin were also used for immortal polymerization.[95] Several studies about the metalloporphyrin system showed that visible light, substitution on the phenyl ring and bulky Lewis acids were favorable for the polymerization, resulting in a monomer loading capacity of up to 20000 equivalents.[95-96]

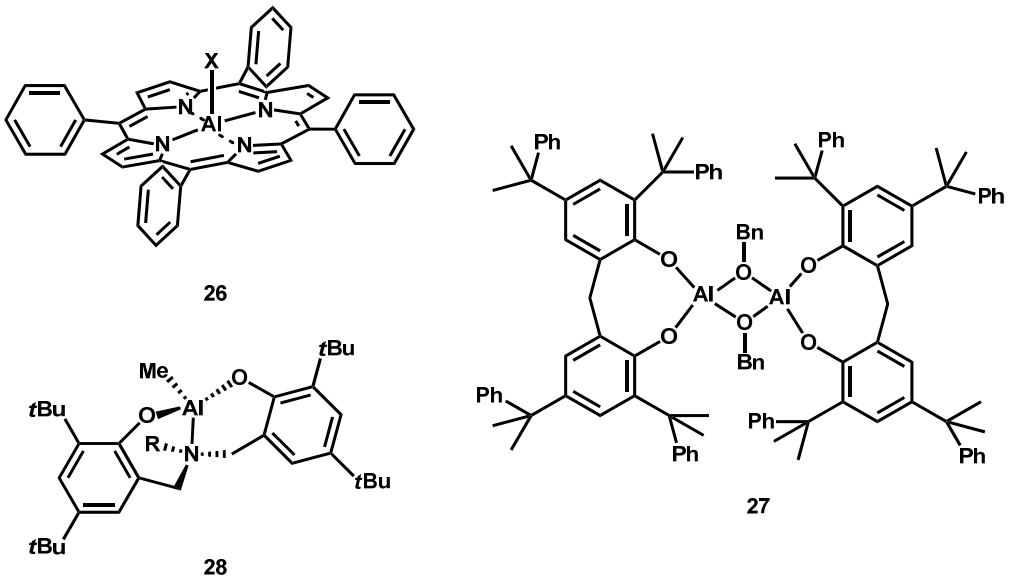

Figure 1.10 Selective catalysts for iROP of cyclic esters

Aluminum complexes based on other ligands, such as thiolates and phenolates, were used to perform iROP of caprolactone and lactide. For example, bulky bidentate phenolate aluminum complexes bridged by a benzyl alkoxide (**27**, Figure 1.10) and aluminum complexes bearing

dianionic amine bis(phenolate) ligands (**28**, Figure 1.10) were found to be able to yield polymers with low PDI at a high loading of alcohol.[96b, 97] Complexes for iROP based on other metals were also discovered, like Zn[97] and group 3 metals[68, 98].

The choice of CTA can introduce special architectures and functionalities to the polymers. For example, a star-shaped alcohol triethanolamine was used work as a CTA during the ROP of *rac*-LA, resulting in a star-shaped PLA.[98c] The reaction was catalyzed by an yttrium alkyl complex bearing an O,N,N,O-tetradentate salan ligand. Carpentier *et al.* used functionalized alcohols as CTA to synthesized end-functionalized PLA.[97] These functionalized PLAs were used as macroinitiators in the controlled nitroxide-mediated polymerization of styrene, resulting in PLA-*b*-poly(styrene).

Most of the reported examples are for the iROP of LA and CL. In contrast to these systems, there are only a few examples of iROP of BBL. As has mentioned above, side reaction is easier to occur during the polymerization of BBL. Therefore, it's possible that the high criteria of the robustness and activity of the catalyst restricts the number of catalysts successful in iROP of BBL with high loading CTA.

Several of the catalysts active in the ROP of LA and BBL mentioned in the above sections were also found to be active in immortal ROP of BBL. The amino-alkoxy-bis(phenolate) yttrium complexes (**23**, Figure 1.9) reported by Carpentier *et al.* can stereoselectively polymerize *rac*-LA and *rac*-BBL in the presence of an alcohol.[99] Up to 50 equivalents of alcohol can be added to the polymerization of *rac*-LA. 800 equivalents of *rac*-BBL was converted within 5 min with 3 equivalents of *i*PrOH ([**23a**] = 0.0038mmol/mL, M_n = 21.9 kDa, PDI = 1.17).

The lanthanide alkoxide complex supported by bis(guanidinate) (**25**, Figure 1.9) was capable of iROP with 2000 equivalents of *rac*-LA in the presence of 50 equivalents of *i*PrOH.[87] It took 26 h to reach 70% conversion at 20 °C in toluene ([**25**] = 0.0005 mmol/mL, M_n = 6 kDa, PDI = 1.14). If no alcohol was added, PDI range was wide, from 1.12 to 1.77. These

complexes were able to polymerize BBL stereoselectively, with P_r around 0.8. Reactions were all done at 20 °C, requiring several hours (M_n = 2.5–28.2 kDa, PDI = 1.09–1.48, [**25**] = 0.03 mmol/L) to reach completion.

The Coates' zinc BDI complex discovered in 2002[78a] was recently slightly modified by Carpentier *et al.* to apply iROP to BBL with as many as 50 equivalents of alcohol (M_n = 1.5 kDa, PDI = 1.12) (Scheme 1.13).[100] It was shown that the zinc complex/iPrOH binary system could perform the bulk polymerization of *rac*-BBL. However, long heating time (up to 20 h) was needed, and not much detail of the resulting polymers was provided.

Scheme 1.13 Immortal ROP of *rac*-BBL with a BDI zinc catalyst

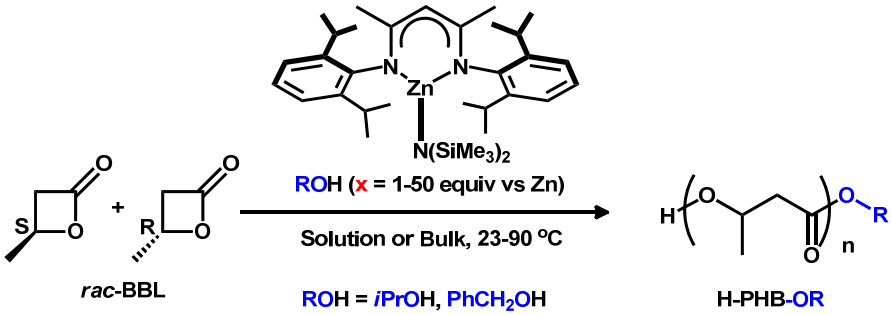

Until recently, iROP with alkaline metal complexes was thought to be very unlikely, as these metals are quite oxophilic and therefore active towards alcohol. However, in 2009, Carpentier *et al.* found that mono anionic complexes of Mg, Ca and Zn supported by a bulky bis(morpholinomethyl)phenoxy ligand were able to perform large-scale ROP of L-LA in the presence of large amounts of alcohol.[101] The zinc complex was able to convert up to 50000 equivalents of L-LA in the presence of up to 1000 equivalents of *i*PrOH (M_n = 2.4–13.5 kDa, PDI = 1.16–1.60). Preliminary studies of iROP of BBL with this catalyst also showed activity. 500 equivalents of BBL was converted at 60 °C within 3 h with 10 equivalents *i*PrOH present (M_n = 4.3 kDa, PDI = 1.07). Later, zinc and magnesium supported by various multidentate amino-ether phenolate ligands possessing comparable catalyst activity were also discovered.[102]

In all these examples, in regards to making equal amounts of polymers with the same molecular weight, lower catalysts loading is needed for immortal ROP than in regular ROP. Thus, the real catalytic role of the complexes is realized through this way, with well-defined polymers provided.

1.9 Block copolymer containing poly(ethylene glycol) and polyesters segments

In immortal ROP, the choice of chain transfer agents can introduce special architectures and functionalities to the polymers. Specially, when a macromolecule is used as a CTA, block copolymers can be synthesized in one step. Copolymerization is an effective way to modify the properties of polymeric materials. In particular, block copolymerization of two dissimilar monomers would provide an attractive method to combine their properties. Since pure atactic PHB has low crystallinity and a large creep behavior, BBL has been copolymerized with various other monomers.[103]

Poly(ethylene glycol) (PEG), also known as poly(ethylene oxide) (PEO), is a hydrophilic and biocompatible material which can be attached to polyesters, thus forming amphiphilic copolymers. These copolymers can self-assemble into nanoparticles of different shapes, which are widely used in drug delivery systems.[103a, 104] Since Perret *et al.* first prepared block copolymers consisting of PEG and PCL by anionic polymerization using a naphthalene-sodium catalyst, there have been many examples of block copolymers of lactide and caprolactone with ethylene glycol.[42, 103-105] ROP, anionic polymerization and polycondensation were all used to form these polymers.

There have been numerous studies on the synthesis and properties investigation of block copolymers of LA and ethylene glycol. For example, Du *et al.* synthesized diblock PLA_x-PEG_{44} (subscripts represent the numbers of the monomeric units in the blocks) block copolymers through ROP in the presence of MePEG 2000.[104b] They found that PLA_{212}-PEG_{44}

was able to form vesicles, the fluctuation of whose membrane further caused various differently shaped vesicles in solution.

Block copolymers of BBL and ethylene glycol has been made *via* transesterification by PEG during fermentation[105b, c], condensation[104a, 105d, 105g], click chemistry[105i], anionic ROP of BBL with PEG macroinitiator[105h], and ROP of BBL in the presence of PEG[103a].

Transesterification is a fast process to make diblock copolymers. Several transition metal complexes are capable of catalyzing transesterification. Block copolymers of PLA and PEG can be synthesized this way. Marchessault *et al.* used catalyzed transesterification to synthesize diblock copolymers of PHB and MePEG in a one-step process.[105c] In the melt, bacterial PHB was depolymerized and then copolymerized with $Sn(Oct)_2$ catalyst. The resulting copolymer has a low PDI, which the authors speculated was due to the low PDI of PEG and dialysis purification. PHB-*b*-PEG was then found to form nanoparticles in different shapes, such as rods, lamellae clusters and core-shell particles.[105e] Ashby *et al.* added PEG oligomers to the fermentation medium of bacteria to get diblock copolymers of PEG and PHB.[105b] PEG was able to perform chain termination through esterification, thus lowering the molecular weight of PHB.

Condensation is a versatile way to design the block structure of these copolymers; however, it requires modification of the monomer or prepolymerization before condensation. Li *et al.* first synthesized PEO-PHB-PEO triblock copolymers by coupling a low molecular weight telechelic hydroxylated PHB chain to two chains of methoxy-PEO-monocarboxylic acid (MePEO-A) (Scheme 1.14).[105d] First PHB diol was made through transesterification of high molecular weight PHB with ethylene glycol. Then the diol underwent esterification with MePEO-A in the presence of dicyclohexylcarbodiimide (DCC) and 4-dimethylaminopyridine (DMAP) to yield block copolymers. The PHB diol had a PDI of 1.46, but the final copolymers had quite narrow molecular weight distribution after isolation and purification through repeated precipitation and fractionation, although only low molecular weight copolymers were obtained.

Scheme 1.14 Synthesis of PEO-PHB-PEO triblock copolymers by Li *et al.*

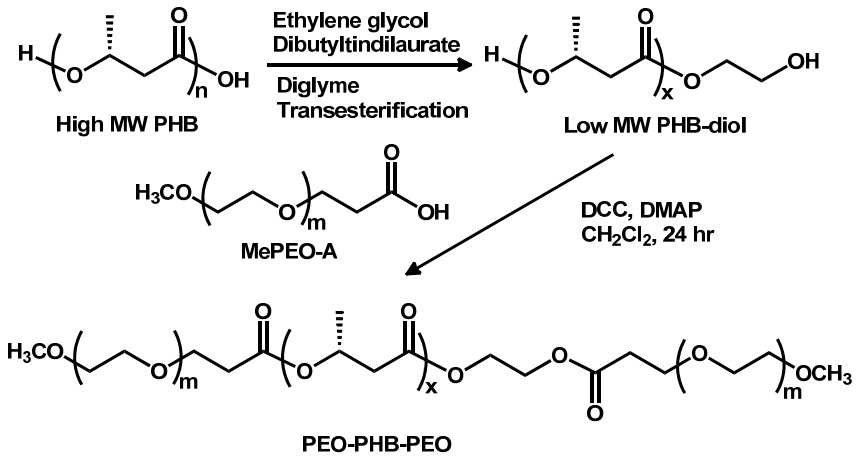

A similar method was later applied to prepare PHB-*alt*-PEG multiblock copolymers.[104a] By coupling PHB-diol and PEG with hexamethylene diisocyanate (HDI), poly(PHB/PEG urethane) was synthesized (Scheme 1.15).[105g] However, this method is not able to control the PHB block or the sequence of PEG and PHB in the polymer.

Scheme 1.15 Synthesis of poly(PHB/PEG urethane)

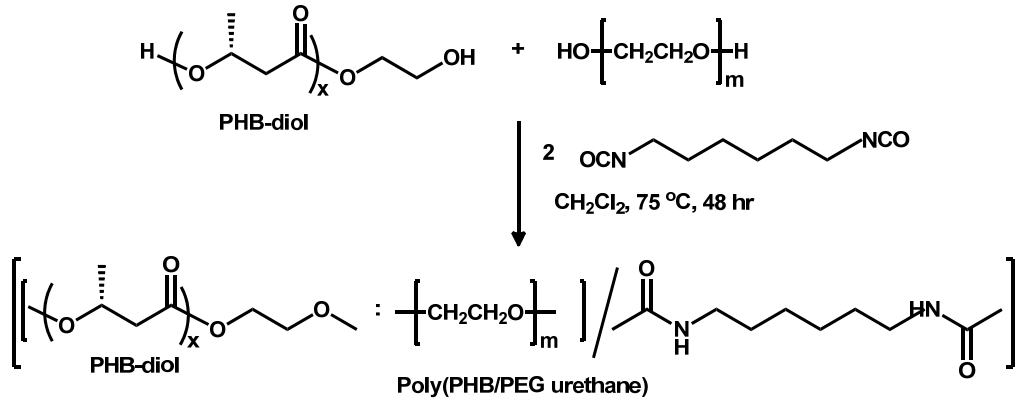

Renard *et al.* synthesized diblock copolymers using click chemistry.[105i] PHA oligomers were obtained through thermal treatment (Scheme 1.16) and then tailored to incorporate a propargylamine end group. Then the click reaction between the modified PHA and an azide-terminated PEG (MW = 5000 g/mol) with a copper catalyst. Though click chemistry is

a versatile way to synthesize well-defined polymers, it is a slow process, as it requires several steps to modify the end groups of both blocks. Also, all these reactions require a considerable amount of heating, reagents and time.

Scheme 1.16 Synthesis PHA-PEG diblock copolymer through click chemistry

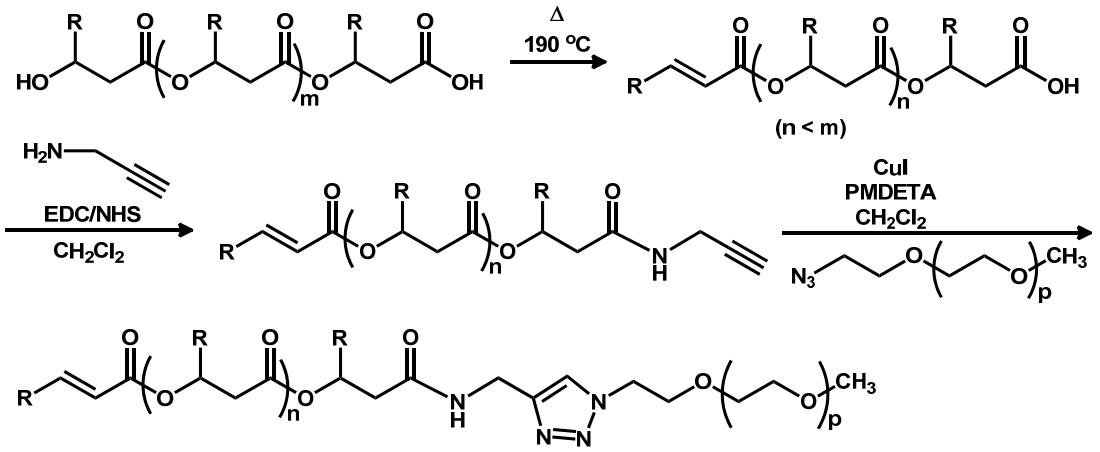

Anionic ROP of BBL with PEG as a macroinitiator is another way to produce block copolymers. PHB-*b*-PEG-*b*-PHB triblock copolymers by ROP of BBL using PEG macroinitiators was reported by Li *et al.* in 2008 (Scheme 1.17).[105h] The PEG macroinitiator $PEG(CO_2Na)_2$, prepared *via* TEMPO-mediated oxidation, was used to initiate anionic ROP of *rac*-BBL by attacking the methine carbon and breaking the alkyl-oxygen bond on the monomer. The polymers possessed the expected molecular weight and a low PDI (~1.1) but the molecular weights were below 10 kDa. In some cases, small portion of higher molecular weight polymers was observed.

Scheme 1.17 Synthesis of PHB-PEG-PHB triblock copolymers using by Li *et al.* in 2008

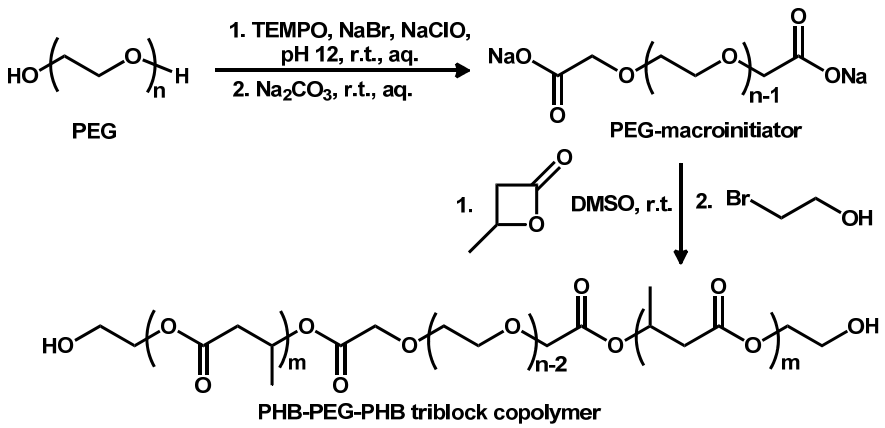

ROP of BBL in the presence of PEG is the only one-step way in which well-defined block copolymers can be made. Chen *et al.* synthesized PHB-*b*-PEG-*b*-PHB triblock copolymers directly by ROP of BBL in the presence of PEG using stannous octanoate.[103a] The resulting polymers could assemble into nanoparticles with a core-shell structure, and the critical micelle concentration values were decreased compared to ABA* style triblocks. However, very little details about the chemistry of these polymers were reported.

To our knowledge there are no reports on the immortal ROP of BBL with PEG. Immortal ROP with PEG as a CTA is a true one-step reaction, and requires much less catalysts. It can proceed under mild conditions, without heating or additional reagents, which may contaminate the resulting polymers. Also, in this way well defined block copolymers can be obtained.

1.10 General chemistry of indium and group 13

Group 13 elements have an electron configuration of ns^2np^1 in their outer shell. They can form compounds in which their oxidation state is +3. Usually these compounds are electron

* Usually, in amphiphilic block polymers, A is used to denote the hydrophilic block and B is used to denote the hydrophobic block.

deficient and work as Lewis acids. The properties of group 13 elements change considerably moving from boron to thallium, making this group versatile in many different applications. Aluminum is a widely used metal for catalysis, especially in polymerization. For example, Ziegler-Natta catalysts for the stereoselective polymerization of α-olefins, with $TiCl_3$-AlR_3 catalysts as the first generation, have been used in the commercial manufacture of various polymeric materials since 1956. Numerous aluminum based complexes, as discussed in the above sections, are capable of the ROP of cyclic esters.[31, 106]

Indium remains a less explored metal in catalysis, but it is gaining more and more interest for its desirable properties, such as its low first ionization potential, lack of toxicity and relative robustness towards moisture and oxygen. For example, indium complexes were found to be able to perform Barbier-Type reactions in aqueous conditions.[107]

There are only few examples utilizing indium complexes for the polymerization of cyclic esters. In 2006, Huang *et al.* reported an indium catalyst **29** (Figure 1.11), which showed moderate catalytic activity toward the ring-opening polymerization of ε-caprolactone.[108] Inspired by this work and the chiral dinuclear indium catalyst reported previously by our group (see below)[109], Hillmyer and Tolman *et al.* reported a simple and robust catalyst system prepared *in situ* from indium trichloride ($InCl_3$), benzyl alcohol (BnOH) and triethylamine (NEt_3), without the addition of any multidentate ligands.[37] This time-saving system was able to afford highly heterotactic (P_r from 0.86 to 0.97) PLA with narrow PDI and controlled molecular weights in good yields.

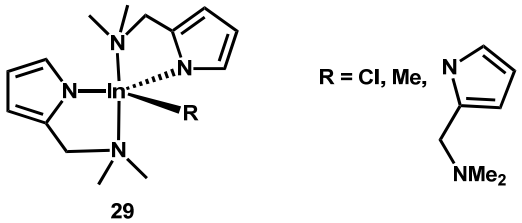

29

Figure 1.11 Indium catalysts for ROP of ε-caprolactone by Huang *et al*. in 2006

The polymerization kinetics of this interesting indium system was studied and showed the

process was first-order in $[InCl_3]_0$ and zero-order in both $[BnOH]_0$ and $[NEt_3]_0$. The rate of *rac*-LA conversion differed with different indium(III) halides (*i.e.*, $t_{1/2}(InCl_3) \approx 43$ min versus $t_{1/2}(InBr_3) \approx 7.5$ h, 21 °C, CD_2Cl_2, $[rac\text{-LA}]_0/[BnOH]_0 \approx 100$, $[rac\text{-LA}]_0 = 0.84$ M, $[InX_3]_0/[BnOH]_0 = 1$) and lactide stereoisomers (*i.e.*, $k_{obs}^{rac\text{-LA}} \approx k_{obs}^{meso\text{-LA}} > k_{obs}^{L\text{-LA}}$). A postulated mechanism is shown in Scheme 1.18. The polymerization goes through a coordination-insertion mechanism with $[InCl_{(3-n)}(OR)_n]_m$ as the propagating species (drawn as a dinuclear complex in Scheme 1.18, with R_3NH^+ as the counterion). Lactide monomer coordinates to the indium center with carbonyl oxygen. Then the nucleophilic LA carbonyl carbon is attacked by the alkoxide (step **i**), resulting in the insertion of LA into indiumalkoxide bond *via* cleavage of the acyl–oxygen bond (step **ii**). The rate and stereocontrol might be determined by the energy differences resulting from a combination of steric and electronic effects created by the halide(s) and multiple stereocenters of the growing polymer chain end.[110]

Scheme 1.18 Postulated Mechanism for LA Polymerization by $InCl_3$/BnOH/NEt_3 system

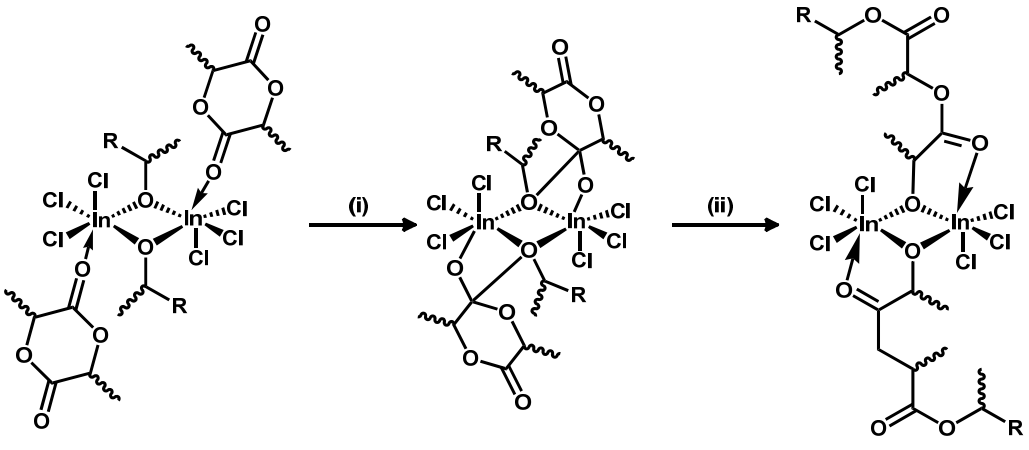

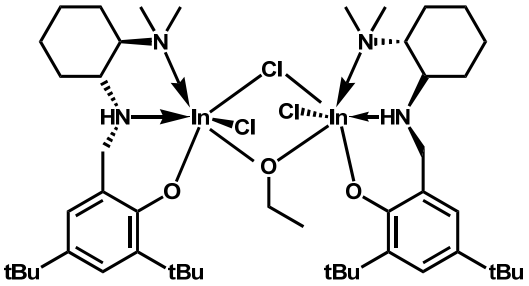

30

Figure 1.12 Structure of a chiral indium catalyst by Mehrkhodavandi *et al.*

In 2008, our group reported a chiral indium catalyst $[(NNO)InCl]_2(\mu\text{-}Cl)(\mu\text{-}OEt)$ **30** (Figure 1.12) which was shown to be a very active, living system for the polymerization of lactide.[109] With 200 equivalents of lactide, over 90% conversion was reached in 30 min, at 25 °C in CH_2Cl_2. Sequential addition of two 100 equivalents aliquots of LA to the polymerization solution showed the polymerization rate was unchanged after the second addition of LA. A more recent study involved the synthesis of a series of the alkoxy-bridged dinuclear indium complexes bearing bulky diaminoaryloxy ligands $[(NNO_R)InX]_2(\mu\text{-}Z)(\mu\text{-}OEt)$.[111] The dinuclear structures in solution were observed in the study of both mono- and bis-alkoxy-bridged complexes *via* 2D nuclear Overhauser enhancement spectroscopy (NOESY). Mechanistic investigations indicated that the complexes remained dinuclear during polymerization.

1.11 *In situ* monitoring of polymerization and characterizations of polymers

In the course of this project there is a need to monitor polymerization *in situ* as well as to characterize polymers and copolymers once they are formed.

In kinetic experiments, if the polymerization is first order with respect to the monomer, the integrated rate law can be derived as shown:

$$-\frac{\mathrm{d}[M]}{\mathrm{d}t} = k_{\mathrm{obs}} \times [M] \tag{1.1}$$

$$\int_{[M]_0}^{[M]_t} -\frac{\mathrm{d}[M]}{[M]} = \int_{t=0}^{t=t} k_{\mathrm{obs}} \mathrm{d}t \tag{1.2}$$

$$\ln \frac{[M]_0}{[M]} = k_{\mathrm{obs}} \times t \tag{1.3}$$

In situ NMR spectroscopy is used to obtain kinetic data for the polymerizations at different temperatures and also with different concentrations of catalyst. Monomer (*M*) concentration during the polymerization process can be monitored by integrating the methine proton for LA and

BBL. By plotting ln[*M*] against time, if a linear relationship is obtained, the hypothesis that the polymerization is first order with respect to the monomer concentration is confirmed. The negative of the slope equals the observed rate constant (k_{obs}). Therefore, by kinetic monitoring, k_{obs} can be measured which is helpful to postulate the mechanism.

1,3,5-trimethoxybenzene (TMB) is used as an internal standard to calibrate the integrations of all spectra, since it is inert in the polymerization media and has distinct chemical shifts corresponding to the methoxy and the arene protons at 3.77 and 6.09 ppm (CD_2Cl_2) respectively (Figure 1.13).

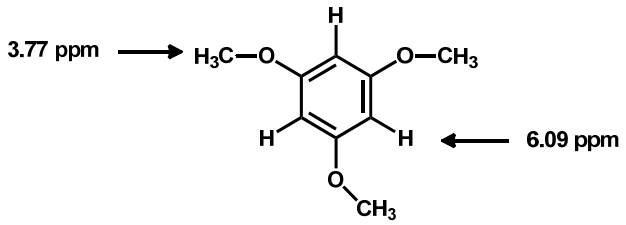

Figure 1.13 Internal standard (1,3,5-trimethoxybenzene) for the polymerization of LA and BBL and its ^{1}H NMR characteristics (CD_2Cl_2, 298 K, 400 MHz)

The Eyring equation represents the relationship between reaction rate constant, temperature and the free energy change in the transition state:

$$\ln\frac{k}{T} = -\frac{\Delta H^{\neq}}{R}\times\frac{1}{T} + \ln\frac{k_b}{h} + \frac{\Delta S^{\neq}}{R} \qquad (1.4)$$

To obtain the thermodynamic parameters, enthalpy ($\Delta H^{\neq}$) and entropy ($\Delta S^{\neq}$) of activation, the rates of polymerization at different temperatures are obtained using *in situ* NMR spectroscopy. Then the natural logarithm of the observed rate over temperature is plotted against the inverse of the temperature. $\Delta H^{\neq}$ and $\Delta S^{\neq}$ during polymerization can be calculated from the slope and the *y*-intercept of the line. The temperatures of the NMR monitoring experiments are calibrated using the reagents and formulae in Table 1.3.

Table 1.3 Formulae for calibrating temperatures

Standard	Temperature	Formula
4% MeOH in MeOH-d_4	270–300 K	$(4.109-\Delta\delta)/0.008708^a$
80% Ethylene Glycol in DMSO-d_6	300–400 K	$(4.218-\Delta\delta)/0.009132^b$

[a]$\Delta\delta$ is the shift difference (ppm) between CH_3 and OH peaks of MeOH. [b]$\Delta\delta$ is the shift difference (ppm) between CH_2 and OH peaks of ethylene glycol.

A polymer sample is a mixture of chains of different lengths. The molecular weight has a strong influence on physical properties of the materials, such as viscosity and tensile strength. Several numbers are used to reflect the distribution of the molecular weight of polymers.[1] The number average molecular weight is:

$$M_n = \frac{\sum M_i N_i}{\sum N_i} = \frac{\sum W_i}{\sum N_i} \tag{1.5}$$

Where:

M_i = Molecular weight of chains in fraction i

N_i = Number of chains in fraction i

W_i = Weight of chains in fraction i

Similarly, the weight number average weight and z average molecular weight are:

$$M_w = \frac{\sum M_i^2 N_i}{\sum M_i N_i} = \frac{\sum M_i W_i}{\sum W_i} \tag{1.6}$$

$$M_z = \frac{\sum M_i^3 N_i}{\sum M_i^2 N_i} = \frac{\sum M_i^2 W_i}{\sum M_i W_i} \tag{1.7}$$

The molecular weight distribution is indicated by the polydispersity index (PDI):

$$\mathrm{PDI} = \frac{M_\mathrm{w}}{M_\mathrm{n}} \tag{1.8}$$

The PDI, which is larger than 1, indicates how uniform the molecular weights of the chains in the polymer are. A PDI close to 1, *i.e.* a low PDI, indicates the molecular weight distribution in the polymer chains is narrow. Living polymerization can provide polymers with PDI close to 1.

Gel permeation chromatography (GPC) is the most commonly used method to determine molecular weights of polymers. When a polymer solution passes through the GPC column, which is packed with crosslinked polymer microspheres to have pores of various sizes on the surfaces, polymers of different sizes can enter different amounts of pores: the smaller the polymer is, the more pores the polymer molecule can enter. Thus, it takes a longer time for smaller polymers to elute from the column. The signal of the eluent is recorded versus time. The molecular weight of each fraction is calculated to plot the molecular weight distribution. Various detectors based on different properties are used, such as refractive index and viscosity. Specially, a light scattering detector is able to determine the absolute molecular weights of polymers. The only prerequisite is that for different polymers, the dn/dc value should be known, either from the literature or measurement on the GPC machine.[1]

Glass transition temperature (T_g) and melting temperature (T_m) are two thermal parameters indicating the extent of motions in the polymer. An amorphous polymer transforms from a glassy to a rubbery state when the temperature goes above the glass transition temperature. As temperature keeps increasing, a crystalline or semi-crystalline polymer undergoes the transition to an amorphous phase, showing the melting temperature.[1]

Differential scanning calorimetry (DSC) is used to analyze the thermal properties of polymer samples as a function of temperature. The polymer is placed in an insulated cell on a heater with another identical reference cell. The temperature of the two cells is increased at the same rate and the heat difference required to keep the two cells at the same temperature is recorded.

The heat flow is plotted versus temperature, which is called a thermogram. Thermograms provide information of the transitions which occurs in the polymers among the temperature range.[1] Positive peaks in thermograms indicate endothermic process while negative peaks indicate exothermic process. In a thermogram of a polymer sample, glass transition and melting can be observed as positive peaks. Sometimes negative curve can be observed before T_m, which is caused by partial crystallization in some region of the material, due to the increased movement of the polymer chain as a result of the increased temperature.

Goals of this Work

The goals of my project were to expand our active indium catalyst to the polymerization of BBL as well as other cyclic esters, explore its competence in living and iROP of cyclic esters, and synthesize previously unexplored well-defined block copolymers based on PLA and PHB. In a collaborative project with Prof. Savvas G. Hatzikiriakos and Norhayani Othman in Chemical and Biological Engineering we aimed to study the special properties of controlled micro- and macrostructure biodegradable polymers generated by this catalyst. By investigating the iROP of cyclic esters with different alcohols at higher loading, we aimed to develop diblocks of cyclic esters and PEG, to be used as drug delivery agents in collaboration with Prof. Helen Burt and Dr. Kevin Letchford in Pharmaceutical Sciences.

CHAPTER 2. Living Polymerization of Cyclic Esters

2.1 Introduction

As discussed in Chapter 1, a limited number of catalysts for the polymerization of β-butyrolactone (BBL) have been reported. However, most systems are slow and only yield low molecular weight PHB. Stereoselective systems are even more rare.

In 2008, our group reported a chiral indium catalyst **30** (Figure 1.12) which was highly active for the living polymerization of lactide to form iso-rich PLA ($P_m \approx 0.6$).[109] The synthesis of the proligand (±)-HNNO and the subsequent metal complex [(NNO)InCl]$_2$(μ-OEt)(μ-Cl) (**30**) is shown in Schemes 2.1 and 2.2.).[109]

Scheme 2.1 Synthesis of the proligand (±)-HNNO

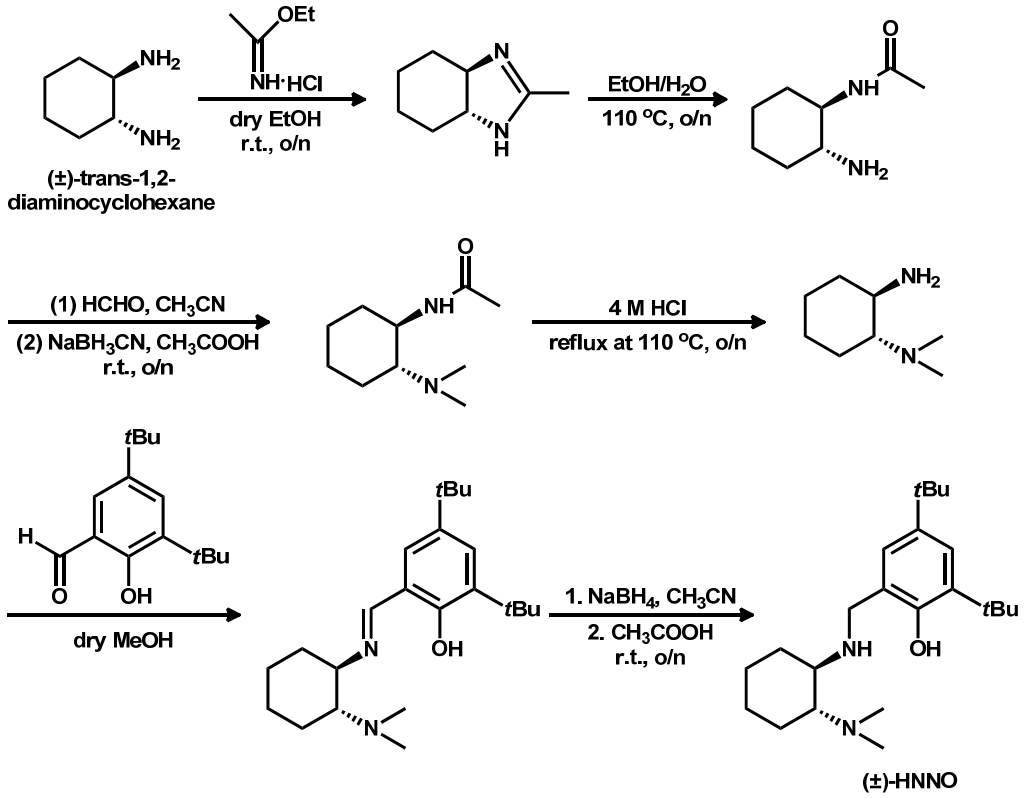

First (±)-trans-diaminocyclohexane was reacted with a Pinner salt, ethylacetimidate

hydrochloride. The imidazoline intermediate was hydrolyzed to generate the acyl protected diamine. The unprotected amine group on the product was then methylated by reductive amination with formaldehyde and sodium cyanoborohydride. Then the amide group was deprotected and condensed with 3,5-di-*tert*-butylsalicylaldehyde to form the corresponding imine. The imine was purified effectively by recrystallization in CH_3CN. Then the imine was reduced to the desired proligand with sodium borohydride. The crude product was recrystallized in CH_3CN several times to obtain a white pure compound, with an overall yield of 22%.

Scheme 2.2 Synthetic route from proligand (±)-HNNO to (*S*,*S*/*S*,*S*)- and (*R*,*R*/*R*,*R*)--[(NNO)InCl]$_2$(μ-OEt)(μ-Cl)

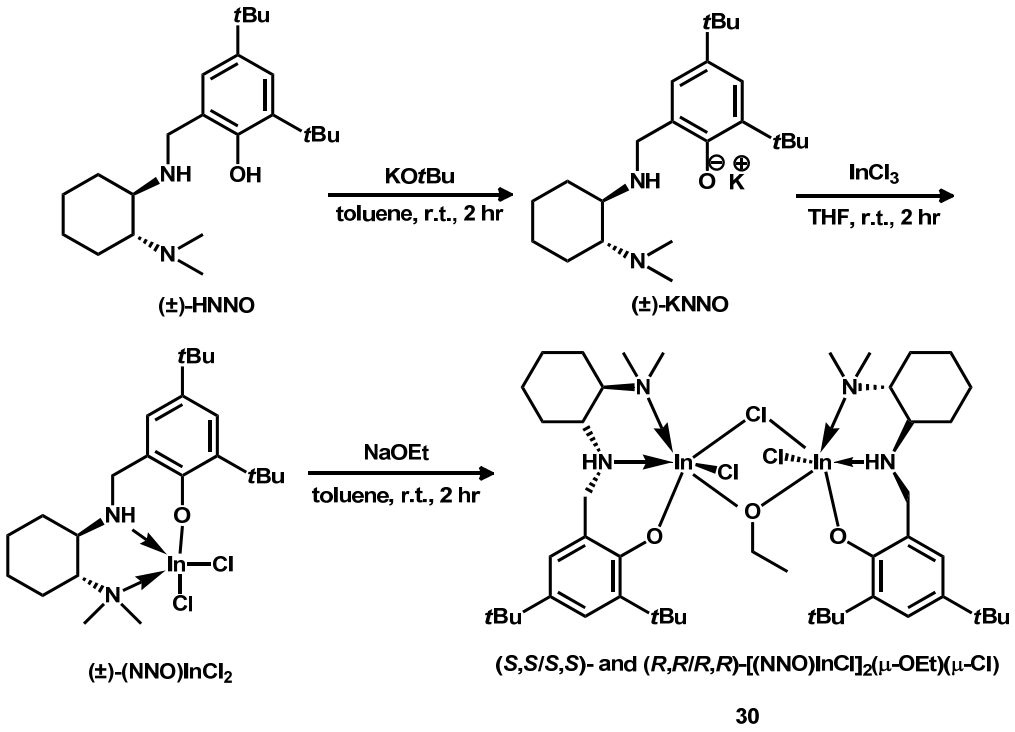

The synthesis of the catalyst **30** is shown in Scheme 2.2. A slightly modified literature procedure was used.[109] The proligand (±)-HNNO was deprotonated by potassium *tert*-butoxide and then reacted with one equivalent of $InCl_3$ to yield (±)-(NNO)$InCl_2$. Subsequent reaction of the indium dichloride complex with sodium ethoxide afforded the dinuclear catalyst **30**, bridged by a chloride and an ethoxy group. The optimum amount of

NaOEt, 0.88 equivalents, produced the desired product while minimizing the undesired dialkoxy-bridged side product.

In this chapter, the monomer scope of the catalyst $[(NNO)InCl]_2(\mu\text{-}OEt)(\mu\text{-}Cl)$ (**30**) is examined by applying it to the polymerization of lactide as well as other cyclic esters. Diblock and triblock copolymers containing lactide were synthesized *via* sequential addition method thanks to the living characteristic of this polymerization. For BBL, polymerizations were carried out in different solvents to explore the solvent effect. The relationship between molecular weights and the [BBL]:[**30**] was studied. Rates were measured at different temperatures and also with different concentrations of **30** to obtain activation parameters during transition station and the rate order to the catalyst. Other cyclic esters, ε-caprolactone and a functionalized β-lactone were also studied initially.

With a living polymerization, block copolymers can be synthesized through the sequential addition of different monomers. Synthesis of block copolymers of either LA or ε-caprolactone (CL) by sequential addition of monomers in living polymerization systems has been reported by several groups.[112] In this chapter, the behavior of our catalyst in building block copolymers is discussed. The rheology and mechanical properties of the synthesized block copolymers, tested in collaboration with Prof. Savvas G. Hatzikiriakos and Norhayani Othman in Chemical and Biological Engineering, are discussed briefly.

2.2 Results and discussion

The polymerization scope for our catalyst **30** is summarized in Scheme 2.3.

Scheme 2.3 Monomer scope for the polymerization of cyclic esters by **30**

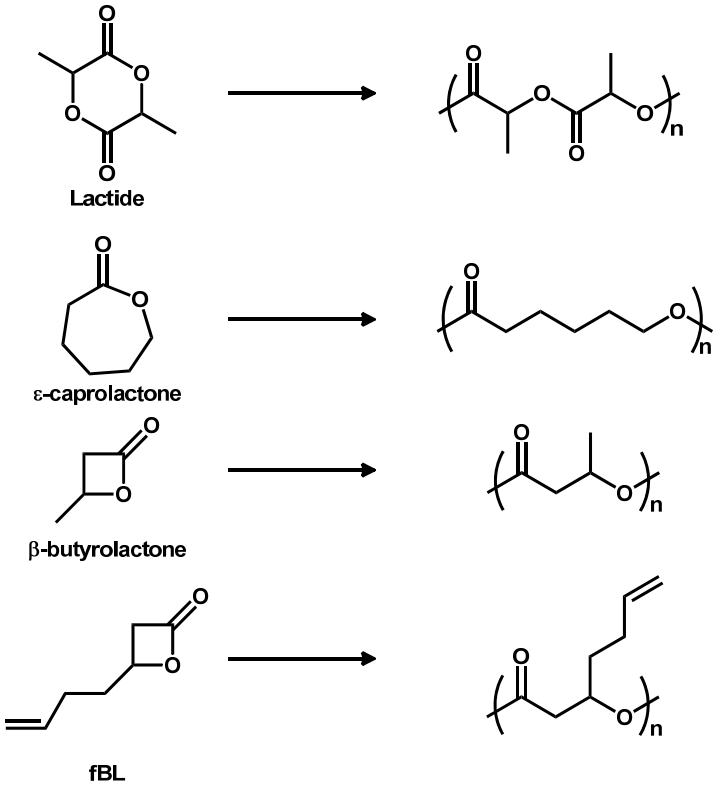

Block copolymerization of lactide

In the study of polymerization of LA by our previous group members, polymerization of up to 500 equivalents LA was reported, providing polymers with M_n values close to theoretical molecular weights and PDIs between 1.1 and 1.2.[109]

In my work, I explored the range of molecular weights accessible for the ring opening polymerization of LA with **30** (CH_2Cl_2, 25 °C). GPC data shows that for up to 2080 equivalents of LA, M_n values fit theoretical values and the PDI values are around 1.1 (Figure 2.1). Thus we can produce well-defined PLA up to 300 kDa with this catalyst.

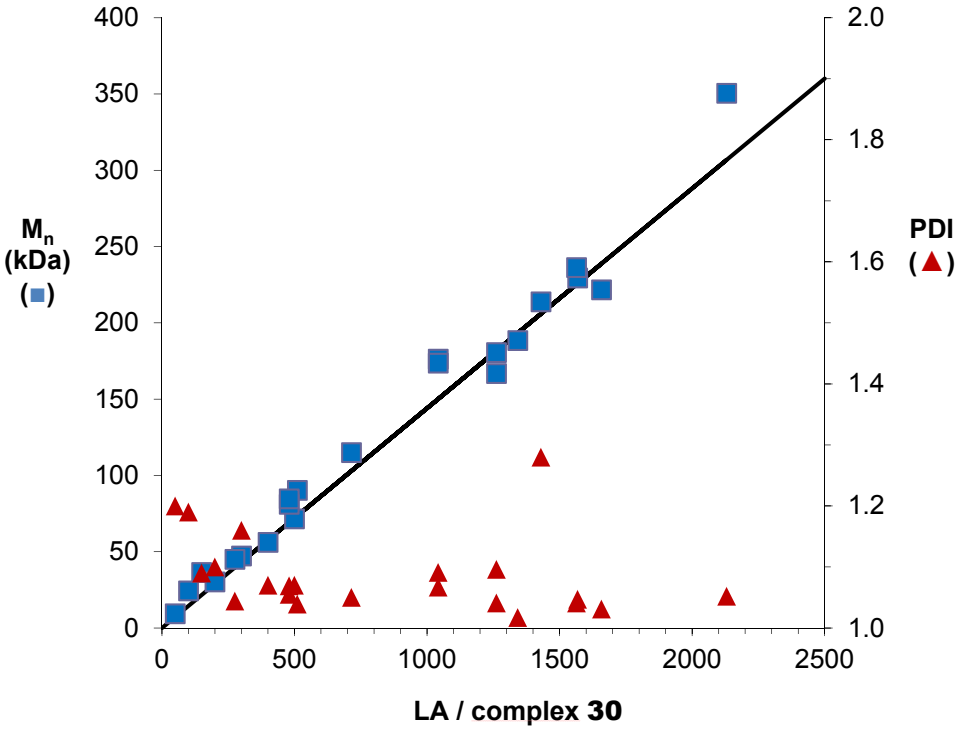

Figure 2.1 Plot of the observed molecular weight (M_n = ■) and molecular weight distributions (PDI = ▲) of PLA as a function of added monomer (calculated values for the molecular weights are shown using the line). Reactions were carried out in CH_2Cl_2, 25 °C, with [**30**] ≈ 0.3 mM and conversion > 97%.

These data, along with studies conducted previously in the group, confirm that **30** is indeed a living catalyst for the polymerization of LA and thus should be capable of generating block copolymers of lactide. To illustrate this, different compositions of nearly monodispersed diblock copolymers of DL-LA or D-LA with L-LA were synthesized by sequential living ring-opening polymerization with **30** (Scheme 2.4).

The diblock polymers, such as entry 3 in Table 2.1 were synthesized in a two-step process: In the first step L-LA (283 equiv.) was added to a solution of the catalyst and the reaction was stirred at room temperature overnight. The conversion (> 98%) and molecular weight ($M_{n,theo}$ = 40.8 kDa, $M_{n,expt}$ = 51.8 kDa, PDI = 1.10) of the PLLA were measured. DL-LA (743 equiv.) was added only after L-LA was fully converted so that each block only contained the expected amount of the corresponding monomer. The conversion (> 98%) and molecular weights of the resulting copolymers were then measured to ensure that a true diblock was

formed. Overlaid GPC traces of the PLLA block and the diblock copolymer ($M_{n,theo}$ = 147.8 kDa) (Figure 2.2) show that the peak corresponding to the PLLA block is not observed after addition of DL-LA, thus no chain termination events occurred.[113]

Scheme 2.4 Synthesis of poly(L-lactide)-*b*-poly(DL-lactide)

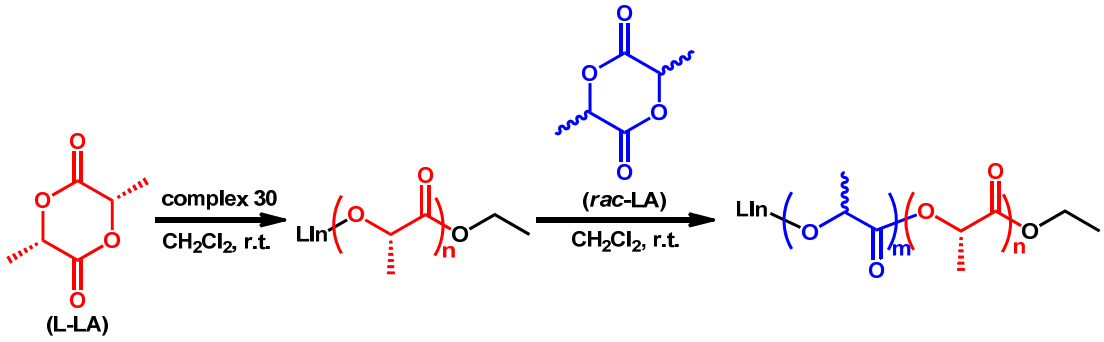

Table 2.1 Summary of diblock copolymers synthesized[113]

Entry[a]	Samples[b]	Monomers (M_1+M_2)	Equiv. (M_1+M_2)	$M_{n,theo}$[c] (kDa)	$M_{n,expt}$ (kDa)	PDI
1	75L-b170-25DL	L+DL	755+288	150.2	163.3	1.09
2	50L-b170-50DL	L+DL	516+516	148.6	163.2	1.08
3	25L-b170-75DL	L+DL	283+743	147.8	165.6	1.06
4	84L-b150-16DL	L+DL	800+156	137.5	149.5	1.05
5	50L-b170-50D	L+D	508+508	146.3	150.9[d]	1.12[d]
6	75L-b170-25D	L+D	736+280	146.3	149.2[d]	1.16[d]

[a]Reactions were carried out in CH_2Cl_2, 25 °C, with [**30**] ≈ 1 mmol/L during polymerization of the first monomer and 0.5 mmol/L of the second monomer, with conversion over 99%. [b]These block copolymers were denoted by their composition and their overall molecular weight *i.e.* 75L-b170-25DL denotes a block copolymers with an overall molecular weight of about 170 kDa with a block of L-LA (75% of the total molecular weight) and a block of DL-LA (about 25% of the total molecular weight). [c]Calculated from $M_{n,theo}$ = MW_{LA} × Equiv.$_{(M1+M2)}$. [d]Samples were highly insoluble in THF and therefore GPC measurement was run in $CHCl_3$, calibrated with monodispersed polystyrene standards. The results were multiplied by a Mark Houwink factor of 0.58 for PLA.

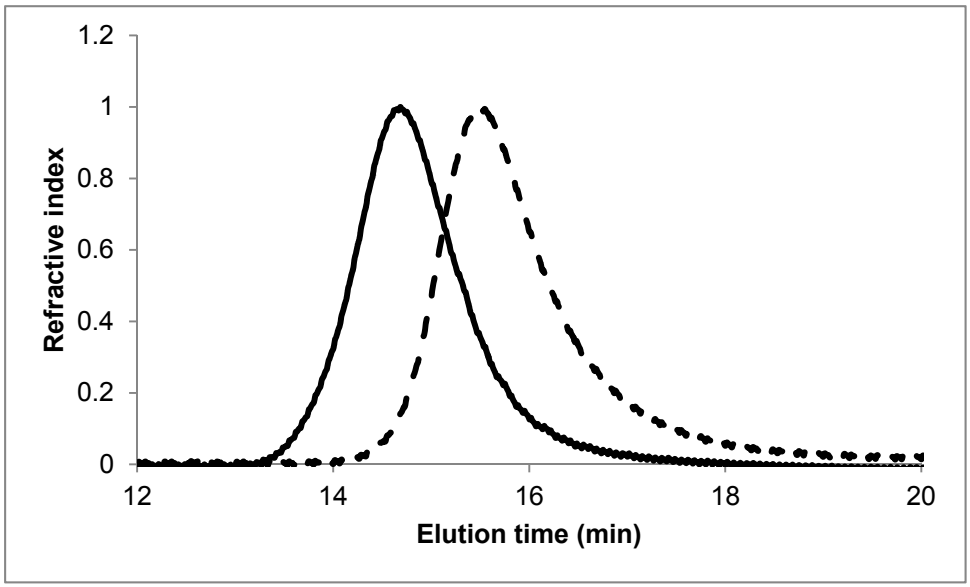

Figure 2.2 GPC trace of the polymers. Left (solid line): PLLA-*b*-PDLLA (M_n = 165.6 kDa, PDI = 1.09); right (dashed line): PLLA block in the copolymer (M_n = 51.8 kDa, PDI = 1.10).

Table 2.2 Specific optical rotation and thermal properties of L- and DL-lactide diblock copolymers[113]

Entry[a]	Samples	[α] (°)	L-LA content	T_g (°C)	T_{m1} (°C)	T_{m2} (°C)
1	75L-b170-25DL	−121.7	0.75[d]	58.5	176.0	-
2	50L-b170-50DL	−81.8	0.50[d]	56.8	174.0	-
3	25L-b170-75DL	−49.6	0.30[d]	55.2	-	-
4	84L-b170-16DL	−142.3	0.87[d]	59.9	170.9	-
5	50L-b170-50D	−4.4	0.49[e]	55.0	162.0	210.0
6	75L-b170-25D	−73.8	0.71[e]	53.0	169.0	204.0
7[b]	DL30[c]	−0.99	-	-	-	-
8[b]	L194[c]	−162.6	-	-	-	-
9[b]	D201[c]	+148.6	-	-	-	-

[a]Samples were dissolved in chloroform with a concentration close to 1 g/L and measured with Jasco P-2000 Polarimeter under a wavelength of 589 nm at room temperature. Each sample was measured five times and the average was calculated. [b]Entries 7, 8 and 9 were used as references to calculate the content of respective monomers in the copolymers. [c]Homopolymers are denoted with letters indicating the monomer type (L means L-LA, D means D-LA and DL means *rac*-LA) and numbers indicating the molecular weight in kDa. [d]Calculated as x based on the equation: $x\cdot(-162.6) + (1-x)\cdot(-0.99) = [\alpha](\text{sample})$. [e]Calculated as x based on the equation: $x\cdot(-162.6) + (1-x)\cdot(+148.6) = [\alpha](\text{sample})$.

Specific optical rotation of these copolymers was measured to determine the ratios of respective monomers in the copolymers (Table 2.2). Poly(DL-LA), poly(L-LA) and

poly(D-LA) homopolymers (entries 7, 8 and 9) were used as references. Their specific optical rotations were measured to be −0.99°, −162.6° and +148.6°, which are close to literature values ($[\alpha]_D^{25} = -151°$ for L-LA, $[\alpha]_D^{25} = +151°$ for D-LA).[114]

The ratios of monomers calculated from this data agree well with the feeding ratios in the synthesis of the polymers. This supports the controlled and living nature of our catalyst for the polymerization of lactide.

These DL- and L-lactide diblock copolymers were used to investigate the effects of molecular weight and block length ratio on their rheological behavior. For comparison, blends of PDLLA and PLLA homopolymers of equivalent molecular weights to the diblock copolymers were prepared. Homopolymers of LA were designed and blended to mimic the diblock copolymers in Table 2.1. For each component in the blend, the molecular weight and its ratio in blending were calculated to ensure that the blend and the corresponding copolymer share these parameters: (1) overall weight average molecular weight (M_w); (2) ratio of the amounts of L-LA and DL-LA; (3) ratio of the lengths of PLLA and PDLLA chains. The properties of these homopolymers and blends are summarized in Table 2.3.[113]

The thermal properties of these diblock copolymers and blendings were investigated using differential scanning calorimetry (DSC) and results are listed in Table 2.2 and Table 2.3. Figure 2.3 shows the thermograms of the second heating sequence of PLLA, L240 (**a**), PDLLA, DL90 (**e**) and their blends at different compositions (**b**, **c** and **d**). The peak around 180 °C indicates the melting temperature (T_m) and the peak between 50 and 60 °C indicates glass transition temperature (T_g). The negative curve might be caused by partial crystallization in some region of the materials. DL90 does not exhibit crystallization and melting, showing that it is completely amorphous. In the blends single and narrow peaks for the T_g and T_m can be seen, indicating that L240 and DL90 are miscible in the molten state, although the intensity of the melting peak decreases with decreasing content of L240. These observations agree well with previous studies on PLLA\PDLLA blends.[20, 115, 113]

Table 2.3 Characteristics and thermal properties of PLA homopolymers and blends[113]

Entry	Samples[a]	$M_{n,expt}$ (kDa)	$M_{w,expt}$ (kDa)	PDI	T_g (°C)	T_m (°C)
1	L200	180.6	197.9	1.10	60.3	180.7
2	L190	176.3	192.4	1.09	59.2	179.5
3	L90	84.7	90.6	1.07	53.6	178.1
4	DL190	173.6	185.2	1.07	53.2	-
5	DL170	166.8	173.7	1.04	52.6	-
6	DL85	81.07	85.51	1.06	51.5	-
7	75 L200\25 DL85	-	166.8[b]	-	57.0	179.2
8	50 L192\50 DL190	-	188.8[b]	-	56.3	179.0
9	25 L90\75 DL170	-	150.7[b]	-	57.0	-
10	L240	229.5	240.3	1.05	61.0	183.1
11	75 L240\25 DL90	-	203.7[b]	-	60.0	175.8
12	50 L240\50 DL90	-	167.0[b]	-	56.0	177.4
13	25 L240\75 DL90	-	130.4[b]	-	55.9	177.7
14	DL90	90.2	93.7	1.04	52.6	-

[a]Homopolymers are denoted with letters indicating the monomer type (L means L-LA, D means D-LA and DL means *rac*-LA) and numbers indicating the molecular weight in kDa. For the notation of blendings, take 75 L200\25 DL85 as an example. It means that the blend was made from around 75 wt% L200 and 25 wt% DL85 (actual weight percentage is 72% for L200). [b]Calculated by $M_{w,blend} = x_{PLLA}M_{wPLLA} + (1-x)M_{wPDLLA}$, where x is the weight fraction of PLLA.

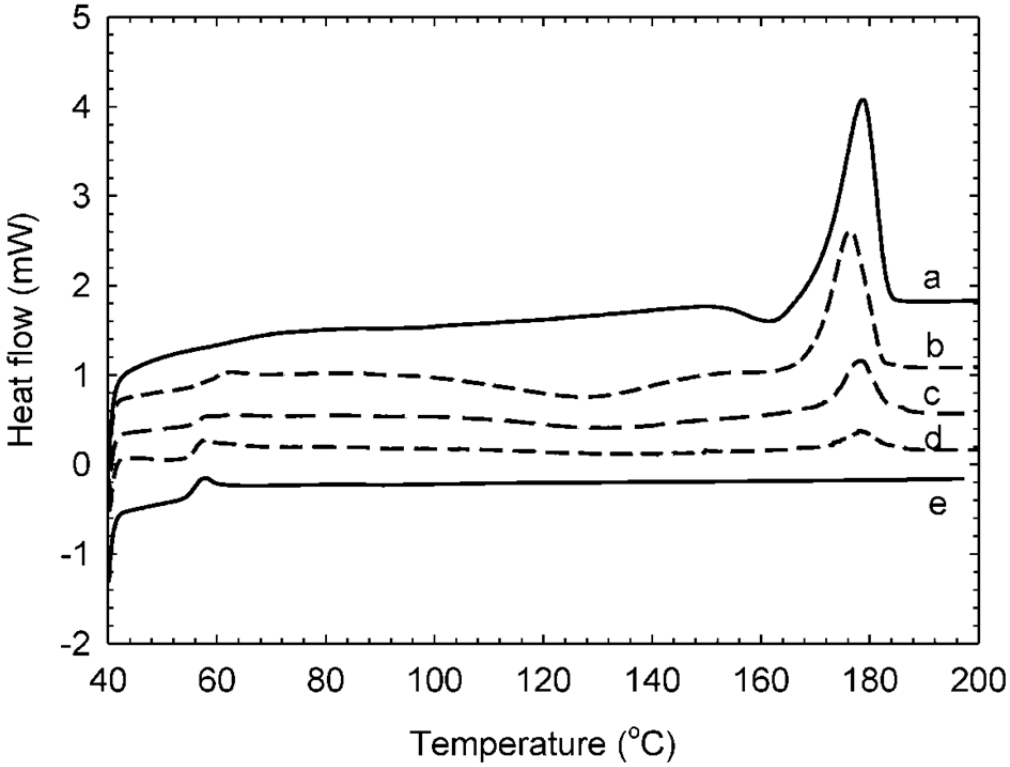

Figure 2.3 DSC thermograms of L240(a), DL90(e) and their blends with different L240 weight fractions 0.75(b),0.50(c) and 0.25(d).[113]

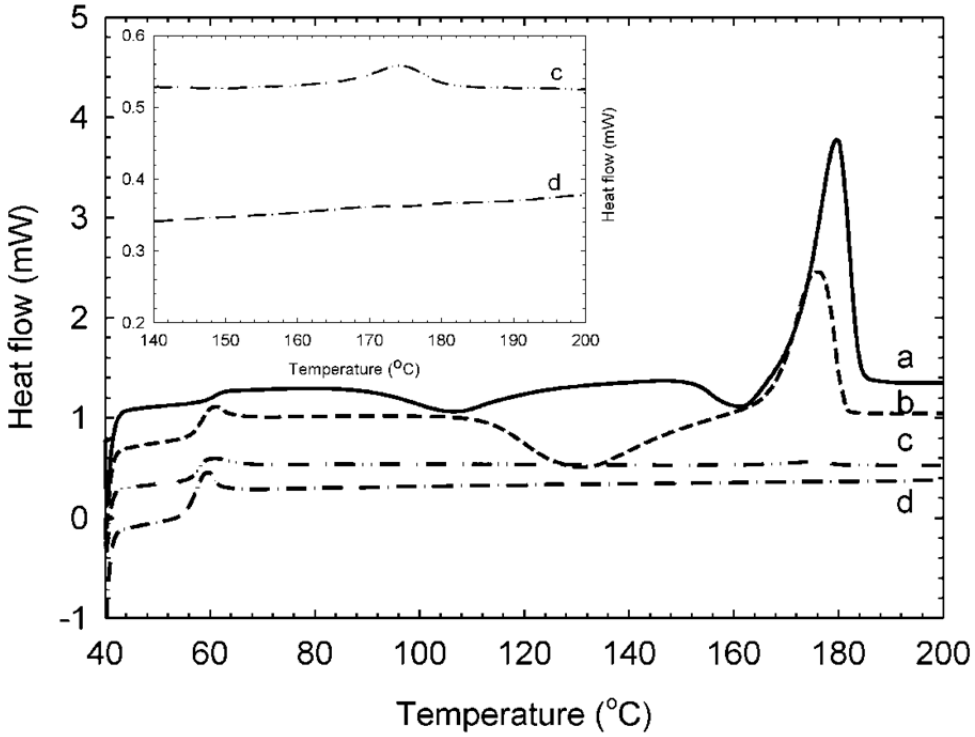

Figure 2.4 DSC thermograms of diblock copolymers with different block length ratios a) L190 b) 75L-b170-25DL c) 50L-b170-50DL d) 25L-b170-75DL.[113]

Figure 2.4 depicts the thermograms of diblock copolymers having the same molecular weight and different compositions of the blocks (Table 2.2, entries 1–3). For comparison the thermogram of PLLA with approximately the same molecular weight is shown as well (L190, Table 2.3, entry 3). The presence of a DL block (amorphous) shifts the T_m to lower temperatures and with increasing DL block content the T_m decreases. At high amounts of DL blocks (*ca.* 75%), the T_m disappears and the diblock copolymer becomes completely amorphous. The depression of T_m in diblock copolymers is due to shorter L-LA lengths in the diblock copolymers. Diblock copolymers with similar lengths of L-LA and DL-LA show small broad melting peaks (see inset in Figure 2.4). The reduced degree of crystallinity of diblock copolymers compared to that of the corresponding blend is also attributed to the segmental connection between PLLA and PDLLA chains, which somehow hinders the free movement of the PLLA chains of the diblock copolymers during crystallization.[113]

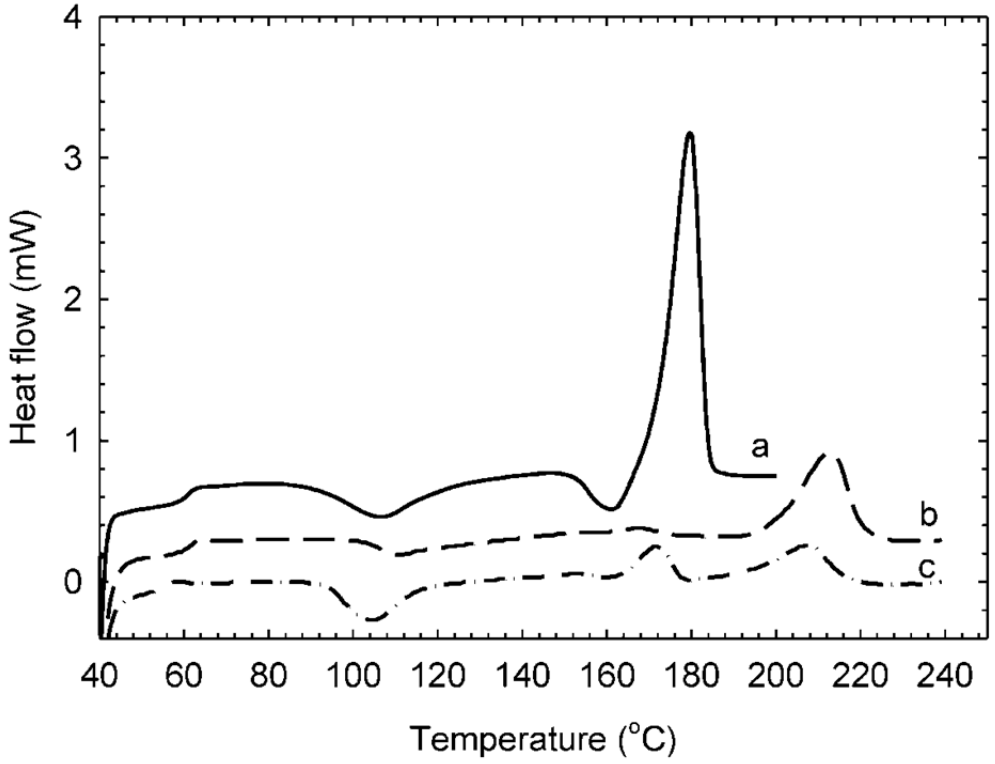

Figure 2.5 DSC thermograms of diblock copolymers with different block length ratio a) L190 b) 50L-b170-50D c) 25L-b170-75D.[113]

PLLA-*b*-PDLA diblock copolymers (Table 2.2, entries 5 and 6) possess double melting peaks (Figure 2.5); the low melting point is detected at about 170 °C and the high melting

temperature peak at about 210 °C. The lower melting temperatures are close to melting temperature of pure PLLA. The higher melting temperatures are attributed to the formation of stereocomplexes between PLLA block and PDLA block, which is in agreement with reported values.[29, 116] As the block ratio deviates from 1:1, coexistence of a homocrystal phase, *i.e.* the crystal phase of PLLA and PDLA separately, can be found particularly at low crystallization temperatures. It has been reported in the literature that the mixture of PLLA and PDLA in 1:1 ratio prefer to form a stable stereocomplex. When the molar ratio deviates from 1:1, the fraction of the stereocomplexes decreases steadily.[117] Similar results have been reported by Li *et al.* for PLLA-*b*-PDLA diblock copolymers.[118, 113]

Triblock copolymers of LA isomers were also synthesized (Scheme 2.5, Table 2.4). The incorporation of *rac*-LA in the middle block and L-LA or D-LA in the outer blocks was intended to enhance the mechanical properties while maintaining polymer flexibility. In PLLA-*b*-PDLLA-*b*-PDLA triblocks, the PLLA and PDLA blocks can form stereocomplexes while the atactic block in the middle provides some flexibility to the copolymer.

Scheme 2.5 Synthesis of PLLA-*b*-PDLLA-*b*-PLLA and PLLA-*b*-PDLLA-*b*-PDLA

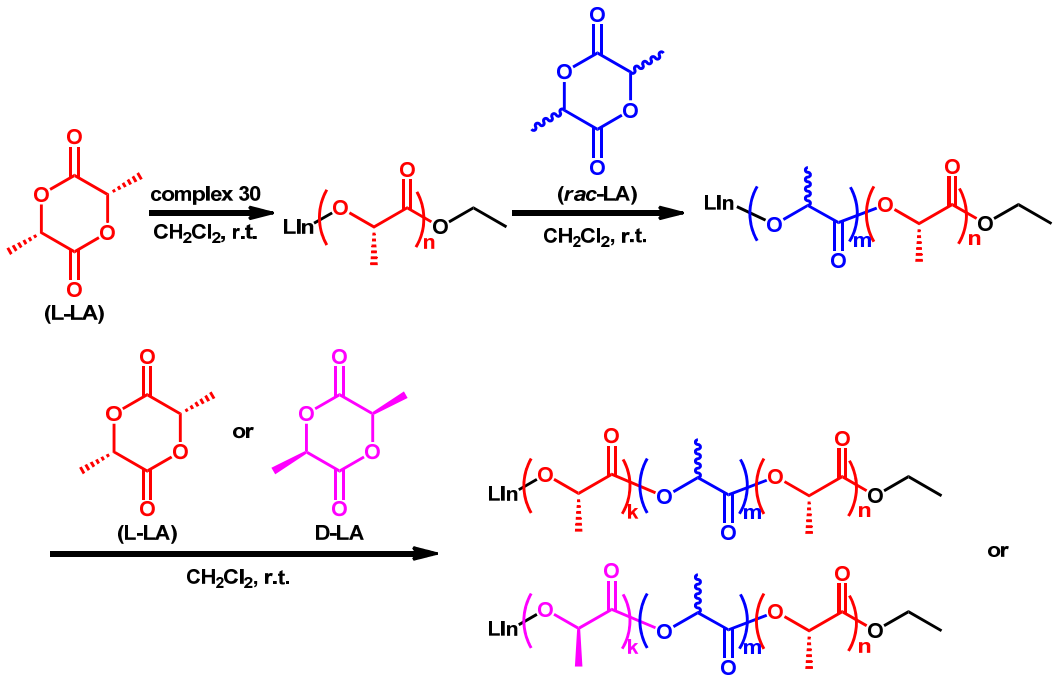

Table 2.4 Summary of synthesized lactide triblock copolymers

Entry[a]	Monomers (M_1+M_2+M_3)	Equiv. (M_1+M_2+M_3)	$M_{n,theo}$[b] (kDa)	$M_{n,expt}$ (kDa)	PDI
1	L+*rac*-LA+L	423+322+423	168	169.1	1.06
2	L+*rac*-LA+L	294+505+294	157	190.3	1.24
3	L+*rac*-LA+D	426+325+426	170	152.9[c]	1.15[c]
4	L+*rac*-LA+D	294+505+294	157	153.0[c]	1.16[c]

[a]Reactions were carried out in CH_2Cl_2, 25 °C, with [**30**] ≈ 1 mmol/L during polymerization of the first monomer, 0.5 mmol/L of the second monomer and 0.3 mmol/L of the third monomer, with conversion over 99%. [b]Calculated from $M_{n,theo} = MW_{LA} \times Equiv._{(M1+M2+M3)}$. [c]Samples were highly insoluble in THF and therefore GPC measurement was run in $CHCl_3$, calibrated with monodispersed polystyrene standards. The results were multiplied by a Mark Houwink factor of 0.58 for PLA.

Formation of stereoblocks causes a significant decrease in polymer solubility. It is difficult to dissolve copolymers containing both L and D blocks (Table 2.4, entries 3 and 4; Table 2.1, entries 5 and 6) in most common solvents, including THF at room temperature and trichlorobenzene at elevated temperature. Under heating and sonicating, these triblock copolymers can be slowly dissolved in CH_2Cl_2 and chloroform. To the best of our effort, the GPC measurements of these triblocks and the aforementioned L-LA and D-LA diblocks were carried out on a facility equipped with a refractive index detector using $CHCl_3$ as the solvent (notated as GPC-RI). To compare the differences between results from different GPC facilities, entry 2 was run with GPC-RI and its result is 174.9 kDa with a PDI of 1.19. The molecular weight result is smaller than the value in Table 2.4 (190.3 kDa, run with a GPC facility equipped with a light scattering detector, notated as GPC-LS), indicating a slight deviation of results obtained by GPC-RI from GPC-LS. In general, the molecular weights of these synthesized triblock copolymers are in good agreement with theoretical values. The studies on the physical properties of these triblock copolymers are ongoing. As far as we know, triblock copolymers consisting of PLLA and PDLA blocks in each end respectively and a racemic block in the center have not been previously reported.

Polymerization of β-butyrolactone

As mentioned in Chapter 1, there are only a few examples of highly active catalysts for the ROP of BBL. Among them, the β-diiminate zinc catalysts **6** by Coates *et al.* and bis(phenolate) yttrium complexes **23** by Carpentier *et al.*, both of which had been reported to be active initiators for ROP of lactide, are also active and living for the polymerization of BBL (Figure 2.6).[78] Complex **6c** was able to polymerize BBL to high molecular weight PHB (M_n = 144 kDa) rapidly under mild conditions without stereoselectivity (in benzene at r.t., with [BBL] = 2.45 M, 200 equivalents BBL was converted 91% in 70 min).[78a] Complexes **23c** and **23d** were able to generate highly syndiotactic PHB (P_r up to 0.94) with the highest activity to date (in toluene and benzene at room temperature, with [BBL] = 2.44 M, 200 equivalents BBL could be converted 97% in 1 minute).[78b] For our indium catalyst **30** (Figure 1.12), the ROP of BBL was studied and is discussed below.

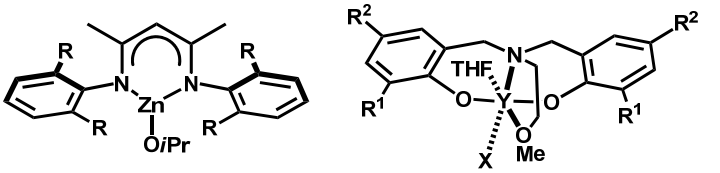

6a: R = Et
6b: R = *n*Pr
6c: R = *i*Pr

23a: X = N(SiHMe$_2$)$_2$, R^1 = R^2 = CMe$_2$Ph
23b: X = N(SiHMe$_2$)$_2$, R^1 = R^2 = CMe$_3$
23c: X = O*i*Pr, R^1 = R^2 = CMe$_2$Ph
23d: X = O*i*Pr, R^1 = R^2 = CMe$_3$

Figure 2.6 Highly active catalysts for ROP of BBL

First, we explored the activity of **30** for the ROP of BBL under a variety of conditions. Polymerization reactions were carried out in different solvents, at both room temperature and 60 °C. Results show that the rate of BBL polymerization with **30** is highly solvent dependent (Table 2.5). In general, reactions with BBL are slower than those with LA. For example, room temperature reactions in CD_2Cl_2 have a rate of LA ROP ($k^{rac\text{-LA}}$ = 0.63 (±0.12) $s^{-1}\cdot M^{-1}$) that is more than an order of magnitude greater than that for BBL (k^{BBL} = 0.013 $s^{-1}\cdot M^{-1}$) (see below for discussion of kinetics). Room temperature polymerizations in toluene, CH_2Cl_2, and CH_3CN reach conversion after many hours, while reactions in THF reach full conversion

(> 99%) in one hour. Heating the reactions to 60 °C increases the rates significantly and allows all reactions to reach full conversion (> 99%) in about 4 hours.

Table 2.5 Solvent dependence of BBL polymerization by **30**

Entry[a]	Solvent	Temp (°C)[b]	Time (h)	Conv. (%)[c]
1	Toluene	25	8.4	89
2	Toluene	60	4	> 99
3	CH_2Cl_2	25	8.5	98
4	CH_2Cl_2	60	0.8	> 99
5	CH_3CN	25	8.5	98
6	CH_3CN	60	0.5	98
7	THF	25	1.0	97

[a]Reactions were carried out with [**30**] = 0.0045 mol/L and M/I = 200. [b]The temperature indicated was the oil bath temperature. [c]Determined by ^{1}H NMR spectroscopy on Bruker AV300.

Importantly, the polymerization reactivity follows the following trend: k_{obs} THF-d_8 (2.9×10^{-4} s^{-1}) >> CD_2Cl_2 (6.1×10^{-5} s^{-1}) > CD_3CN (5.5×10^{-5} s^{-1}) >> toluene (rate not measurable at room temperature). Referring to polarity indices of these solvents (Table 2.6), the reactivity difference may be a result of the polarity difference.[119] However, the high reactivity in THF cannot be solely explained by the polarity index. The coordinating ability of the solvent towards the indium center may be another important factor in explaining this trend.

Table 2.6 Polarity indices of selected solvents[119]

Solvent	Toluene	CH_2Cl_2	CH_3CN	THF
Polarity	2.4	3.1	5.8	4.0

Interestingly, the solvent effect of BBL polymerization may be catalyst dependent. The reactivity of **30** for ROP of BBL is greatest in THF, although the rates are one order of magnitude lower than complex **23**.[78b] Carpentier *et al.* observed a dramatic reversal in the solvent effect in their system. Polymerization of BBL by complex **23c** was almost 2 magnitudes faster in toluene than in THF.[78b] Complex **6** had a less significant solvent effect in this order: benzene > THF > CH_2Cl_2.[78a] These results may suggest some mechanistic

difference in ROP of BBL between the aforementioned systems. Molecular modeling and DFT calculations may be helpful in explaining this effect.

A differential scanning calorimetry study on the resulting PHB showed a thermogram in Figure 2.7, with both the first and second heating curves. From the second heating curve, a glass transition temperature of 5.6 °C was observed. This agrees with literature data, where both isotactic and atactic PHB had identical T_g of around 4 °C.[120] No melting temperature was observed, indicating the synthesized PHB is amorphous. However, the peak at 49.2 °C during the first heating cycle could be caused by the melting of some crystalline zones in the polymer formed in the precipitation process. Compared to polylactide, whose T_g, depending on molecular weight and microstructures, ranges from 50 to 60 °C, the T_g of PHB is much lower.

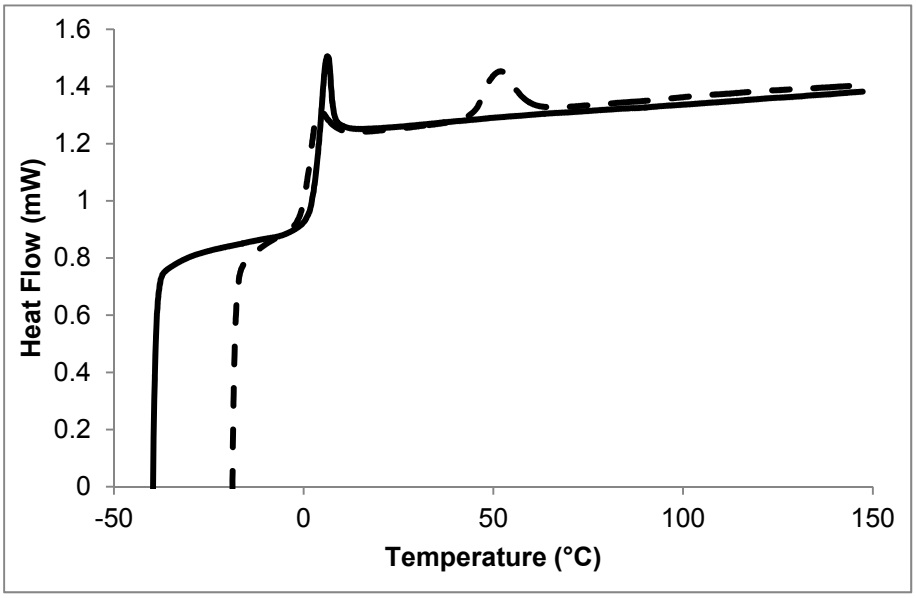

Figure 2.7 DSC thermogram of a synthesized PHB with M_n = 17.85 kDa and PDI = 1.02 (polymerization was carried out in CH_2Cl_2 at room temperature with [BBL] = 0.93 mol/L and M/I = 200, overnight.). Solid line: 2nd heating curve; dashed line: 1st heating curve.

As mentioned above, there are only a handful of catalytic systems capable of producing high MW PHB through ROP.[78a, 80, 85] None of these was achieved through high loading of BBL with expected molecular weight. Despite the high internal strain of four-membered rings (thermodynamic parameters for polymerization of β-propiolactone: $\Delta H_{polym} = -82.3$ kJ·mol^{-1},

ΔS_{polym} = −74 J·mol^{-1}·K^{-1}; no data of BBL was available in the literature), BBL is significantly less reactive than related large membered ring lactones such as lactide (ΔH_{polym} = −22.9 kJ·mol^{-1}, ΔS_{polym} = −25 J·mol^{-1}·K^{-1}).[79] Therefore, ensuring that the monomer sample is water-free and pure is critical for synthesis of high molecular weight PHB and accurate measurement of polymerization rates. It is also important to choose an appropriate drying agent: CaH_2 is able to dry BBL without any unwanted reactions while reagents like Na react with BBL.[85] We have found that stirring BBL over CaH_2 for 48 h, followed by distillation under vacuum and several freeze-pump-thaw cycles are necessary before reproducible results can be obtained. Although similar procedures are common in the literature,[78b, 84b, 121] some groups followed the distillation with redistillation over a second batch of freshly powdered CaH_2[78a]. We found that BBL stored in the glovebox freezer (−30 °C) after purification is able to yield reproducible results for two months, after which repurification was necessary.

We carried out polymerization of BBL in THF, with BBL:**30** ratios ranging from 200 to 5000 (Figure 2.8) THF was chosen as the solvent for bulk syntheses due to the higher activity of **30**. CD_3CN was chosen for small scale polymerizations monitored on NMR, due to the prohibitive price of THF-d_8. The GPC results show a linear relationship between M_n and BBL:**30** ratios of up to 5000, allowing us to isolate PHB samples with molecular weights of nearly 300 kDa (Figure 2.8).

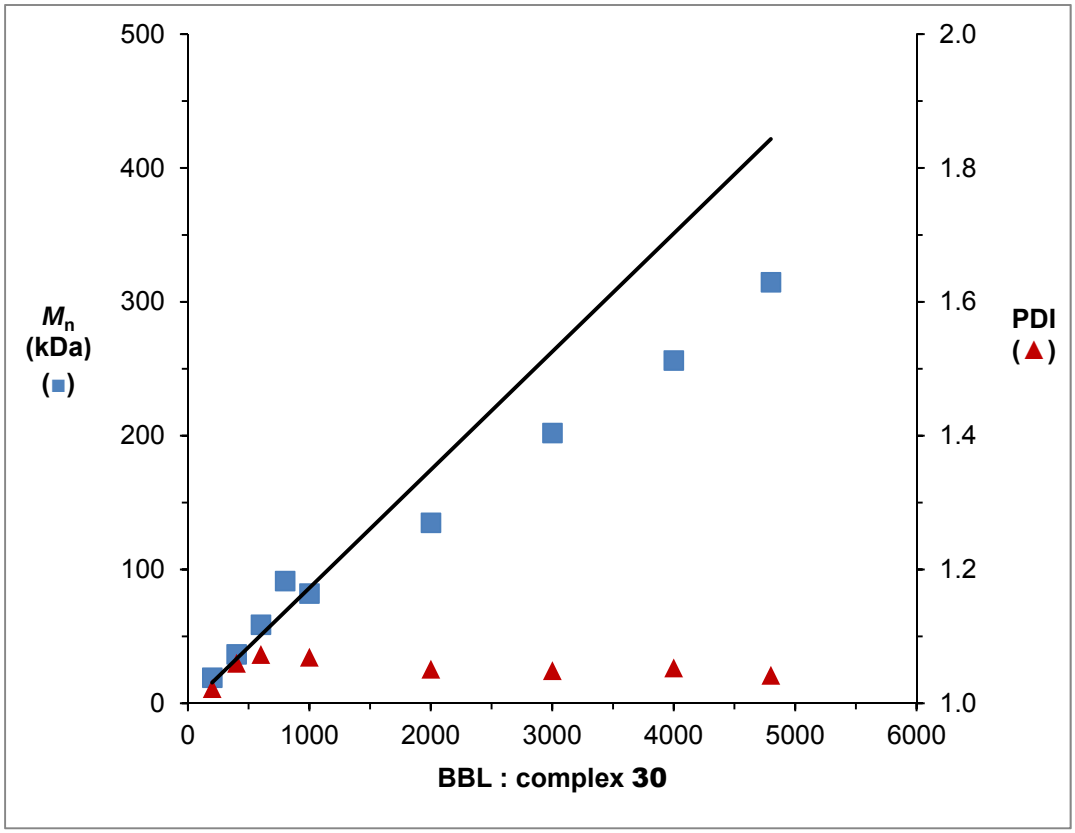

Figure 2.8 Plot of the observed molecular weight (M_n = ■) and molecular weight distributions (PDI = ▲) of PHB as a function of added monomer (calculated values for the molecular weights are shown using the line). Reactions were carried out in THF at room temperature with [BBL] ranging from 1 mol/L to 2.5 mol/L, overnight.

A comparison of Figure 2.8 with the analogous plot obtained for LA (Figure 2.1) shows differences at high molecular weights. Although the plot of M_n versus BBL:**30** is linear, for ratios over 1000 the experimental polymer molecular weights are lower than the theoretical values. As the equivalents of BBL are increased, the deviation from theoretical values increases. With 5000 equivalents BBL, deviation from the calculated molecular weight reaches 27%. Regardless, the molecular weight distributions for these polymer samples are uniformly lower than 1.10, showing a very controlled reaction. Lower than expected molecular weights for BBL:initiator ratios over 1000 were observed by other groups as well.[39b, 78a] Coates *et al.* attributed this phenomenon to: 1) poor calibration of PHB molecular weights by polystyrene standards in GPC measurements; 2) side reactions such as transesterification and elimination catalyzed by the metal complex; 3) the presence of impurities in the monomer. In our indium system, molecular weights were obtained from a GPC equipped with a light scattering detector, so results of molecular weights should be

reliable. Also, low PDI should indicate no obvious side reactions. However, the presence of trace impurities in the monomer cannot be ruled out, since it's known that BBL is difficult to prepare in > 99.9% purity.

To test the tacticity of PHB generated with our catalyst system, $^{13}C\{^{1}H\}$ NMR spectra of our samples were obtained, as the ^{13}C NMR resonances are sensitive to the PHB chain conformation (Figure 2.9). In the carbonyl region of PHB, the upfield (169.0 ppm) and downfield (169.1 ppm) signals correspond to the meso (*m*) diad sequences, *R*-*R* and *S*-*S*, and the racemic (*r*) diad sequences, *R*-*S* and *S*-*R*, respectively.[54, 78b] Figure 2.9 shows that the peaks corresponding to the racemic (*r*) and meso (*m*) diads integrate to 0.52 and 0.48 respectively, indicating the formation of atactic PHB. The methylene region (40.5–40.8 ppm) shows triad sensitivity, with four peaks corresponding to *rm*, *mm*, *rr* and *mr* sequences from left to right. Their integrations are 0.27, 0.32, 0.27 and 0.25, respectively, also indicating an atactic microstructure of PHB. PHB synthesized in different solvents, either at room temperature or 60 °C, was also atactic.

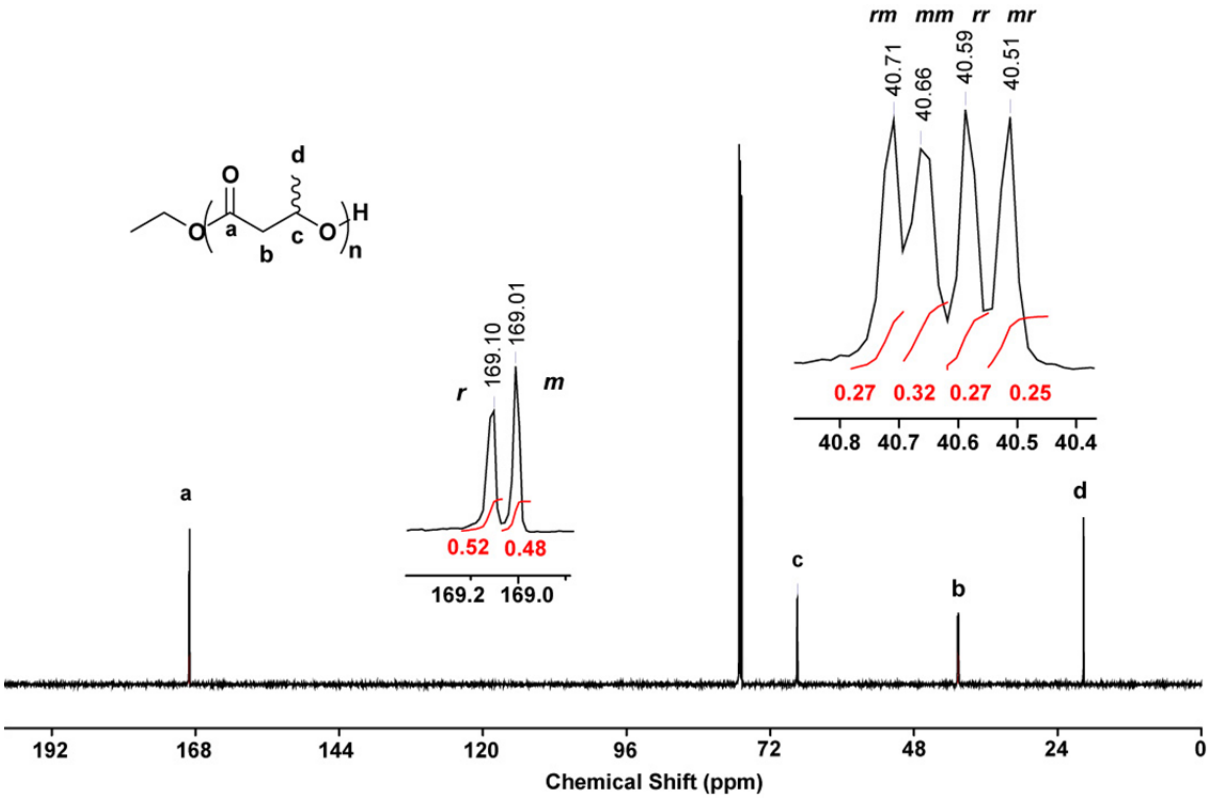

Figure 2.9 ^{13}C NMR spectra of PHB in $CDCl_3$, 150 MHz and 298 K; polymerization was performed in CH_3CN at 60 °C with 1000 equivalent BBL.

In situ ^{1}H NMR spectroscopy was used to monitor the polymerization of BBL to further investigate the rate and mechanism of controlled polymerization. The rate of polymerization of BBL was determined by observation of the decrease in intensity of the methine proton of BBL. A plot of the natural log of [BBL] vs time is linear and indicates first order polymerization of BBL until approximately 90% conversion (Figure 2.10). No induction period was observed, indicating the initiation was fast. Above 90% conversion, the slope decayed slightly. The observed polymerization rate (k_{obs}) was obtained from the slope of line for the linear region.

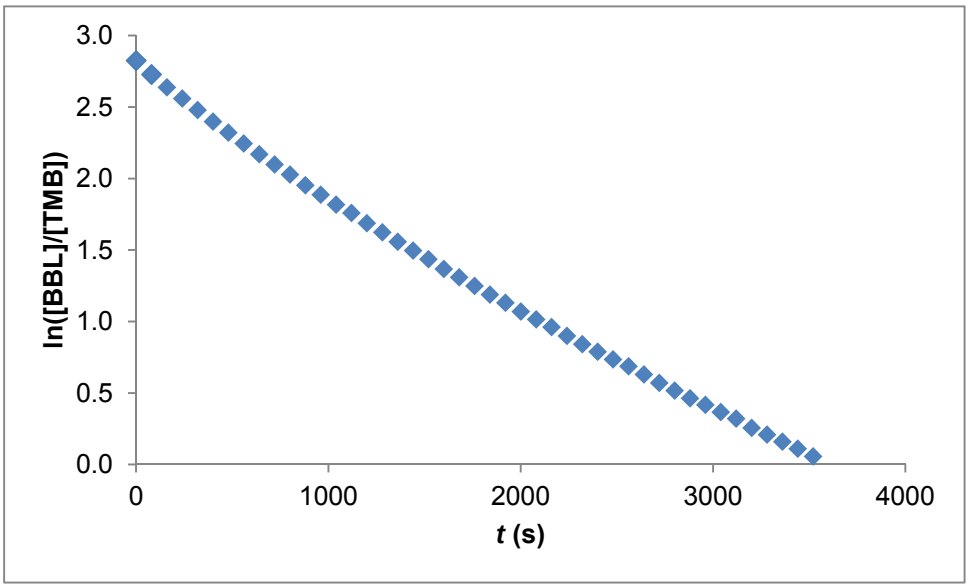

Figure 2.10 Plot of ln([BBL]/[TMB]) versus time for polymerization of BBL (CD_3CN, 358.8 K, [**30**] = 3.7 mM, M/I = 200, 400 MHz ^{1}H NMR spectroscopy).

Polymerization rates with different concentration of **30** were measured by *in situ* ^{1}H NMR spectroscopy (Table 2.7, Figure 2.11). These data show that the polymerization is first order in concentration of **30**. Since the rate is also first order in [BBL], we can propose an overall rate equation during propagation:

$$rate = k \times [\mathrm{BBL}] \times [\mathbf{30}] \qquad (2.1)$$

in which

$$k \times [\mathbf{30}] = k_{obs} \qquad (2.2)$$

The rate constant *k* was calculated from the slope of Figure 2.11 to be 0.22(±0.11) $M^{-1} \cdot s^{-1}$.

Table 2.7 k_{obs} of polymerization of BBL with different concentration of **30**

Entry[a]	[**30**] (mol/L)	k_{obs} (*10^{-5} s^{-1})
1	0.0045	88.2
2	0.0037	78.2
3	0.0030	53.9
4	0.0023	39.5
5	0.0016	27.1

[a]All the experiments were run in CD_3CN at 60.6 °C, with [BBL]/[**30**] = 200, monitored *in situ* on a Bruker AV 400 MHz spectrometer by observing the intensity of methine proton of the monomer.

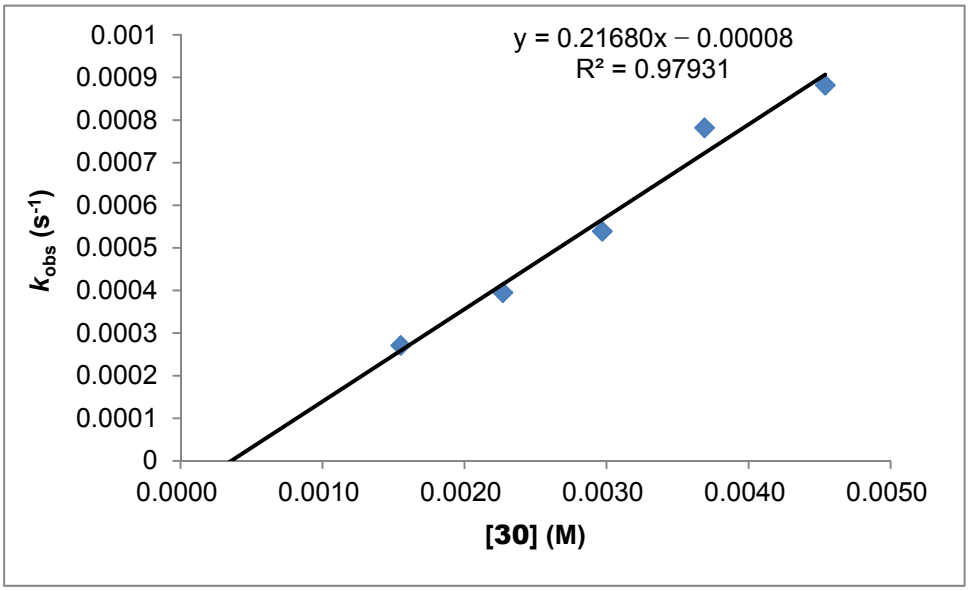

Figure 2.11 Dependence of the observed polymerization rate on [**30**].

According to transition state theory, the Eyring equation (Equation 2.3) was used to obtain the thermodynamic parameters, enthalpy ($\Delta H^{\neq}$) and entropy ($\Delta S^{\neq}$) of activation of polymerization:

$$\ln\frac{k}{T} = -\frac{\Delta H^{\neq}}{R}\times\frac{1}{T} + \ln\frac{k_b}{h} + \frac{\Delta S^{\neq}}{R} \qquad (2.3)$$

Polymerizations of BBL at temperatures ranging from 29 to 76 °C were monitored with *in situ* NMR spectroscopy (Table 2.8). By plotting the natural logarithm of the observed rate over temperature against the inverse of the temperature, $\Delta H^{\neq}$ and $\Delta S^{\neq}$ during polymerization were calculated from the slope and the *y*-intercept of the line (Figure 2.12). Usually in literatures the observed rate k_{obs} was used to plot out ln(k_{obs}/T) vs 1/T. However, since k_{obs} is affected by the concentration of the catalyst, which leads to a change in $\Delta S^{\neq}$ from different concentration of the catalyst used, here the rate constant *k* is also used to plot out ln(*k*/T) vs 1/T as a comparison (Figure 2.13).

From Figure 2.12, activation parameters for the polymerization $\Delta H^{\neq}$ and $\Delta S^{\neq}$ are 58(±4) kJ/mol and −128(±9) J/(mol·K) respectively, compared with 49(±2) kJ/mol and −140(±12) J/(mol·K) for racemic lactide.[109] The corresponding free energies of activation for the polymerization process of BBL and *rac*-LA at room temperature were calculated to be 96 kJ/mol and 91 kJ/mol. The closeness of these thermodynamics data for BBL and LA might indicate a similar mechanism of BBL polymerization to LA. With regard to the differences between k_{obs} and *k*, if ln(*k*/T) was used to draw the Eyring plot, $\Delta H^{\neq}$ would be the same as the above. However, $\Delta S^{\neq}$ would be –83(9) J $mol^{-1}K^{-1}$ instead.

Table 2.8 Rates for polymerization of BBL by **30** at variable temperatures

Entry[a]	Temp[b] (°C)	1/T (K^{-1})	k_{obs} ($*10^{-5}\cdot s^{-1}$)	*k* ($M^{-1}\cdot s^{-1}$)[c]	ln(k_{obs}/T)	ln(*k*/T)
1	22.4	0.003384	5.5	0.0120	−15.497	−10.104
2	29.2	0.003307	11.3	0.0246	−14.800	−9.427
3	40.2	0.003191	24.9	0.0541	−14.045	−8.672
4	51.2	0.003083	71.9	0.156	−13.019	−7.646
5	60.6	0.002996	88.2	0.192	−12.844	−7.357
6	72.2	0.002896	215.4	0.468	−11.985	−6.592

[a]All the experiments were run in CD_3CN, monitored *in situ* by ^1H NMR spectroscopy, [**30**] = 0.0046 M, [TMB] = 0.029 mol/L and [BBL]/[**30**] = 200. [b]The temperatures are calibrated with 80% ethylene glycol in DMSO-d_6. [c]The rate constant k is calculated as: $k = k_{obs}/[\mathbf{30}]$.

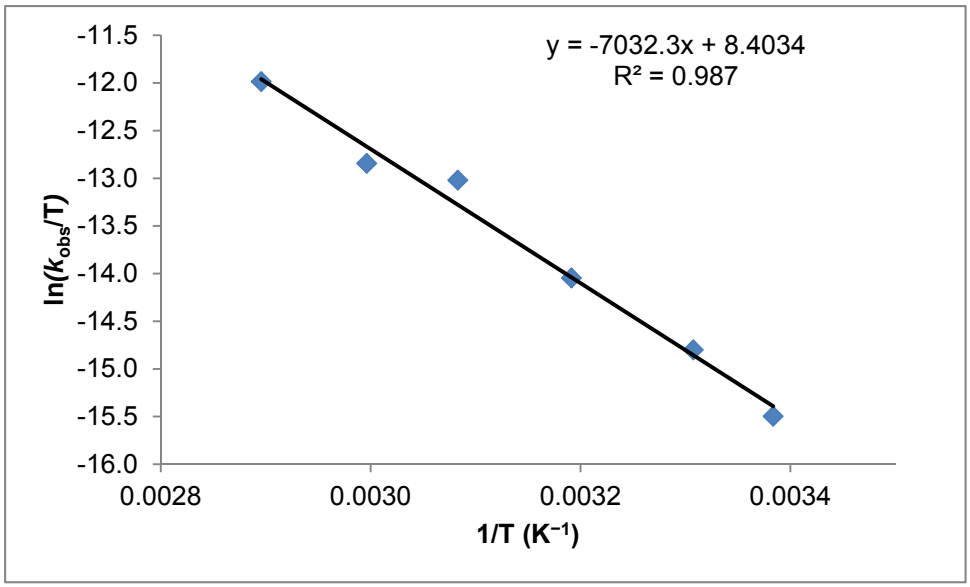

Figure 2.12 Plot of $\ln(k_{obs}/T)$ vs 1/T for polymerization of BBL with **30** in CD_3CN. ([**30**] = 0.0046 mol/L, [BBL]/[**30**] = 200).

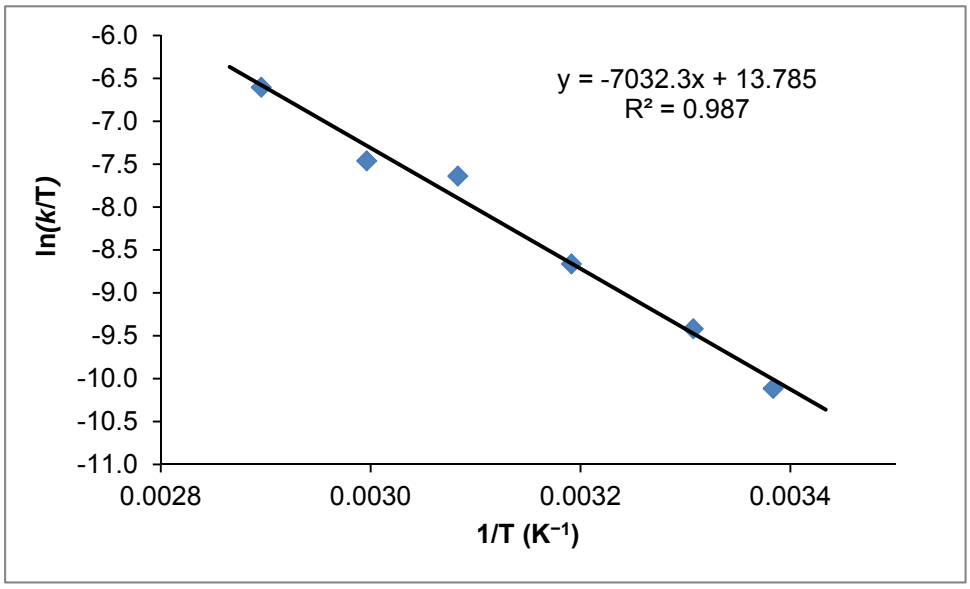

Figure 2.13 Plot of $\ln(k/T)$ vs 1/T for polymerization of BBL with **30** in CD_3CN. [**30**] = 0.0046 mol/L, [BBL]/[**30**] = 200).

Based on the results shown above, the polymerization of BBL by our indium catalyst is controlled. Kinetic observation and GPC data of sequentially adding two aliquots of monomer shows that the catalyst retains its activity over multiple additions. In an experiment

involving sequential addition of two aliquots of BBL (100 equivalents each), the natural logarithm of the relative integration of the methine proton of BBL was plotted versus time (Figure 2.14). The plot during each addition was linear, with rate first order in [BBL]. Compared to the same experiment with LA in which the two rates before and after the second addition were almost the same (0.56 $s^{-1} \cdot M^{-1}$ and 0.59 $s^{-1} \cdot M^{-1}$), the rates of BBL ROP decreased after the second addition from 0.28 $s^{-1} \cdot M^{-1}$ to 0.15 $s^{-1} \cdot M^{-1}$, indicating a slow degradation during polymerization. This is most likely due to impurities in BBL, as described above.

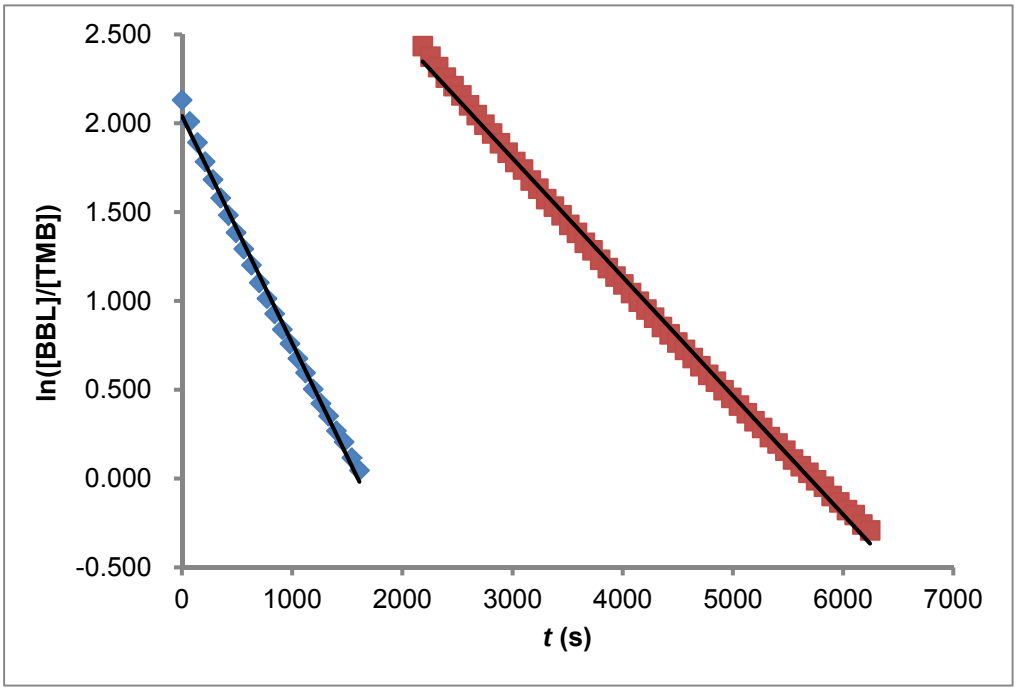

Figure 2.14 Plot of ln([BBL]/[TMB]) versus time for two sequential additions of BBL, (♦ = 1st addition of 100 equivalents; ■ = 2nd addition of 100 equivalents) (CD_3CN, 358.8 K, 400 MHz NMR spectroscopy).

As discussed above, the ROP of BBL with **30** is controlled. Therefore it is possible to synthesize well-defined diblock or triblock copolymers of BBL and LA with this catalyst system by sequential addition. In a representative experiment, two aliquots of BBL (200 equivalents each) were added to a solution of **30** (THF, room temperature, [**30**] = 0.0045 mol/L) sequentially. The resulting PHB sample had M_n corresponding to 400 enchained units (42.8 kDa) and PDI of 1.05 (Figure 2.15). No obvious peak corresponding to 200 units of

PHB was observed in the GPC trace but the peak is a bit tailing, indicating a minimal amount but not obvious chain termination occurred, which also agrees with the decreased rate upon the second addition observed in the kinetic experiment above.

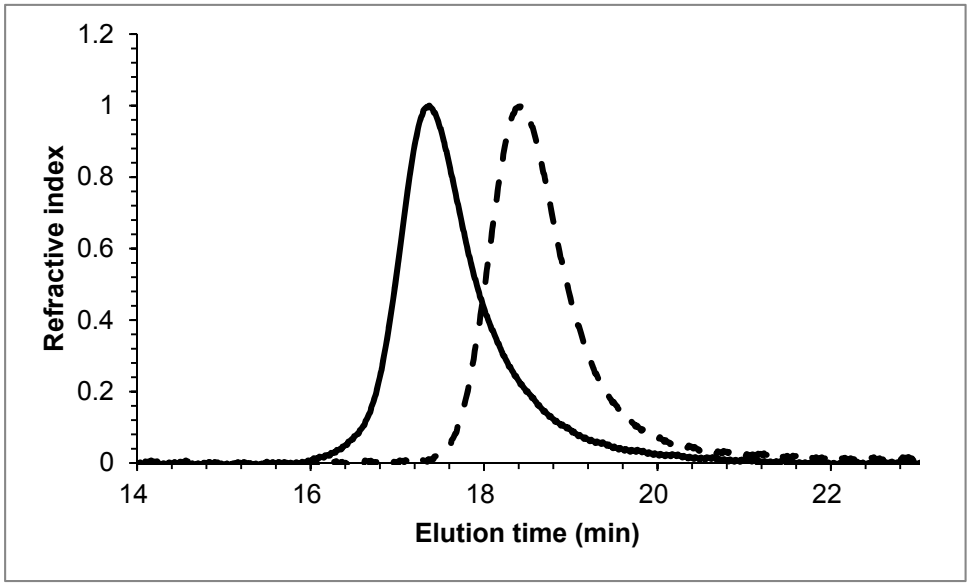

Figure 2.15 GPC traces of the polymers produced by consecutive additions of 200 equivalent BBL to a solution of **30**. Left (solid line): PHB produced by sequentially adding two aliquots of 200 equivalents BBL to **30** (M_n = 42.8 kDa, PDI =1.05); right (dashed line): PHB produced by only adding one aliquot of 200 equivalents BBL to **30** (M_n = 20.4 kDa, PDI =1.02). Reactions were carried out in THF at room temperature with [**30**] = 0.0045 mol/L.

Table 2.9 Summary of synthesized PLLA-*b*-PHB-*b*-PDLA

Entry[a]	Monomers (M_1+M_2+M_3)	Equiv. (M_1+M_2+M_3)	$M_{n,theo}$[b] (kDa)	$M_{n,expt}$ (kDa)	PDI
1	L+*rac*-BBL+D	426+544+426	170	153.0[c]	1.14[c]
2	L+*rac*-BBL+D	530+197+530	170	-[d]	-[d]

[a]Reactions were carried out in CH_2Cl_2, 25 °C, with [**30**] ≈ 1 mmol/L during polymerization of the first monomer, 0.5 mmol/L of the second monomer and 0.3 mmol/L of the third monomer, with conversion over 99%. [b]Calculated from $M_{n,theo} = MW_{LA} \times Equiv._{(M1+M3)} + MW_{BBL} \times Equiv._{M2}$. [c]The sample was highly insoluble in THF and therefore GPC measurement was run in $CHCl_3$, calibrated with monodispersed polystyrene standards. The results were multiplied by a Mark Houwink factor of 0.58 for PLA. [d]The sample was hardly dissolved in $CHCl_3$ either and therefore molecular weight was not able to be determined with existing facilities.

A series of triblock copolymers containing different weight percentages of racemic PHB as the middle segment were also made (Table 2.9). The sample in entry 1 contains 27 wt% PHB,

designed to be a comparable analogue to entry 1 in Table 2.4 which contains 27 wt% PDLLA for the middle block. Entry 2 represents a sample with even less racemic content, containing only 10 wt% PHB. The properties of these triblock copolymers are currently under investigation.

Polymerization of caprolactone and functionalized monomers

Poly(ε-caprolactone) (PCL), which is derived from the ROP of ε-caprolactone (CL), has a central position among aliphatic polyesters due to the desirable combination of biocompatibility, permeability and good mechanical properties. As with LA, and BBL, our indium catalyst **30** is active for the polymerization of CL. Rates of polymerization of CL in CD_3CN were obtained at two different temperatures and show a two fold increase in rate with a ten degree increase in temperature (Table 2.10). Compared to the rate of LA (k = 0.55 $s^{-1}\cdot M^{-1}$, CD_2Cl_2, 25 °C), the rate of CL is slower even at elevated temperature (k = 0.23 $s^{-1}\cdot M^{-1}$, CD_3CN, 50 °C). It is worth noting that the polymerization of CL is usually faster than the polymerization of lactide.[122] Catalysts which polymerize LA faster than CL are very rare.[123] Further theoretical calculations would be helpful to explain the unusual result for our indium catalyst **30**.

Table 2.10 Polymerization of CL monitored by *in situ* ^{1}HNMR

Entry	Solvent	Temp[a] (°C)	[**30**] (mmol/L)	M/I	k_{obs} ($*10^{-5}$ s^{-1})
1	CD_3CN	40.3	4.6	200	45.5
2	CD_3CN	50.8	4.6	200	105.8

[a]Monitored *in situ* on a Bruker Avance 400 MHz spectrometer. The temperature was calibrated with 80% ethylene glycol in DMSO-d_6.

Importantly, **30** is able to ring open polymerize functionalized monomers. Allyl-β-butyro-lactone (fBL) (Scheme 2.3) were synthesized according to known procedures *via* carbonylation of epoxide precursors[55] by Dr. Pothupitiya in our group. Preliminary

copolymerization experiments of BBL/LA and small percentages of fBL were carried out (Table 2.11). For all three copolymerizations, ^{1}H NMR spectra showed fBL was converted over 97% in approximately 18 hours. GPC data showed that the molecular weights are consistent with theoretical calculations. The molecular weight of PLLA-*b*-poly(fBL) (entry 2) has a 50% deviation from the calculated value, which might be a result of poor initiation of fBL by the growing polylactide chain. These results support the activity of **30** towards functionalized β-lactones and the feasibility of synthesizing functionalized copolymers with this catalyst.

Table 2.11 Copolymerization based on fBL

Entry[a]	Copolymer type	M_1	M_2	Equiv. (M_1+M_2)	$M_{n,\,theo}$ (kDa)	$M_{n,\,gpc}$ (kDa)	PDI
1	random	BBL	fBL	100+20	10.1	12.5	1.01
2	block	BBL	fBL	100+20	11.1	15.8	1.01
3	block	L-LA	fBL	100+20	16.9	25.5	1.20

[a]Entries 1 and 2 were carried out in THF at 25 °C. Entry 3 was carried in CH_2Cl_2 at 25 °C for the polymerization of L-LA and at 50 °C for the polymerization of fBL.

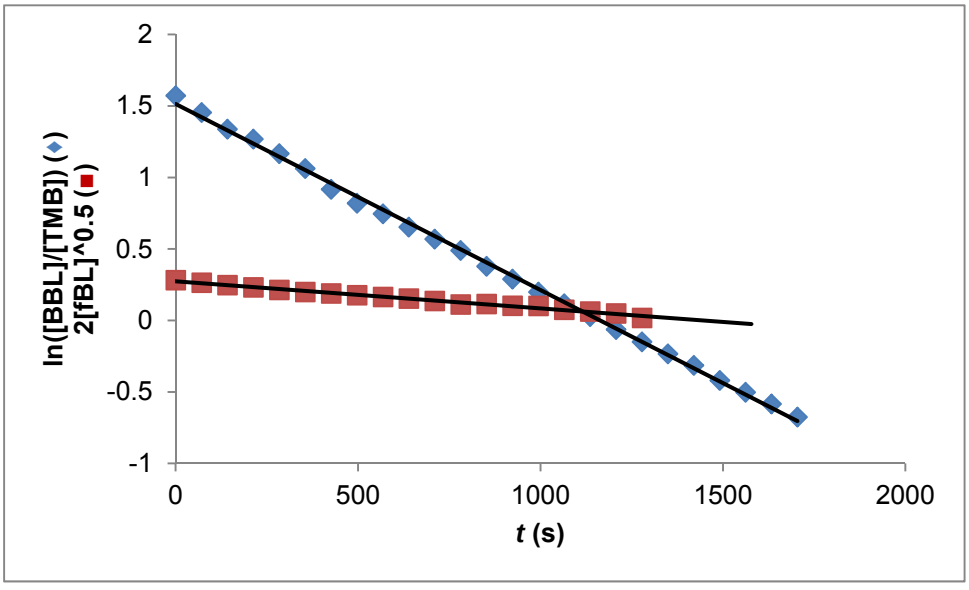

Figure 2.16 Preliminary data of concentration of BBL and fBL versus time in a random copolymerization. (♦ = ln([BBL]/[TMB]); ■ = 2[fBL]^0.5) Polymerization was carried out in CD_3CN at 60.6 °C, monitored *in situ* with 400 MHz ^{1}H NMR spectroscopy, with [**30**] = 0.0047 M, [BBL] = 0.45 M and [fBL] = 0.086 M.

Carpentier *et al.* have reported homopolymerizations and copolymerizations of fBL.[124] They observed a significantly slower rate for fBL than for BBL by more than two orders of magnitude with catalyst **23b**. As a consequence, the presence of the allyl-β-butyrolactone decreased the overall polymerization rate. However, in our study, kinetic monitoring of the copolymerization of BBL and fBL ([BBL]/[fBL] = 5:1) showed that both monomers were consumed within half an hour. The rate of BBL was still first order in [BBL] (Figure 2.16), with the rate constant not affected by the added fBL ($k^{BBL}_{copolymerization}$ = 0.29 $s^{-1}\cdot M^{-1}$, compared to $k^{BBL}_{homopolymerization}$ = 0.28 $s^{-1}\cdot M^{-1}$). The rate of fBL was half order in [fBL] (Figure 2.16). Confirmation of these results and further work with these functionalized monomers is ongoing.

2.3 Conclusion

Our indium catalyst **30** exhibits activity towards a variety of cyclic esters and living characteristics towards lactide and BBL *via* ring-opening polymerization. The range of molecular weights corresponding to the feeding ratios of LA was expanded to 300 kDa with narrow PDIs. A series of well-defined diblock copolymers PLLA-*b*-PDLLA with different ratios of L-LA and DL-LA were made for the first time, *via* a sequential addition technique. The thermal, rheological and mechanical properties of these diblock copolymers and their equivalent blends have been investigated.[113] The crystalline content in the blends of homopolymer PLAs decreases with addition of amorphous PLA, while the melting points remain unchanged. The crystallization of diblock copolymers is different from that of equivalent blends as a result of the covalent connection between L and DL chains that restricts molecular flexibility for ease of molecular orientation. As a result, the crystallinity of diblocks decreases compared to that of the corresponding blends. For PLLA-*b*-PDLA diblocks, formation of stereocomplex crystallites leads to a high melting point (> 200 °C). Also, unprecedented triblock copolymers PLLA-*b*-PDLLA-*b*-PLLA and PLLA-*b*-PDLLA--*b*-PDLA were made and studies on their properties are ongoing.

The polymerization rate of BBL with **30** is highly solvent dependent. The polymerization reactivity follows the trend THF >> CH_3CN > CH_2Cl_2 >> toluene, indicating the importance of solvent polarity and coordinating ability for this indium system. The relationship between molecular weight and [BBL]:[**30**] was studied with [BBL]:[**30**] up to 5000, providing PHB with molecular weight up to 300 kDa, which makes **30** the only catalyst to our knowledge that produces PHB with high MW in agreement with theoretical values to some extent. Unlike the polymerization of LA with **30**, which yields slightly isotactic PLA (P_m ~ 0.65), polymerization of BBL only affords atactic PHB. Kinetic studies on the relationship between the rate and concentration of **30** shows that the rate is first order in [**30**]. An Eyring plot was created *via* studies on the rates of polymerizations at variable temperatures. $\Delta H^{\neq}$ and $\Delta S^{\neq}$ were obtained as 58(±4) kJ/mol and −128(±9) J/(mol·K) respectively. Experiments of sequential addition of BBL show that the polymerization of BBL is controlled. Thus triblock copolymers PLLA-*b*-PHB-*b*-PDLA were made for the first time, *via* a sequential addition technique. Studies on the properties of these triblock copolymers are being carried out.

For other cyclic esters, preliminary polymerization of CL with **30** shows a slower rate than LA, which is an unusual phenomenon. The high activity of **30** towards ally-β-butyrolactone allowed us to prepare copolymers containing alkene functionality in a pendent group to the main PHB chain.

In conclusion, our indium catalyst **30** is highly active in living/controlled ring-opening polymerization of a variety of cyclic esters and well-defined block copolymers of polyesters were made with their properties under investigation.

2.4 Experimental

General Considerations. All the air and moisture sensitive manipulations were carried out in an MBraun glove box or using standard Schlenk line techniques. A Bruker Avance 300 MHz or 400 MHz spectrometer was used to record ^1H and ^{13}C spectra. A Bruker Avance 600 MHz

spectrometer was used to acquire homonuclear decoupled $^{1}H\{^{1}H\}$ spectra of polylactide and inverse gated $^{13}C\{^{1}H\}$ spectra for poly(hydroxybutyrate) operating at 150 MHz for determination of polymer tacticities. ^{1}H NMR chemical shifts are given in ppm versus residual protons in deuterated solvents as follows: δ 7.27 $CDCl_3$, δ 5.34 CD_2Cl_2, δ 3.58 THF-d_8 (O-CH_2), δ 2.09 Tol-d_8 (methyl), δ 1.94 CD_3CN. ^{13}C NMR chemical shifts are given in ppm versus residual ^{13}C in solvents as follows: δ 77.23 $CDCl_3$. Molecular weights and polydispersity indices were determined by triple detection gel permeation chromatography using a Waters liquid chromatograph equipped with a Waters 515 HPLC pump, a Waters 717 plus autosampler, Waters Styragel columns (4.6 × 300 mm) HR5E, HR4 and HR2, a Waters 2410 differential refractometer, a Wyatt tristar miniDAWN laser light scattering detector and a Wyatt ViscoStar viscometer. A flow rate of 0.5 mL/min was used and samples were dissolved in tetrahydrofuran (THF) (*ca.* 2 mg/mL). The measurements were carried out at laser wavelength of 690 nm, at 25 °C. The data were processed using the Astra software provided by Wyatt Technology Corp. A differential scanning calorimeter (DSC) Q1000 (TA Instruments) was employed to measure the glass transition (T_g) and melting (T_m) temperatures. Optical rotation of PLA was measured in chloroform with a concentration of 1 g/L with Jasco P-2000 Polarimeter under a wavelength of 589 nm at room temperature.

Materials. Toluene and THF were taken from an IT Inc. solvent purification system with activated alumina columns and degassed before use. CH_2Cl_2 and CH_3CN were refluxed with CaH_2, distilled and degassed before use. EtOH, $CDCl_3$, CD_2Cl_2 and CD_3CN were dried over CaH_2, transferred under vacuum and degassed through freeze-pump-thaw cycles before use. Toluene-d_8 and THF-d_8 were dried over Na/benzophenone, transferred under vacuum and degassed through freeze-pump-thaw cycles before use. DL-, L- and D-lactide were donated by Purac Biomaterials and recrystallized twice in toluene. Beta-butyrolactone, purchased from Aldrich, was stirred with CaH_2 for 48 hours, distilled under vacuum, degassed through freeze-pump-thaw cycles and kept in the freezer at −30 °C. The catalyst $[In(NNO)Cl_2]_2(\mu\text{-}OCH_2CH_3)(\mu\text{-}Cl)$ (**30**) was prepared by previously published procedures.[109]

NMR scale polymerization of β-butyrolactone. A teflon sealed J. Young NMR tube was

calibrated to have a 1.00 mL mark with pure NMR solvent by a 1.00 mL syringe. Complex **30** (5.0 mg, 0.0045 mmol) and 1,3,5-trimethoxybenzene (5.0 mg, 0.0030 mmol) were dissolved in CD_3CN and transferred to the tube. Then BBL (74.1 μL, 0.909 mmol) was added to the tube. CD_3CN was added until the total volume of the solution reached 1.00 mL. The reaction mixture was immediately cooled in liquid nitrogen. On a 400 MHz Bruker Avance NMR spectrometer, the target temperature was set at 60.0 °C. Ethylene glycol in DMSO-d_6 was used to calibrate the temperature of the spectrometer. Then the reaction tube was warmed up to room temperature and inserted into the spectrometer. Polymerization was monitored using ^{1}H NMR spectroscopy until over 90% conversion was reached.

Large-scale polymerization of β-butyrolactone. Complex **30** (5.0 mg, 0.0045 mmol) was dissolved in 1.00 mL THF and added into a vial with a magnetic stir bar. While stirring, BBL (74.1 μL, 0.909 mmol) was slowly added to this solution. The reaction was allowed to stir for 16 hours and then was quenched with acidic Et_2O (0.5 mL of 1.5 M HCl in Et_2O). A few drops of the reaction mixture were removed with a pipette to test conversion with ^{1}H NMR spectroscopy. The remaining reaction mixtures was dried under vacuum and dissolved in a minimum amount of CH_2Cl_2. The polymer was precipitated with cold methanol. The supernatant was decanted off and the polymer was then washed with cold methanol (1 × 3 mL) and dried under vacuum for 16 hours.

Synthesis of diblock polylactide. Complex **30** (18.3 mg, 0.0166 mmol) was dissolved in CH_2Cl_2 and transferred to a round bottom flask. While stirring, a solution of L-LA in CH_2Cl_2 (1.810 g, 12.6 mmol) was added slowly. The polymerization was allowed to stir overnight. A few drops of the reaction mixture were removed to check the conversion and molecular weight data of the first block before adding the solution of the second monomer. Then a solution of the second monomer *rac*-LA in CH_2Cl_2 (0.690 g, 4.79 mmol) was added to the reaction mixture. The reaction was allowed to stir overnight and then was quenched with acidic Et_2O (0.5 mL of 1.5 M HCl in Et_2O). A few drops of the mixture were removed to check conversion and the remaining mixture was concentrated under vacuum and the polymer was precipitated with cold MeOH. The resulting polymer was washed with cold

MeOH (3 × 3 mL) and dried under vacuum. The polymer was then redissolved in dry CH_2Cl_2, a thermal stabilizer (tris(nonylphenyl)phosphite (TNPP), 20.5 mg) was added and the solvent was removed under vacuum overnight.

Synthesis of triblock copolymers. Complex **30** (22.7mg, 0.0206 mmol) was dissolved in CH_2Cl_2 and transferred to a round bottom flask. While stirring, a solution of L-LA in CH_2Cl_2 (1.267 g, 8.80 mmol) was added slowly. The polymerization was allowed to stir for a few hours and then a solution of the second monomer *rac*-LA (0.966 g, 6.71 mmol) in CH_2Cl_2 was added to the reaction. The polymerization was allowed to stir overnight and a solution of the third monomer D-LA (1.267 g, 8.80 mmol) in CH_2Cl_2 was added to the reaction mixture. The reaction was allowed to stir overnight and then quenched with acidic Et_2O (0.5 mL of 1.5 M HCl in Et_2O). A few drops of the mixture were removed to check conversion and the remaining mixture was concentrated under vacuum and the polymer was precipitated with cold MeOH. The resulting polymer was washed with cold MeOH (3 × 3 mL) and dried under vacuum. The polymer was then redissolved in dry CH_2Cl_2, a thermal stabilizer (TNPP, 35.0 mg) was added and the solvent was removed under vacuum overnight. Parallel experiments of the synthesis of only the first block and the first two block polymers were carried out under the same condition to get information of the molecular weight of each block.

Synthesis of the PLLA and PDLLA homopolymers for blending. Complex **30** (22.1 mg, 0.0201 mmol) was dissolved in CH_2Cl_2 and transferred to a round bottom flask. While stirring, a solution of L-LA in CH_2Cl_2 (3.000 g, 20.8 mmol) was added slowly. The next day, the reaction was quenched with acidic Et_2O (0.5 mL of 1.5 M HCl in Et_2O). A few drops of the mixture were removed to test conversion with ^1H NMR spectroscopy. The remaining reaction mixture was concentrated and the polymer was precipitated with cold MeOH. The resulting polymer was washed with cold MeOH (3 × 3 mL) and dried under vacuum. The polymer was redissolved in dry CH_2Cl_2, a thermal stabilizer (TNPP, 30.0 mg) was added and the solvent was removed under vacuum overnight.

DSC measurement of PLA homopolymers and copolymers. Approximately 2–3 mg of the samples were weighed and sealed in an aluminum pan. The experiments were carried out under a nitrogen atmosphere. The samples were heated at a rate of 10 °C/min from 40 to 200 °C and held isothermally for 5 min to destroy any residual nuclei before cooling at 5 °C/min. The transition and melting temperatures were obtained from a second heating sequence, performed at 10 °C/min.

DSC measurement of polyhydroxybutyrate. The same as the procedure for PLA polymers, except that the sample was heated from −40 to 150 °C.

Optical rotation measurement of polylactide. 10.0 mg of PLA was dissolved in dry $CHCl_3$ and diluted into 10.00 mL with a volumetric flask. The optical rotation of the solution was measured under a wavelength of 589 nm at room temperature for five times with the interval as 10 seconds. The average of the results were calculated and used.

CHAPTER 3. Immortal Polymerization of Cyclic Esters

3.1 Introduction

As described in Chapter 2, in living polymerization the polymer chain ends remain active even after the consumption of monomer, and when fresh monomer is added, polymerization resumes. Along with the absence of a termination or irreversible chain transfer, another property is that the initiation rate is much faster than the propagation rate allowing all the chain ends to grow at the same rate. In a living system the polymer molecular weight is determined by the monomer:initiator ratio, therefore the molecular weight is linear with conversion. The polymers produced *via* living polymerization have predictable molecular weights and narrow molecular weight distributions.[90]

In a living polymerization, the amount of growing polymer chains equals the total number of active sites available from the catalyst molecules. For sing-site catalysts such as ours, this is equal to the amount of the catalyst (Scheme 3.1). The catalytic productivity therefore is low, since to grow each polymer chain needs one molecule of catalyst. In consequence, the contamination of the polymers from catalyst residues is considerably large. Nevertheless, immortal ring-opening polymerization can overcome these limitations.[91]

In contrast, immortal ROP (iROP) provides an efficient alternative to living ROP. This process involves a binary system consisting of a catalyst and an external nucleophile which plays the role of the chain transfer agent (CTA). As shown in Scheme 3.1, the number of growing polymer chains in an iROP exceeds the number of catalyst molecules and is equal to the amount of CTA plus the catalyst (in the case when the metal complex reacts with one molecule of CTA to form initiators in *situ*, the number of growing chains is equal to only the amount of CTA). Through iROP, less catalyst is required, thus cutting the work of ligand synthesis and decreasing the metal contamination in the synthesized materials.[91]

Scheme 3.1 Illustration of the distinction between living and immortal ROP processes

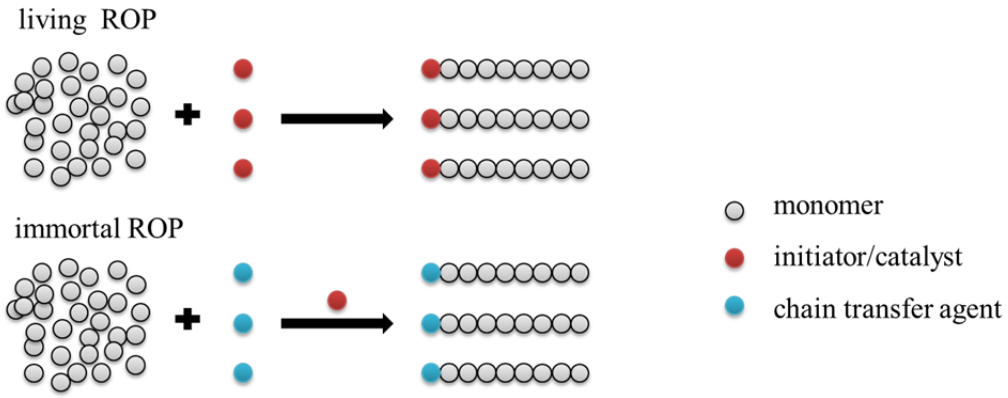

Scheme 3.2 Chain transfer in an immortal ROP

$$LnM(OR^1) + R^2OH \xrightarrow[k_{tr} \gg k_p]{k_{tr}} LnM(OR^2) + R^1OH \qquad (3.1)$$

Several features are necessary to achieve a successful iROP. The initiation must proceed faster than propagation and irreversible termination reactions must be absent or very minimal. Most importantly, the reversible transfer reactions must proceed faster than propagation (Scheme 3.2) so that all the chains can grow at the same rate. Catalysts that are stable under high loading of protic compound are necessary for iROP. The CTAs used are usually alcohols and sometimes amines. Functional alcohol can be used to introduce functional groups to the chain end of polymers.[97] Meanwhile, if macromolecular alcohols such as poly(ethylene glycol) (PEG) can work as CTA, copolymers containing PEG blocks can be achieved *via* iROP in one step.

There have been numerous studies on the synthesis and properties of PEG and polyesters block copolymers.[42, 103-105] Since PEG is hydrophilic and polyesters are usually hydrophobic, their block copolymers are amphiphilic. Amphiphilic block copolymers are able to form a range of different nanoparticulate structures. These include micelles, nanospheres, nanocapsules, and polymersomes, which have great potential as drug delivery carriers.[125] Popular methods to prepare nanoparticles from preformed copolymers include thin film

rehydration and nanoprecipitation/dialysis. In a nanoprecipitaion/dialysis process, the polymer is dissolved in a water-miscible organic solvent and the solution is then added to the aqueous phase with or without a surfactant. The organic solvent immediately diffuses out, resulting in the precipitation of the polymer and formation of nanoparticles. In the thin film rehydration method, a volatile organic solvent such as chloroform is used to dissolve the polymer and then evaporated under a stream of nitrogen gas, leaving the polymer as a thin film on the surface of the container. Under vigorous stirring, sonication and extrusion, the film is rehydrated with the aqueous phase, thus affording submicron vesicles with a narrow size distribution.[125]

There are fewer studies on the block copolymers of ethylene glycol and BBL than those with lactide or caprolactone. Poly(ethylene glycol) and poly(β-hydroxybutyrate) block copolymers have been made using: transesterification by PEG during fermentation[105b, c], condensation[104a, 105d, 105g], click chemistry[105i], anionic ROP of BBL with PEG macroinitiator[105h], and ROP of BBL in the presence of PEG[103a]. As mentioned in Chapter 1, there has been no report on iROP of BBL with PEG until present. Such a reaction would be a true one step reaction under mild condition, without heating and other reagents, which might contaminate the material. As an added bonus, better defined block copolymers can be obtained.

In this chapter, iROP of LA and BBL using our catalyst in the presence of ethanol and different-length PEG monomethyl ether (MePEG) was investigated. Block copolymers were made and their potential as drug carriers was evaluated in collaboration with Dr. Kevin Letchford at UBC Pharmaceutical Sciences.

3.2 Results

Immortal ring-opening polymerization of lactide

Immortal ROP was studied first with lactide (

Table **3.1**). Different equivalents of EtOH (based on the amount of catalyst) were added. The

molecular weight decreases as more EtOH was added. It is in an inverse relationship to the amount of initiation species, *i.e.*, the total amount of catalyst and alcohol. During the polymerization, the alcohol acts as a chain transfer agent (CTA), thus the propagating chain is switched between the alkoxides from catalyst and alcohol. The PDI value and P_m remain similar to those in the absence of the alcohol, making iROP an attractive way to decrease catalyst usage and scale up polymerization.

Table 3.1 Polymerization of *rac*-LA with different equivalents of EtOH

Entry[a]	[EtOH]/[**30**]	Conv.	$M_{n,theo}$[b] (kDa)	$M_{n,expt}$ (kDa)	PDI	P_m
1	0	99	144.0	109.4	1.02	0.57
2	1	98	72.0	75.53	1.03	0.60
3	2	99	48.0	48.29	1.02	0.60
4	3	98	36.0	33.46	1.01	0.58
5	4	98	28.8	30.79	1.01	0.59

[a]All the experiments were done in CH_2Cl_2, with 5.0 mg catalyst, [*rac*-LA]/[**30**] = 1000. [b]Calculated from: $M_n = MW_{LA} \times [LA]/([\mathbf{30}] + [EtOH]) \times Conv.$.

Immortal ROP of LA with low molecular weight MePEG (M_n = 350 g/mol, denoted as $MePEG_7$ with the subscript 7 representing the number of units of ethylene oxide in the molecule) results in well-defined polymers with low PDIs (Table 3.2, entries 1–5). The molecular weights of the resulting polymers were much lower than those in the situation without $MePEG_7$. As the amount of $MePEG_7$ used increases, the molecular weights of the polymers produced decreases. The experimental molecular weights fit the theoretical values very well, proving that in the short chain MePEG, the hydroxy group is active enough to perform chain transfer with the growing polymer chain during the polymerization.

In the experiments of iROP of LA with higher molecular weight MePEG (M_n = 5000 g/mol, denoted as $MePEG_{114}$ with the subscript 114 representing the number of units of ethylene oxide in the molecule) (Table 3.2, entries 6–10), **30** was stirred with $MePEG_{114}$ for 30 min and pumped down to dryness to remove the generated ethanol. Therefore the amount of

initiating group equals the amount of $MePEG_{114}$. The molecular weights of the resulting polymers were close to the theoretical values. PDI values are higher with shorter chain PLA segments in the copolymers, likely due to the larger PDI of the commercially available $MePEG_{114}$ itself. Since $MePEG_{114}$ is not as monodispersed as the homopolymers made with our living catalyst, the incorporation of $MePEG_{114}$ increases the PDI of the copolymers. As the PLA block gets longer, the differences of the copolymer chain lengths caused by $MePEG_{114}$ become less significant, thus resulting in a lower PDI. Another possible reason accounting for the high PDI is that THF is not a good solvent for this copolymer. Long chain PEG is not soluble in THF, which is the same situation for copolymers containing $MePEG_{114}$. Also, copolymers might form aggregates in THF, which can be detected by the light scattering detector of GPC, although no peaks were observed from the refractive index detector, due to low concentrations.

Table 3.2 Polymerization of L-LA with different equivalent of MePEG

Entry[a]	ROH	[LA]/[ROH]/[**30**]	Conv.	$M_{n,\,theo}$ (kDa)	$M_{n,\,expt}$ (kDa)	PDI
1	$MePEG_7$	1000/0/1	98	141.1[b]	144.2	1.06
2	$MePEG_7$	1000/1/1	99	71.30[b]	72.41	1.04
3	$MePEG_7$	1000/2/1	99	47.53[b]	49.54	1.03
4	$MePEG_7$	1000/3/1	98	35.29[b]	39.14	1.02
5	$MePEG_7$	1000/4/1	99	28.52[b]	29.79	1.02
6	$MePEG_{114}$	1000/5/1	> 99	33.8[c]	31.90	1.14
7	$MePEG_{114}$	520/5/1	> 99	20.0[c]	23.36	1.46
8	$MePEG_{114}$	500/10/1	> 99	12.2[c]	15.95	2.30
9	$MePEG_{114}$	250/10/1	> 99	8.6[c]	10.01	2.21

[a]All the experiments were done in CH_2Cl_2 at 25 °C. [b]Calculated from: $M_n = MW_{LA} \times [LA]/([\mathbf{30}] + [MePEG_7]) \times Conv. + 350$ g/mol. [c]Calculated from: $M_n = MW_{LA} \times [LA]/[MePEG_{114}] \times Conv. + 5000$ g/mol.

The formation of nanoparticles composed of $MePEG_{114}$-*b*-PLA_{105} (Table 3.2, entry 7, the subscripts 114 and 105 represent the numbers of the units of ethylene oxide and lactide

respectively in the copolymer blocks) and $MePEG_{114}$-*b*-PLA_{200} (Table 3.2, entry 6) was investigated *via* thin film rehydration and nanoprecipitation/dialysis methods.

Using thin film rehydration, $MePEG_{114}$-*b*-PLA_{200} did not solubilize and remained as a film on the side of the vial wall. $MePEG_{114}$-*b*-PLA_{105} fragmented and remained as a milky precipitate after rehydration and stirring overnight. These results might indicate that the copolymers with more than 100 units of lactide are too hydrophobic to be an effective substrate for thin film rehydration.

In nanoprecipitation, dimethylformamide (DMF) was used as the water miscible organic solvent. $MePEG_{114}$-*b*-PLA_{105} precipitated into a nanodispersion as indicated by the formation of an opalescent solution. The average diameter of these nanoparticles is approximately 50 nm with a polydispersity index of 0.079 (Figure 3.1).*

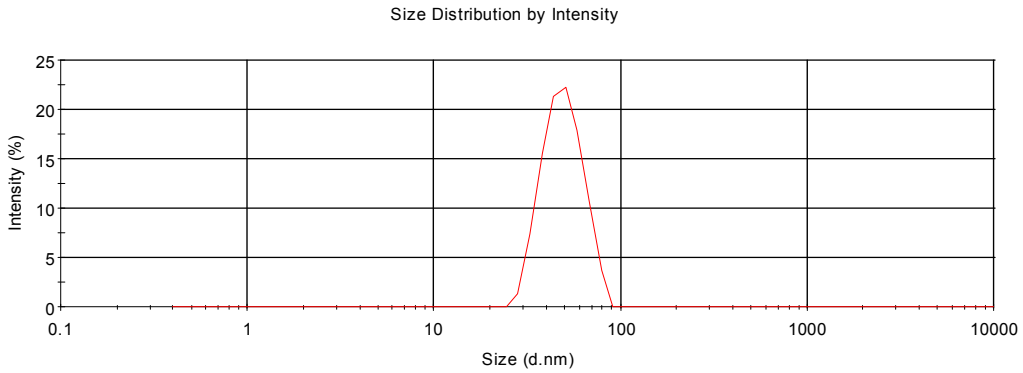

Figure 3.1 Representative plot of the particle size distribution of $MePEG_{114}$-*b*-PLA_{105} nanoparticles prepared by nanoprecipitation and dialysis using a 1:4 ratio of DMF:H_2O

Using nanoprecipitation, $MePEG_{114}$-*b*-PLA_{200} did not precipitate but formed a gel when added to water. Therefore, different DMF:H_2O ratios were used: 1) dissolved in1 mL DMF and dripped into 2 mL H_2O; 2) dissolved in 2 mL DMF and dripped into 1 mL H_2O; 3) dissolved in 3 mL DMF without addition to H_2O. It was found that only addition of

*The polydispersity index (PI) of nanoparticles is used to indicate the uniformity of the nanoparticles. Nanoparticles with a PI around 0.05 are considered as monodisperse. The PI here was provided by the Malvern Nano ZS software.

DMF:water (with copolymer dissolved in the DMF) in a 2:1 ratio resulted in a nanodispersion. Particles have an average diameter of approximately 100 nm with a polydispersity index of 0.169 (Figure 3.2). This is quite promising as we have previously not been able to prepare nanoparticles composed of copolymers with such a long hydrophobic block by nanoprecipitation. Studies on the drug encapsulation and release by these MePEG-*b*-PLA nanoparticles are on-going.

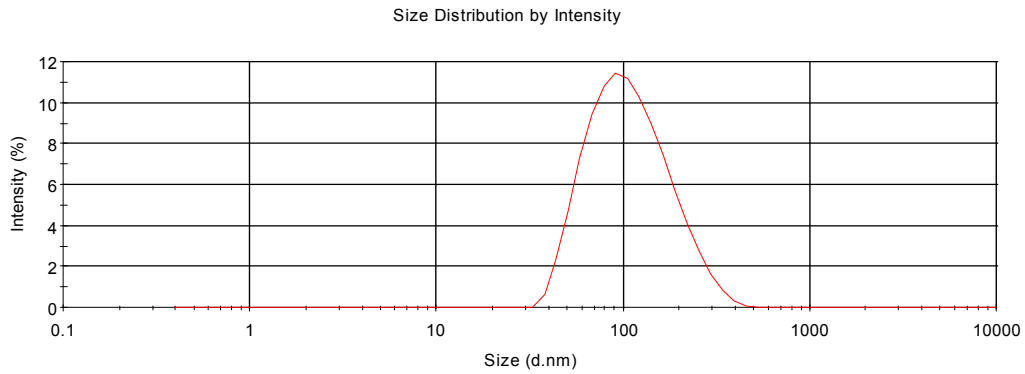

Figure 3.2 Representative plot of the particle size distribution of $MePEG_{114}$-*b*-PLA_{200} nanoparticles prepared by nanoprecipitation and dialysis using a 2:1 ratio of DMF:H_2O

Immortal ring-opening polymerization of β-butyrolactone

Immortal ROP was then expanded to BBL. Ethanol and $MePEG_7$ were used as the CTA as well. Results are summarized in Table 3.3. Polymerization of BBL with different amounts of ethanol shows that the molecular weight of the resulting polymer decreases as more EtOH was added as well. It is in inverse proportion to the amount of initiation species, *i.e.*, the total amount of catalyst and ethanol. With a high loading of BBL (as high as 4000 equivalents), polymerization at the presence of 10 equivalents of EtOH still yielded nearly monodispersed PHB. Similar results are observed during the polymerization of BBL with $MePEG_7$. Remarkably, entries 12 to 14, BBL loading as high as 10000 can be used (Table 3.3, entries 12–14). Reactions reached conversions over 90%, yielding polymers with molecular weights close to theoretical calculation. Based on our knowledge, 10000 equivalents of BBL with 100 equivalents $MePEG_7$ is the highest monomer and alcohol loadings ever used in iROP of BBL.

All these results proved that iROP of BBL with different alcohols were active and proficient.

Table 3.3 Immortal ROP of BBL with EtOH and $MePEG_7$

Entry[a]	ROH	[BBL]/[ROH]/[**30**]	$M_{n,theo}$ (kDa)	$M_{n\ expt}$ (kDa)	PDI
1	-	1000/0/1	86.09[b]	82.89	1.07
2	EtOH	1000/1/1	43.04[b]	39.97	1.02
3	EtOH	1000/2/1	28.70[b]	28.34	1.01
4	EtOH	1000/3/1	21.52[b]	21.85	1.01
5	EtOH	1000/4/1	17.22[b]	16.77	1.01
6	EtOH	4000/10/1	31.31[b]	44.02	1.01
7	$MePEG_7$	1000/1/1	43.24[c]	42.67	1.02
8	$MePEG_7$	1000/2/1	28.95[c]	27.97	1.01
9	$MePEG_7$	1000/3/1	21.80[c]	21.07	1.01
10	$MePEG_7$	1000/4/1	17.51[c]	17.07	1.02
11	$MePEG_7$	1000/10/1	8.149[c]	7.824	1.03
12	$MePEG_7$	10000/20/1	40.92[c]	36.09	1.01
13	$MePEG_7$	10000/50/1	16.89[c]	14.90	1.01
14	$MePEG_7$	10000/100/1	8.359[c]	7.569	1.03

[a]All the experiments were done in THF at r.t., overnight to reach > 99% conversion, except 14, whose conversion is 94%. [b]Calculated from $M_{n,theo} = MW_{BBL} \times [BBL]/([\mathbf{30}] + [EtOH]) \times Conv.$. [b]Calculated from $M_{n,theo} = MW_{BBL} \times [BBL]/([\mathbf{30}] + [MePEG_7]) \times Conv. + 350$ g/mol.

Immortal polymerization of BBL with $MePEG_{114}$ and application of the polymers in drug encapsulation and delivery are being studied by Dr. Kevin Letchford and Prof. Helen Burt at UBC Pharmaceutical Sciences.

3.3 Conclusions and future work

Immortal polymerization of LA and BBL with our catalyst is very rapid, with monomer loading capacity up to 4000–10000 in the presence of 100 equivalents of alcohol. With this

method, block copolymers containing $MePEG_{114}$ were made. These copolymers can form nanoparticle with sizes suitable for drug delivery. Further investigations are being carried out on other polymer properties.

Further studies on the polymerization of BBL with **30** are necessary to elucidate the mechanism in deep. Polymerization in other solvents can be carried out to estimate the significance of each factor that induces the rate difference. The polymerization rates should be obtained in a polar but non-coordinating solvent and a nonpolar but coordinating solvent to estimate the effects from polarity and coordinating ability. Modeling and calculations will be helpful to elucidate the detailed mechanism of polymerization.

Studies of ROP of CL with **30** should be carried out to confirm reactivity of **30** towards CL. If CL is truly polymerized more slowly by **30** than LA, this piece of information might be useful in understanding the difference between these two monomers and the novelty of our indium catalyst compared to other catalysts.

The copolymers containing allyl-β-butyrolactone should be further crosslinked through the alkene functionality to prepare 3D network materials. Beta-lactones bearing other functionalities can be synthesized *via* carbonylation of epoxides.

Kinetic studies on the immortal polymerization of LA and BBL should be carried out to further investigate the mechanism of iROP. The drug delivery study of the resulting MePEG and PLA block copolymers should be carried out and compared with copolymers synthesized from other methods, in order to explore the advantage of iROP. PEG and PHB block copolymers with different lengths of PHB blocks should be synthesized to investigate how the block length of PHB will affect the drug encapsulation and release.

3.4 Experimental

General Consideration. The same as section 2.4.

Materials. The same as section 2.4. $MePEG_7$ and $MePEG_{114}$ (molecular weights 350 and 5000 g/mol) were purchased from Sigma-Aldrich and dried by adding dry toluene and pumping down to dryness for 2 cycles.

Immortal polymerization of *rac*-LA with 30 in the presence of ethanol. A 20 mL scintillation vial vas charged with a stirring bar and a 0.25 mL solution of **30** in CH_2Cl_2 (**30**, 0.0182 M, 0.0045 mmol). 13.4 μL of ethanol in CH_2Cl_2 (0.685 M, 0.0092 mmol) was added to the stirring catalyst solution. Subsequently, *rac*-LA (654 mg, 4.5 mmol) was dissolved in CH_2Cl_2 and slowly added in to the stirring solution. The total volume of the solution was around 4 mL. The reaction was stirred overnight and then quenched with acidic Et_2O (0.5 mL of 1.5 M HCl). A few drops of the reaction mixture were removed to test conversion with ^1H NMR spectroscopy. The remaining reaction mixture was dried under vacuum and dissolved in a minimum amount of CH_2Cl_2 and the polymer was precipitated with cold methanol. The supernatant was decanted off and the polymer was then washed with cold methanol (1× 3 mL) and dried under vacuum overnight.

Immortal polymerization of L-LA with 30 in the presence of $MePEG_7$. A 20 mL scintillation vial vas charged with a stirring bar and a 0.90 mL solution of **30** in CH_2Cl_2 (**30**, 0.00309 M, 0.00278 mmol). 44.7 μL of $MePEG_7$ in CH_2Cl_2 (0.0622 M, 0.00278 mmol) was added to the stirring catalyst solution. Subsequently, *rac*-LA (401 mg, 2.78 mmol) was dissolved in CH_2Cl_2 and slowly added in to the stirring solution. The total volume of the solution was around 5 mL. The reaction was stirred overnight and then quenched with acidic Et_2O (0.5 mL of 1.5 M HCl). A few drops of the reaction mixture were removed to test conversion with ^1H NMR spectroscopy. The remaining reaction mixture was dried under vacuum and dissolved in a minimum amount of CH_2Cl_2 and the polymer was precipitated with cold methanol. The supernatant was decanted off and the polymer was then washed with

cold methanol (1× 3 mL) and dried under vacuum overnight.

Immortal polymerization of BBL with 30 in the presence of ethanol. A 20 mL scintillation vial vas charged with a stirring bar and a 0.90 mL solution of **30** and TMB in THF (**30**, 0.00305 M, 0.00275 mmol; TMB, 0.0346 M, 0.0311 mmol). 32.1 μL of ethanol in THF (0.171 M, 0.00550 mmol) was added to the stirring catalyst solution. Subsequently, 224 μL BBL (2.75 mmol) was slowly added in to the stirring solution. The reaction was stirred overnight and then quenched with acidic Et_2O (0.5 mL of 1.5 M HCl). A few drops of the reaction mixture were removed to test conversion with ^1H NMR spectroscopy. The remaining reaction mixture was dried under vacuum and dissolved in a minimum amount of CH_2Cl_2 and the polymer was precipitated with cold methanol. The supernatant was decanted off and the polymer was then washed with cold methanol (1× 3 mL) and dried under vacuum overnight.

Immortal polymerization of BBL with 30 in the presence of $MePEG_7$. A 20 mL scintillation vial vas charged with a stirring bar and a 0.90 mL solution of **30** and TMB in THF (**30**, 0.00304 M, 0.00273 mmol; TMB, 0.0357 M, 0.0321 mmol). 43.9 μL of $MePEG_7$ in THF (0.0622 M, 0.0027 mmol) was added to the stirring catalyst solution. Subsequently, 223 μL BBL (2.73 mmol) was slowly added in to the stirring solution. The reaction was stirred overnight and then quenched with acidic Et_2O (0.5 mL of 1.5 M HCl). A few drops of the reaction mixture were removed to test conversion with ^1H NMR spectroscopy. The remaining reaction mixture was dried under vacuum and dissolved in a minimum amount of CH_2Cl_2 and the polymer was precipitated with cold methanol. The supernatant was decanted off and the polymer was then washed with cold methanol (1× 3 mL) and dried under vacuum overnight.

Immortal polymerization of *rac*-LA with 30 in the presence of $MePEG_{114}$. A round bottom flask was charged with **30** in CH_2Cl_2 (73.5 mg, 0.0668 mmol) and $MePEG_{114}$ in THF (1.67 g, 0.334 mmol). The mixture was allowed to stir for half an hour and dried under vacuum. CH_2Cl_2 was added to dissolve the dry residue again. While stirring, *rac*-LA in CH_2Cl_2 (5.00 g, 34.7 mmol) was added slowly to the solution. The reaction was allowed to stir overnight and then was quenched with acidic Et_2O (0.5 mL of a 1.5 M HCl in Et_2O). A

few drops of the reaction mixture were removed to check conversion with ^{1}H NMR spectroscopy. The remaining mixture was dried under vacuum and dissolved in a minimum amount of CH_2Cl_2 and the polymer was precipitated in 1:1 Et_2O/hexane. The supernatant was decanted off and the polymer was washed with 1:1 Et_2O/hexane (3 × 3 mL) and dried under vacuum overnight.

Nanoparticles preparation from PEG-*b*-PLA *via* thin film rehydration. In a vial, 20 mg of copolymer was dissolved with 0.5 mL of CH_2Cl_2. The solvent was evaporated by N_2 flow to allow the polymer to form a thin film coating on the wall of the vial. Then 2 mL of deionized H_2O at 60 °C was added to the film and the mixture was allowed to stir at 200 rpm overnight.

Nanoparticles preparation from PEG-*b*-PLA *via* nanoprecipitation and dialysis. In a vial, 30 mg of copolymer was dissolved with 0.5 mL dimethylformamide. The solution was added dropwise to 2 mL of deionized water stirring at 1600 rpm. Then the mixture was transferred to 3500 MWCO dialysis tubing and dialysed against deionized H_2O overnight.

Measurement of the sizes of the nanoparticles prepared from PEG-*b*-PLA. The nanoparticles were prepared at a concentration of 10mg/mL and in phosphate buffered saline (10 mM, pH 7.4) and sized on a Malvern Nanosizer ZS at 25 °C using a 633nm laser with detection at 175 degrees (back scattering).

Bibliography

1.Peacock, A. J.; Calhoun, A. *Polymer Chemistry - Properties and Applications*, 1st ed.; Hanser Publishers: Munich, 2006.

2.*BP Statistical Review of World Energy*; 2011.

3.Mecking, S. *Angew. Chem. Int. Ed.* **2004**, *43*, 1078-1085.

4.Okada, M. *Prog. Polym. Sci.* **2002**, *27*, 87-133.

5.(a) Dubois, P.; Narayan, R. *Macromol. Symp.* **2003**, *198*, 233-243; (b) Ciardelli, G.; Chiono, V.; Vozzi, G.; Pracella, M.; Ahluwalia, A.; Barbani, N.; Cristallini, C.; Giusti, P. *Biomacromolecules* **2005**, *6*, 1961-1976.

6.Doi, Y. *Microbial Polyesters*; VCH-Publisher: New York, 1990.

7.Gao, H. J.; Wu, Q. N.; Chen, G. Q. *FEMS Microbiol. Lett.* **2002**, *213*, 59-65.

8.Chen, G. Q. *Chem. Soc. Rev.* **2009**, *38*, 2434-2446.

9.Chen, G. Q.; Wu, Q. *Biomaterials* **2005**, *26*, 6565-6578.

10.Bianco, B.; Castaldo, L.; del Gaudio, A.; Maglio, G.; Palumbo, R.; La Cara, F.; Peluso, G.; Petillo, O. *Polym. Bull.* **1997**, *39*, 279-286.

11.(a) Kylma, J.; Seppala, J. V. *Macromolecules* **1997**, *30*, 2876-2882; (b) van Dijkhuizen-Radersma, R.; Roosma, J. R.; Kaim, P.; Metairie, S.; Peters, F. L. A. M. A.; de Wijn, J.; Zijlstra, P. G.; de Groot, K.; Bezemer, J. M. *J. Biomed. Mater. Res. A* **2003**, *67A*, 1294-1304; (c) Guan, H.-L.; Deng, C.; Xu, X.-Y.; Liang, Q.-Z.; Chen, X.-S.; Jing, X.-B. *J. Polym. Sci., Part A: Polym. Chem.* **2005**, *43*, 1144-1149.

12.Demicheli, A.; Russo, S.; Mariani, A. *Polymer* **2000**, *41*, 1481-1486.

13.Drumright, R. E.; Gruber, P. R.; Henton, D. E. *Adv. Mater.* **2000**, *12*, 1841-1846.

14.(a) Madhavan Nampoothiri, K.; Nair, N. R.; John, R. P. *Bioresour. Technol.* **2010**, *101*, 8493-8501; (b) Lasprilla, A. J. R.; Martinez, G. A. R.; Lunelli, B. H.; Jardini, A. L.; Filho, R. M. *Biotechnol. Adv.* **2012**, *30*, 321-328.

15.NatureWorks LLC. http://www.natureworksllc.com/ (accessed Dec 20, 2011).

16.PURALACT by PURAC. http://www.purac.com/EN/Bioplastics/PLA/Brands.aspx (accessed Dec 20, 2011).

17.Kalb, B.; Pennings, A. J. *Polymer* **1980**, *21*, 607-612.

18.Fukushima, K.; Hirata, M.; Kimura, Y. *Macromolecules* **2007**, *40*, 3049-3055.

19.(a) Jun, C. L. *J. Polym. Environ.* **2000**, *8*, 33-37; (b) Chen, C.-C.; Chueh, J.-Y.; Tseng, H.; Huang, H.-M.; Lee, S.-Y. *Biomaterials* **2003**, *24*, 1167-1173.

20.Tsuji, H.; Ikada, Y. *J. Appl. Polym. Sci.* **1995**, *58*, 1793-1802.

21.Ikada, Y.; Jamshidi, K.; Tsuji, H.; Hyon, S. H. *Macromolecules* **1987**, *20*, 904-906.

22.Fukushima, K.; Kimura, Y. *Polym. Int.* **2006**, *55*, 626-642.

23.(a) Stayshich, R. M.; Meyer, T. Y. *J. Am. Chem. Soc.* **2010**, *132*, 10920-10934; (b) Li, J.; Stayshich, R. M.; Meyer, T. Y. *J Am Chem Soc* **2011**, *133*, 6910-6913.

24.(a) Duda, A.; Kowalski, A. Thermodynamics and Kinetics of Ring-Opening Polymerization. In *Handbook of Ring-Opening Polymerization*, Dubois, P.; Coulembier, O.; Raquez, J.-M., Eds.; Wiley-VCH Verlag GmbH & Co. KGaA: Weinheim, 2009; pp 1-51; (b) Thomas, C. M. *Chem. Soc. Rev.* **2010**, *39*, 165.

25.Malcolm, C.; Zhiping, Z. Stereoselective Polymerization of Lactide. In *Stereoselective Polymerization with Single-Site Catalysts*, CRC Press: 2007; pp 645-660.

26.Dechy-Cabaret, O.; Martin-Vaca, B.; Bourissou, D. *Chem. Rev.* **2004**, *104*, 6147-6176.

27.Ovitt, T. M.; Coates, G. W. *J. Am. Chem. Soc.* **1999**, *121*, 4072-4073.

28.Ovitt, T. M.; Coates, G. W. *J. Am. Chem. Soc.* **2002**, *124*, 1316-1326.

29.Spassky, N.; Wisniewski, M.; Pluta, C.; LeBorgne, A. *Macromol. Chem. Phys.* **1996**, *197*, 2627-2637.

30.Zhong, Z. Y.; Dijkstra, P. J.; Feijen, J. *Angew. Chem. Int. Ed.* **2002**, *41*, 4510-4513.

31.Nomura, N.; Ishii, R.; Akakura, M.; Aoi, K. *J. Am. Chem. Soc.* **2002**, *124*, 5938-5939.

32.Hormnirun, P.; Marshall, E. L.; Gibson, V. C.; White, A. J. P.; Williams, D. J. *J. Am. Chem. Soc.* **2004**, *126*, 2688-2689.

33.Arnold, P. L.; Buffet, J. C.; Blaudeck, R. P.; Sujecki, S.; Blake, A. J.; Wilson, C. *Angew. Chem. Int. Ed.* **2008**, *47*, 6033-6036.

34.Chamberlain, B. M.; Cheng, M.; Moore, D. R.; Ovitt, T. M.; Lobkovsky, E. B.; Coates, G. W. *J. Am. Chem. Soc.* **2001**, *123*, 3229-3238.

35.Chisholm, M. H.; Gallucci, J. C.; Phomphrai, K. *Inorg. Chem.* **2004**, *43*, 6717-6725.

36.Chmura, A. J.; Chuck, C. J.; Davidson, M. G.; Jones, M. D.; Lunn, M. D.; Bull, S. D.; Mahon, M. F. *Angew. Chem. Int. Ed.* **2007**, *46*, 2280-2283.

37.Pietrangelo, A.; Hillmyer, M. A.; Tolman, W. B. *Chem. Commun.* **2009**, 2736-2737.

38.Amgoune, A.; Thomas, C. M.; Carpentier, J.-F. *Pure Appl. Chem.* **2007**, *79*, 2013-2030.

39.(a) Cai, C. X.; Amgoune, A.; Lehmann, C. W.; Carpentier, J.-F. *Chem. Commun.* **2004**, 330-331; (b) Amgoune, A.; Thomas, C. M.; Roisnel, T.; Carpentier, J.-F. *Chem. Eur. J.* **2006**, *12*, 169-179.

40.Zhao, K.; Deng, Y.; Chen, J. C.; Chen, G. Q. *Biomaterials* **2003**, *24*, 1041-1045.

41.Wang, Z. X.; Itoh, Y.; Hosaka, Y.; Kobayashi, I.; Nakano, Y.; Maeda, I.; Umeda, F.; Yamakawa, J.; Kawase, M.; Yagi, K. *J. Biosci. Bioeng.* **2003**, *95*, 541-543.

42.Shah, M.; Naseer, M. I.; Choi, M. H.; Kim, M. O.; Yoon, S. C. *Int. J. Pharm.* **2010**, *400*, 165-175.

43.Cheng, G. X.; Cai, Z. J.; Wang, L. *J. Mater. Sci.-Mater. M.* **2003**, *14*, 1073-1078.

44.Kemnitzer, J. E.; McCarthy, S. P.; Gross, R. A. *Macromolecules* **1992**, *25*, 5927-5934.

45.Tsuji, H.; Suzuyoshi, K. *Polym. Degrad. Stabil.* **2002**, *75*, 347-355.

46.Jendrossek, D.; Schirmer, A.; Schlegel, H. G. *Appl. Microbiol. Biotechnol.* **1996**, *46*, 451-463.

47.Abe, H.; Doi, Y. *Macromolecules* **1996**, *29*, 8683-8688.

48.Metabolix. http://www.metabolix.com/ (accessed Dec 20, 2011).

49.Calabia, B. P.; Tokiwa, Y. *Biotechnol. Lett.* **2006**, *28*, 383-388.

50.Zhang, X.; Luo, R.; Wang, Z.; Deng, Y.; Chen, G.-Q. *Biomacromolecules* **2009**, *10*, 707-711.

51.Getzler, Y. D. Y. L.; Mahadevan, V.; Lobkovsky, E. B.; Coates, G. W. *J. Am. Chem. Soc.* **2002**, *124*, 1174-1175.

52.Getzler, Y. D. Y. L.; Mahadevan, V.; Lobkovsky, E. B.; Coates, G. W. *Pure Appl. Chem.* **2004**, *76*, 557-564.

53.Schmidt, J. A. R.; Mahadevan, V.; Getzler, Y. D. Y. L.; Coates, G. W. *Org. Lett.* **2004**, *6*, 373-376.

54.Schmidt, J. A. R.; Lobkovsky, E. B.; Coates, G. W. *J. Am. Chem. Soc.* **2005**, *127*, 11426-11435.

55.Kramer, J. W.; Lobkovsky, E. B.; Coates, G. W. *Org. Lett.* **2006**, *8*, 3709-3712.

56.Church, T. L.; Getzler, Y. D. Y. L.; Coates, G. W. *J. Am. Chem. Soc.* **2006**, *128*,

10125-10133.

57.Choi, J.; Lee, S. Y. *Appl. Microbiol. Biotechnol.* **1999**, *51*, 13-21.

58.(a) Lee, J. T.; Alper, H. *Macromolecules* **2004**, *37*, 2417-2421; (b) Allmendinger, M.; Molnar, F.; Zintl, M.; Luinstra, G. A.; Preishuber-Pflugl, P.; Rieger, B. *Chem. Eur. J.* **2005**, *11*, 5327-5332.

59.Stridsberg, K. M.; Ryner, M.; Albertsson, A. C. Controlled ring-opening polymerization: Polymers with designed macromolecular architecture. In *Degradable Aliphatic Polyesters*, Albertsson, A. C., Ed. Springer-Verlag Berlin: Berlin, 2002; Vol. 157, pp 41-65.

60.(a) Uyama, H.; Kobayashi, S. *Chem. Lett.* **1993**, 1149-1150; (b) Knani, D.; Gutman, A. L.; Kohn, D. H. *J. Polym. Sci., Part A: Polym. Chem.* **1993**, *31*, 1221-1232.

61.(a) Mei, Y.; Kumar, A.; Gross, R. *Macromolecules* **2003**, *36*, 5530-5536; (b) Yang, Y.; Yu, Y.; Zhang, Y. X.; Liu, C. B.; Shi, W.; Li, Q. S. *Process Biochem.* **2011**, *46*, 1900-1908.

62.Matsumura, S. *Adv. Polym. Sci.* **2006**, *194*, 95-132.

63.Okamoto, Y. *Macromol. Chem., Macromol. Symp.* **1991**, *42-3*, 117-133.

64.Hayakawa, M.; Mitani, M.; Yamada, T.; Mukaiyama, T. *Macromol. Chem. Physic.* **1997**, *198*, 1305-1317.

65.Nomura, N.; Taira, A.; Tomioka, T.; Okada, M. *Macromolecules* **2000**, *33*, 1497-1499.

66.Samantaray, M. K.; Katiyar, V.; Roy, D.; Pang, K. L.; Nanavati, H.; Stephen, R.; Sunoj, R. B.; Ghosh, P. *Eur. J. Inorg. Chem.* **2006**, 2975-2984.

67.Milione, S.; Grisi, F.; Centore, R.; Tuzi, A. *Organometallics* **2006**, *25*, 266-274.

68.Clark, L.; Cushion, M. G.; Dyer, H. E.; Schwarz, A. D.; Duchateau, R.; Mountford, P. *Chem. Commun.* **2010**, *46*, 273-275.

69.(a) Kurcok, P.; Matuszowicz, A.; Jedliński, Z. *Macromol. Rapid Comm.* **1995**, *16*, 201-206; (b) Monsalve, M.; Contreras, J. M.; Laredo, E.; Lopez-Carrasquero, F. *Express Polym. Lett.* **2010**, *4*, 431-441.

70.(a) Kurcok, P.; Matuszowicz, A.; Jedliński, Z.; Kricheldorf, H. R.; Dubois, P.; Jérôme, R. *Macromol. Rapid Comm.* **1995**, *16*, 513-519; (b) Jedlinski, Z.; Kowalczuk, M.; Kurcok, P.; Adamus, G.; Matuszowicz, A.; Sikorska, W.; Gross, R. A.; Xu, J.; Lenz, R. W. *Macromolecules* **1996**, *29*, 3773-3777; (c) Adamus, G.; Kowalczuk, M. *Biomacromolecules* **2008**, *9*, 696-703.

71.Jedlinski, Z.; Kowalczuk, M.; Kurcok, P. *J. Macromol. Sci., Pure Appl. Chem.* **1992**, *A29*, 1223-1230.

72.Lenz, R. W.; Jedlinski, Z. *Macromol. Chem., Macromol. Symp.* **1996**, *107*, 149-161.

73.Coulembier, O.; Delva, X.; Hedrick, J. L.; Waymouth, R. M.; Dubois, P. *Macromolecules* **2007**, *40*, 8560-8567.

74.Kawalec, M.; Śmiga-Matuszowicz, M.; Kurcok, P. *Eur. Polym. J.* **2008**, *44*, 3556-3563.

75.Juzwa, M.; Jedlinski, Z. *Macromolecules* **2006**, *39*, 4627-4630.

76.(a) Dubois, P.; Jacobs, C.; Jerome, R.; Teyssie, P. *Macromolecules* **1991**, *24*, 2266-2270; (b) Dubois, P.; Jerome, R.; Teyssie, P. *Macromol. Chem., Macromol. Symp.* **1991**, *42-43*, 103-116; (c) Kricheldorf, H. R.; Berl, M.; Scharnagl, N. *Macromolecules* **1988**, *21*, 286-293.

77.Kurcok, P.; Dubois, P.; Jerome, R. *Polym. Int.* **1996**, *41*, 479-485.

78.(a) Rieth, L. R.; Moore, D. R.; Lobkovsky, E. B.; Coates, G. W. *J. Am. Chem. Soc.* **2002**, *124*, 15239-15248; (b) Amgoune, A.; Thomas, C. M.; Ilinca, S.; Roisnel, T.; Carpentier, J.-F. *Angew. Chem. Int. Ed.* **2006**, *45*, 2782-2784.

79.Carpentier, J.-F. *Macromol. Rapid Commun.* **2010**, *31*, 1696-1705.

80.Zintl, M.; Molnar, F.; Urban, T.; Bernhart, V.; Preishuber-Pflügl, P.; Rieger, B. *Angew. Chem. Int. Ed.* **2008**, *47*, 3458-3460.

81.Ajellal, N.; Durieux, G.; Delevoye, L.; Tricot, G.; Dujardin, C.; Thomas, C. M.; Gauvin, R. M. *Chem. Commun.* **2010**, *46*, 1032-1034.

82.Kemnitzer, J. E.; Mccarthy, S. P.; Gross, R. A. *Macromolecules* **1993**, *26*, 1221-1229.

83.Kemnitzer, J. E.; Mccarthy, S. P.; Gross, R. A. *Macromolecules* **1993**, *26*, 6143-6150.

84.(a) Hori, Y.; Suzuki, M.; Yamaguchi, A.; Nishishita, T. **1993**, *26*, 5533-5534; (b) Hori, Y.; Hagiwara, T. *Int. J. Biol. Macromol.* **1999**, *25*, 237-245.

85.Kricheldorf, H. R.; Eggerstedt, S. *Macromolecules* **1997**, *30*, 5693-5697.

86.Ajellal, N.; Bouyahyi, M.; Amgoune, A.; Thomas, C. M.; Bondon, A.; Pillin, I.; Grohens, Y.; Carpentier, J.-F. *Macromolecules* **2009**, *42*, 987-993.

87.Ajellal, N.; Lyubov, D. M.; Sinenkov, M. A.; Fukin, G. K.; Cherkasov, A. V.; Thomas, C. M.; Carpentier, J.-F.; Trifonov, A. A. *Chem. Eur. J.* **2008**, *14*, 5440-5448.

88.Bouyahyi, M.; Ajellal, N.; Kirillov, E.; Thomas, C. M.; Carpentier, J.-F. *Chem. Eur. J.* **2011**, *17*, 1872-1883.

89.Kramer, J. W.; Treitler, D. S.; Dunn, E. W.; Castro, P. M.; Roisnel, T.; Thomas, C. M.; Coates, G. W. *J. Am. Chem. Soc.* **2009**, *131*, 16042-16044.

90.Webster, O. W. *Science* **1991**, *251*, 887-893.

91.Ajellal, N.; Carpentier, J.-F.; Guillaume, C.; Guillaume, S. M.; Helou, M.; Poirier, V.; Sarazin, Y.; Trifonov, A. *Dalton Trans.* **2010**, *39*, 8363-8376.

92.Inoue, S. *J. Polym. Sci., Part A: Polym. Chem.* **2000**, *38*, 2861-2871.

93.Asano, S.; Aida, T.; Inoue, S. *J. Chem. Soc. Chem. Comm.* **1985**, 1148-1149.

94.Aida, T.; Maekawa, Y.; Asano, S.; Inoue, S. *Macromolecules* **1988**, *21*, 1195-1202.

95.(a) Aida, T.; Kawaguchi, K.; Inoue, S. *Macromolecules* **1990**, *23*, 3887-3892; (b) Watanabe, Y.; Aida, T.; Inoue, S. *Macromolecules* **1990**, *23*, 2612-2617.

96.(a) Aida, T.; Inoue, S. *Acc. Chem. Res.* **1996**, *29*, 39-48; (b) Ko, B. T.; Lin, C. C. *Macromolecules* **1999**, *32*, 8296-8300; (c) Sugimoto, H.; Aida, T.; Inoue, S. *Macromolecules* **1990**, *23*, 2869-2875.

97.Poirier, V.; Duc, M.; Carpentier, J.-F.; Sarazin, Y. *ChemSusChem* **2010**, *3*, 579-590.

98.(a) Ma, H. Y.; Okuda, J. *Macromolecules* **2005**, *38*, 2665-2673; (b) Amgoune, A.; Thomas, C. M.; Roisnel, T.; Carpentier, J.-F. *Chem. Eur. J.* **2006**, *12*, 169-179; (c) Zhao, W.; Cui, D. M.; Liu, X. L.; Chen, X. S. *Macromolecules* **2010**, *43*, 6678-6684.

99.Amgoune, A.; Thomas, C. M.; Carpentier, J.-F. *Macromol. Rapid. Comm.* **2007**, *28*, 693-697.

100.Guillaume, C.; Carpentier, J.-F.; Guillaume, S. M. *Polymer* **2009**, *50*, 5909-5917.

101.Poirier, V.; Roisnel, T.; Carpentier, J.-F.; Sarazin, Y. *Dalton Trans.* **2009**, 9820-9827.

102.Poirier, V.; Roisnel, T.; Carpentier, J.-F.; Sarazin, Y. *Dalton Trans.* **2011**, *40*, 523-534.

103.(a) Chen, C.; Yu, C. H.; Cheng, Y. C.; Yu, P. H. F.; Cheung, M. K. *Biomaterials* **2006**, *27*, 4804-4814; (b) Ozturk, T.; Goktas, M.; Hazer, B. *J. Appl. Polym. Sci.* **2010**, *117*, 1638-1645.

104.(a) Li, X.; Liu, K. L.; Li, J.; Tan, E. P. S.; Chan, L. M.; Lim, C. T.; Goh, S. H. *Biomacromolecules* **2006**, *7*, 3112-3119; (b) Du, B. Y.; Mei, A. X.; Yin, K. Z.; Zhang, Q. F.; Xu, J. T.; Fan, Z. Q. *Macromolecules* **2009**, *42*, 8477-8484.

105.(a) Perret, R.; Skoulios, A. *Makromol. Chem.* **1972**, *156*, 143-156; (b) Ashby, R. D.; Solaiman, D. K. Y.; Foglia, T. A. *Appl. Microbiol. Biotechnol.* **2002**, *60*, 154-159; (c) Ravenelle, F.; Marchessault, R. H. *Biomacromolecules* **2002**, *3*, 1057-1064; (d) Li, J.; Li, X.; Ni, X. P.; Leong, K. W. *Macromolecules* **2003**, *36*, 2661-2667; (e) Ravenelle, F.; Marchessault, R. H. *Biomacromolecules* **2003**, *4*, 856-858; (f) Bishara, A.; Kricheldorf, H. R.; Domb, A. J. *Macromol. Symp.* **2005**, *225*, 17-30; (g) Li, X.; Loh, X. J.; Wang, K.; He, C. B.; Li, J. *Biomacromolecules* **2005**, *6*, 2740-2747; (h) Liu, K. L.; Goh, S. H.; Li, J. *Polymer* **2008**, *49*, 732-741; (i) Babinot, J.; Renard, E.; Langlois, V. *Macromol. Chem. Phys.* **2011**, *212*, 278-285.

106.Chen, C. T.; Huang, C. A.; Huang, B. H. *Macromolecules* **2004**, *37*, 7968-7973.

107.Li, C. J.; Chan, T. H. *Tetrahedron* **1999**, *55*, 11149-11176.

108.Hsieh, I. P.; Huang, C. H.; Lee, H. M.; Kuo, P. C.; Huang, J. H.; Lee, H. I.; Cheng, J. T.; Lee, G. H. *Inorg. Chim. Acta* **2006**, *359*, 497-504.

109.Douglas, A. F.; Patrick, B. O.; Mehrkhodavandi, P. *Angew. Chem. Int. Ed.* **2008**, *47*, 2290-2293.

110.Pietrangelo, A.; Knight, S. C.; Gupta, A. K.; Yao, L. J.; Hillmyer, M. A.; Tolman, W. B. *J. Am. Chem. Soc.* **2010**, *132*, 11649-11657.

111.Yu, I.; Acosta-Ramirez, A.; Mehrkhodavandi, P. *Submitted*.

112.(a) Zhang, J.; Gan, Z.; Zhong, Z.; Jing, X. *Polym. Int.* **1998**, *45*, 60-66; (b) Stridsberg, K.; Albertsson, A.-C. *J. Polym. Sci., Part A: Polym. Chem.* **2000**, *38*, 1774-1784; (c) An, S. G.; Cho, C. G. *Macromol. Rapid Commun.* **2004**, *25*, 618-622; (d) Hamley, I. W.; Parras, P.; Castelletto, V.; Castillo, R. V.; Muller, A. J.; Pollet, E.; Dubois, P.; Martin, C. M. *Macromol. Chem. Phys.* **2006**, *207*, 941-953.

113.Othman, N.; Xu, C.; Mehrkhodavandi, P.; Hatzikiriakos, S. *Polymer*, in press.

114.Yoo, D. K.; Kim, D. *Polym Bull.* **2009**, *63*, 637-651.

115.(a) Ren, J. D.; Adachi, K. *Macromolecules* **2003**, *36*, 5180-5186; (b) Xu, J.; Guo, B. H.; Zhou, J. J.; Li, L.; Wu, J.; Kowalczuk, M. *Polymer* **2005**, *46*, 9176-9185.

116.Tsuji, H.; Wada, T.; Sakamoto, Y.; Sugiura, Y. *Polymer* **2010**, *51*, 4937-4947.

117.(a) Tsuji, H.; Horii, F.; Hyon, S. H.; Ikada, Y. *Macromolecules* **1991**, *24*, 2719-2724; (b) Opaprakasit, P.; Opaprakasit, M. *Macromol Symp* **2008**, *264*, 113-120.

118.Li, L. B.; Zhong, Z. Y.; de Jeu, W. H.; Dijkstra, P. J.; Feijen--, J. *Macromolecules* **2004**, *37*, 8641-8646.

119.Polarity index. http://www.chemical-ecology.net/java/solvents.htm (accessed Mar 16th, 2012).

120.(a) Pearce, R.; Brown, G. R.; Marchessault, R. H. *Polymer* **1994**, *35*, 3984-3989; (b) Pearce, R.; Marchessault, R. H. *Polymer* **1994**, *35*, 3990-3997.

121.(a) Nishiura, M.; Hou, Z. M.; Koizumi, T.; Imamoto, T.; Wakatsuki, Y. *Macromolecules* **1999**, *32*, 8245-8251; (b) Grunova, E.; Roisnel, T.; Carpentier, J.-F. *Dalton Trans.* **2009**, 9010-9019.

122.(a) Huang, C. H.; Wang, F. C.; Ko, B. T.; Yu, T. L.; Lin, C. C. *Macromolecules* **2001**, *34*, 356-361; (b) Shueh, M. L.; Wang, Y. S.; Huang, B. H.; Kuo, C. Y.; Lin, C. C.

Macromolecules **2004**, *37*, 5155-5162; (c) Bonnet, F.; Cowley, A. R.; Mountford, P. *Inorg. Chem.* **2005**, *44*, 9046-9055; (d) Yu, T. L.; Wu, C. C.; Chen, C. C.; Huang, B. H.; Wu, J. C.; Lin, C. C. *Polymer* **2005**, *46*, 5909-5917; (e) Huang, B. H.; Lin, C. N.; Hsueh, M. L.; Athar, T.; Lin, C. C. *Polymer* **2006**, *47*, 6622-6629; (f) Dyer, H. E.; Huijser, S.; Susperregui, N.; Bonnet, F.; Schwarz, A. D.; Duchateau, R.; Maron, L.; Mountford, P. *Organometallics* **2010**, *29*, 3602-3621.

123.Chen, H. Y.; Huang, B. H.; Lin, C. C. *Macromolecules* **2005**, *38*, 5400-5405.

124.Ajellal, N.; Thomas, C. M.; Carpentier, J.-F. *J. Polym. Sci., Part A: Polym. Chem.* **2009**, *47*, 3177-3189.

125.Letchford, K.; Burt, H. *Eur. J. Pharm. Biopharm.* **2007**, *65*, 259-269.

Appendix

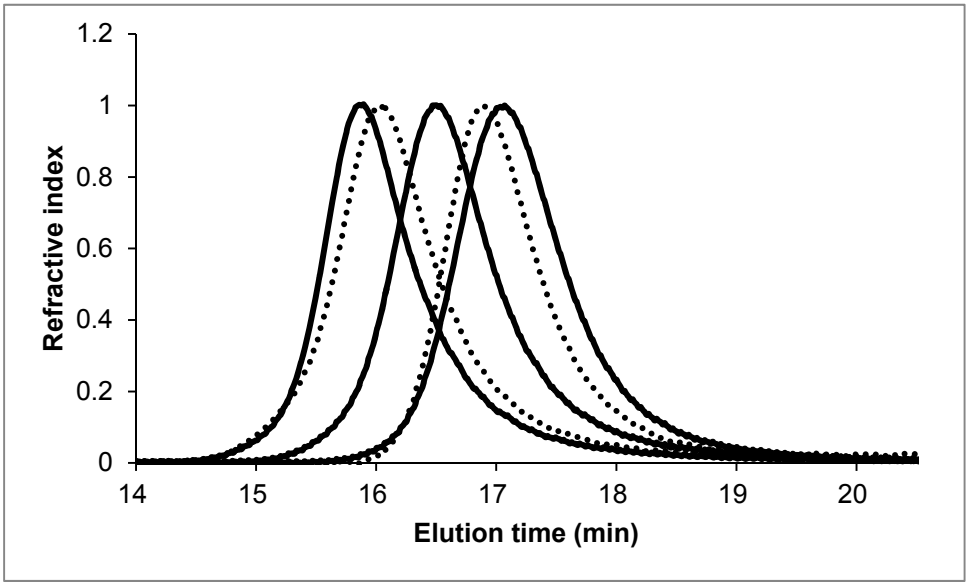

Figure A1 GPC traces of the polymers produced by iROP of *rac*-LA with ethanol by **1**. From left to right, corresponding to entries in Table 3.1: 1. entry 1 (M_n = 109.4 kDa, *PDI* = 1.02); 2. entry 2 (M_n = 75.53 kDa, *PDI* = 1.03); 3. entry 3 (M_n = 48.29 kDa, *PDI* = 1.02); 4. entry 4 (M_n = 33.46 kDa, *PDI* = 1.01); 5. entry 5 (M_n = 30.79 kDa, *PDI* = 1.01).

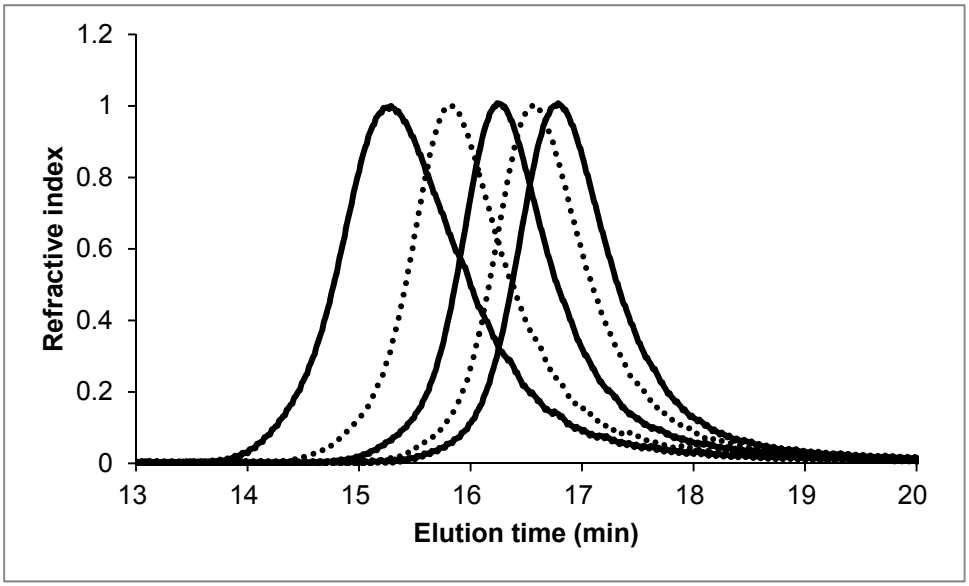

Figure A2 GPC traces of the polymers produced by iROP of L-LA with $MePEG_7$ by **30**. From left to right, corresponding to entries 1–5 in Table 3.2: 1. entry 1 (M_n = 144.2 kDa, *PDI* = 1.06); 2. entry 2 (M_n = 72.41 kDa, *PDI* = 1.04); 3. entry 3 (M_n = 49.54 kDa, *PDI* = 1.03); 4. entry 4 (M_n = 39.14 kDa, *PDI* = 1.02); 5. entry 5 (M_n = 29.79 kDa, *PDI* = 1.02).

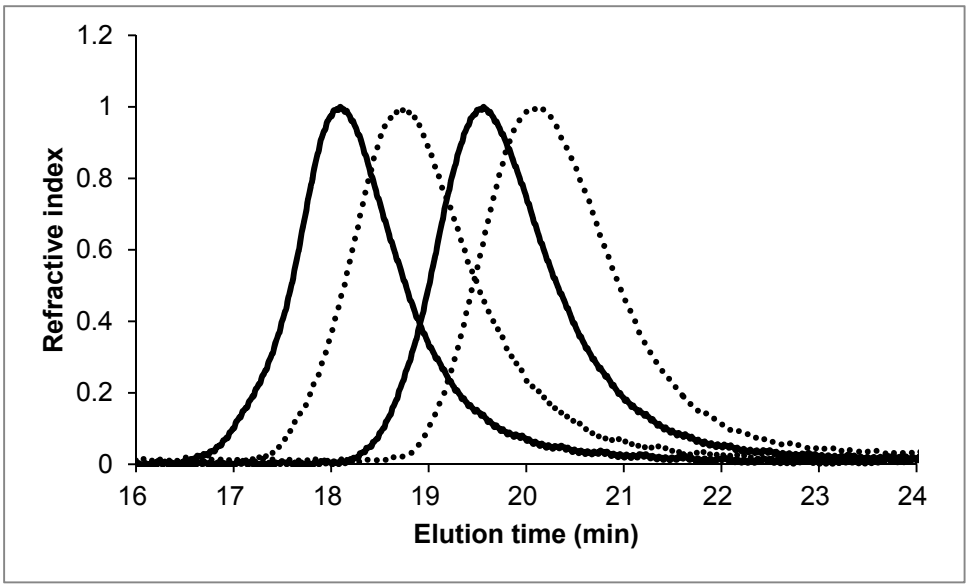

Figure A3 GPC traces of the polymers produced by iROP of L-LA with $MePEG_{114}$ by **30**. From left to right, corresponding to entries 6–9 in Table 3.2: 1. entry 6 (M_n = 31.90 kDa, *PDI* = 1.14); 2. entry 7 (M_n = 23.36 kDa, *PDI* = 1.46); 3. entry 8 (M_n = 15.95 kDa, *PDI* = 2.30); 4. entry 9 (M_n = 10.01 kDa, *PDI* = 2.21).

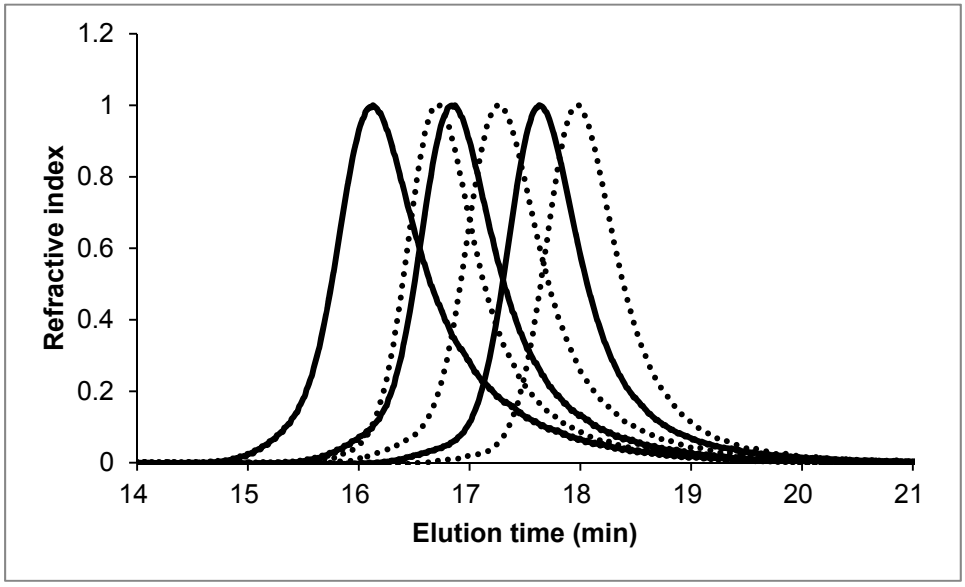

Figure A4 GPC traces of the polymers produced by iROP of BBL with ethanol by **30**. From left to right, corresponding to entries 1–6 in Table 3.3: 1. entry 1 (M_n = 82.89 kDa, *PDI* = 1.07); 2. entry 6 (M_n = 44.02 kDa, *PDI* = 1.01); 3. entry 2 (M_n = 39.97 kDa, *PDI* = 1.02); 4. entry 3 (M_n = 28.34 kDa, *PDI* = 1.01); 5. entry 4 (M_n = 21.85 kDa, *PDI* = 1.01); 6. entry 5 (M_n = 16.77 kDa, *PDI* = 1.01).

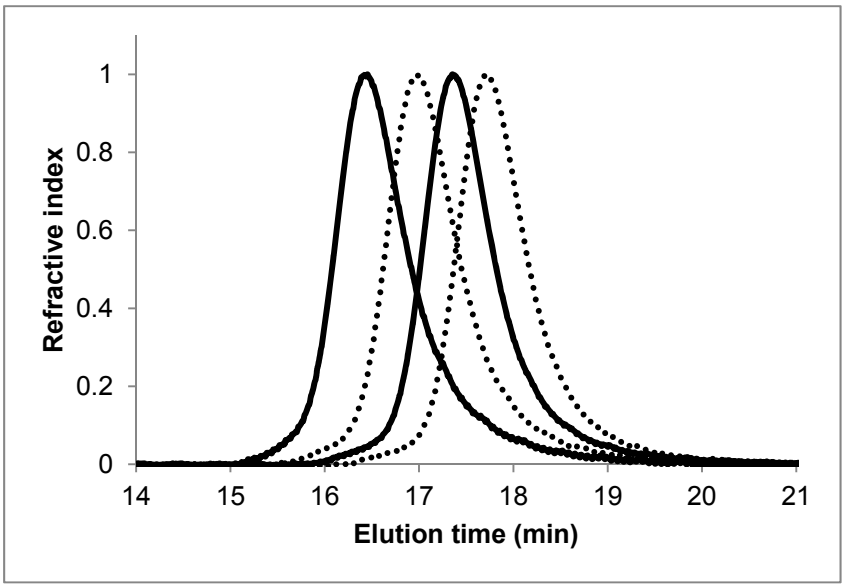

Figure A5. GPC traces of the polymers produced by iROP of BBL with $MePEG_7$ by **30**. From left to right, corresponding to entries 7–10 in Table 3.3: 1. entry 7 (M_n = 42.67 kDa, *PDI* = 1.02); 2. entry 8 (M_n = 27.97 kDa, *PDI* = 1.01); 3. entry 9 (M_n = 21.07 kDa, *PDI* = 1.01); 4. entry 10 (M_n = 17.07 kDa, *PDI* = 1.02).

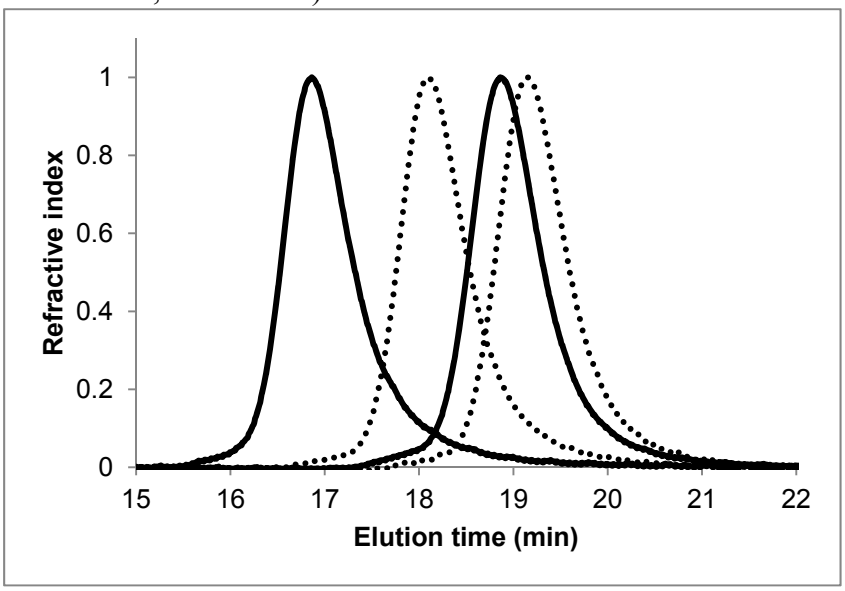

Figure A3. GPC traces of the polymers produced by iROP of BBL with $MePEG_7$ by **30**. From left to right, corresponding to entries 11–14 in Table 3.3: 1. entry 12 (M_n = 36.09 kDa, *PDI* = 1.01); 2. entry 13 (M_n = 14.90 kDa, *PDI* = 1.01); 3. entry 11 (M_n = 7.824 kDa, *PDI* = 1.03); 4. entry 14 (M_n = 7.569 kDa, *PDI* = 1.03).